Summer 8-13-2010

Linear and Nonlinear Auditory Response Properties Of Interneurons In A High Order Avian Vocal Motor Nucleus During Wakefulness

Jonathan N. Raksin
University of Pennsylvania, jraksin@mail.med.upenn.edu

Linear and Nonlinear Auditory Response Properties Of Interneurons In A High Order Avian Vocal Motor Nucleus During Wakefulness

Abstract
Motor-related forebrain areas in higher vertebrates also show responses to passively presented sensory stimuli. Sensory tuning properties in these areas, especially during wakefulness, and their relation to perception, however, are poorly understood. In the avian song system, HVC (proper name) is a vocal-motor structure with auditory responses well defined under anesthesia but poorly characterized during wakefulness. I used a large set of song stimuli including the bird"s own song (BOS) and many conspecific stimuli (CON) to characterize auditory tuning properties in putative interneurons (HVCIN) during wakefulness. My findings suggest that HVC contains a heterogeneity of response types; a third of neurons are either suppressed or show no response to any stimuli and two thirds show excitatory responses to one or more stimuli. A subset of excitatory neurons are tuned exclusively to BOS and show very low linearity as measured by spectrotemporal receptive field analysis (STRF), but many respond well to both BOS and CON stimuli and show response linearity comparable to that previously measured in structures of the ascending auditory pathway. Fourier analysis of the STRFs of linear HVCIN reveals a range of peak spectrotemporal tuning properties, with approximately half of these neurons showing peak sensitivity to modulations occurring with high power in zebra finch song. Previous work has established that HVC lesioned birds are impaired in operant contingency reversals involving CON stimuli and birds with lesions to song nuclei receiving auditory input from HVC are impaired in discriminations between BOS and CON stimuli. The findings of the present study are consistent with these results and suggest a possible role for HVC in species-relevant auditory tasks.

Degree Type
Dissertation

Degree Name
Doctor of Philosophy (PhD)

Graduate Group
Neuroscience

First Advisor
Dr. Marc Schmidt

Keywords
neuroscience, UPenn, auditory, receptive field, songbird

Subject Categories
Systems Neuroscience

LINEAR AND NONLINEAR AUDITORY RESPONSE PROPERTIES OF INTERNEURONS IN A HIGH ORDER AVIAN VOCAL MOTOR NUCLEUS DURING WAKEFULNESS

JONATHAN N. RAKSIN

A DISSERTATION

in

Neuroscience

Presented to the Faculties of the University of Pennsylvania

in

Partial Fulfillment of the Requirements for the Degree of Doctor of Philosophy

2010

_____

Dr. Marc Schmidt, Associate Professor of Biology, Dissertation Supervisor

_____

Dr. Rita Balice-Gordon, Professor of Neuroscience, Graduate Group Chairperson

Dissertation Committee:

Dr. Marcos Frank, Assistant Professor of Neuroscience, Committee Chair

Dr. Diego Contreras, Associate Professor of Neuroscience, Committee Member

Dr. Joshua Gold, Assistant Professor of Neuroscience, Committee Member

Dr. Rita Balice-Gordon, Professor of Neuroscience, Added Committee Member

ABSTRACT

LINEAR AND NONLINEAR AUDITORY RESPONSE PROPERTIES OF INTERNEURONS IN A HIGH ORDER AVIAN VOCAL MOTOR NUCLEUS DURING WAKEFULNESS

Jonathan N. Raksin

Marc F. Schmidt

Motor-related forebrain areas in higher vertebrates also show responses to passively presented sensory stimuli. Sensory tuning properties in these areas, especially during wakefulness, and their relation to perception, however, are poorly understood. In the avian song system, HVC (proper name) is a vocal-motor structure with auditory responses well defined under anesthesia but poorly characterized during wakefulness. I used a large set of song stimuli including the bird's own song (BOS) and many conspecific stimuli (CON) to characterize auditory tuning properties in putative interneurons (HVC_{IN}) during wakefulness. My findings suggest that HVC contains a heterogeneity of response types; a third of neurons are either suppressed or show no response to any stimuli and two thirds show excitatory responses to one or more stimuli. A subset of excitatory neurons are tuned exclusively to BOS and show very low linearity as measured by spectrotemporal receptive field analysis (STRF), but many respond well

to both BOS and CON stimuli and show response linearity comparable to that previously measured in structures of the ascending auditory pathway. Fourier analysis of the STRFs of linear HVC_{IN} reveals a range of peak spectrotemporal tuning properties, with approximately half of these neurons showing peak sensitivity to modulations occurring with high power in zebra finch song. Previous work has established that HVC lesioned birds are impaired in operant contingency reversals involving CON stimuli and birds with lesions to song nuclei receiving auditory input from HVC are impaired in discriminations between BOS and CON stimuli. The findings of the present study are consistent with these results and suggest a possible role for HVC in species-relevant auditory tasks.

Table of Contents

List of Figures

Chapter 1. Introduction

Overview

The goal of this Introduction is to provide context for the work presented in **Chapter 2,** where I describe both 'low order' (e.g. response valence and magnitude) and 'high order' (e.g. linear receptive field structure) properties of a large population of putative interneurons in the high-order vocal motor nucleus HVC (proper name) in awake, unrestrained adult male zebra finches. In Section 1 of this Introduction, I describe HVC in the context it is most commonly studied, as a key structure in the song production circuit. In Section 2, I describe evidence that HVC can also be thought of as a sensory structure, with response properties that have often been found to vary with changes in behavioral state. This section is divided into separate discussions of auditory activity in HVC during song production and activity during passive presentation of complex stimuli, with a focus on auditory properties during wakefulness. A key motivation of the work described in **Chapter 2** is that, though previous studies have shown robust responses to passively presented stimuli during wakefulness, these studies have been limited in multiple ways. These limitations include implementation of recording techniques disruptive to ongoing behavior and yielding few single neurons, stimulus sets insufficiently comprehensive to make strong statements about neural selectivity, and analytical techniques restricted to spike rate-derived measures at the exclusion of the analysis of receptive field structure. In Section 3, I discuss the known involvement of

HVC and its song system afferents in perceptual discriminations between naturalistic, species relevant stimuli, as gleaned from lesion-behavior studies in both operant and semi-naturalistic conditions. These functional results are critical for framing the possible significance of the response features of putative HVC_{IN} described in **Chapter 2**. In Section 4, I discuss evidence that HVC receives auditory input from at least several different ascending sources. Because response properties during wakefulness differ across these afferent structures, these differences may account for a substantial portion of the heterogeneity in response properties of putative HVC_{IN} that I report in **Chapter 2**. Finally, in Section 5, I discuss the nature and functional properties of spontaneous and auditory activity in HVC and its immediate target in the primary song production motor pathway (the robust nucleus of the arcopallium, RA) during sleep. Though this section relates most closely to topics discussed in the Future Directions section (**Chapter 3**), it also has relevance to a type of response during wakefulness that I describe in **Chapter 2** in which neurons show extreme preference for the bird's own song (BOS) as compared to the songs of other birds of the same species (conspecific, or CON).

Section 1. HVC and Vocal Motor Production

HVC is an essential component of the song production circuit in adult songbirds. Large (Nottebohm et al., 1976; Simpson and Vicario, 1990) and small (Thompson and Johnson, 2007; Thompson et al., 2007) bilateral, as well unilateral (Williams et al., 1992), lesions of HVC lead to immediate cessation of production of the learned, stereotyped song and a reversion to production of a highly variable plastic 'subsong' normally seen only in juvenile birds before the onset of learning (Aronov et al., 2008). Destruction of the

axonal output of HVC in the primary motor axis also leads to song degradation (Scharff et al., 2000). Functional recovery of the original song can occur in the wake of partial HVC lesions, though auditory feedback is required for such recovery in a manner that is not yet understood at a mechanistic level (Thompson et al., 2007). While lesion studies merely demonstrate HVC's necessity and not sufficiency for normal stereotyped song production, recent work involving slowing of local network dynamics via cooling suggests that HVC is likely the single most important structure for dictating the timing of song output in normal adult birds (Long and Fee, 2008), though brainstem reafferent (Ashmore et al., 2005) and feed forward cortico-basal ganglia (Williams and Mehta, 1999) loops may also influence timing to some degree.

HVC contains three basic neuronal types that can be readily distinguished from one another based on spontaneous activity (Fee et al., 2004; Hahnloser and Fee, 2002), spike morphology (Rauske et al., 2003; see **Figure 2.3C**), and premotor properties (Hahnloser et al., 2002; Kozhevnikov and Fee, 2007) during vocal motor output. The first class of neuron (HVC_{RA}), projects in the primary motor axis to the robust nucleus of the arcopallium (RA), which is itself divided in to a dorsal area (dRA; see **Figure 1.1**) projecting to brainstem respiratory effectors facilitating the temporal pattern of song output and a ventral area (vRA) projecting to syringial effectors associated with the frequency modulation of song (Vicario, 1991; Wild 1993, 1997). HVC_{RA} neurons have virtually no spontaneous activity during wakefulness and exhibit just a single, precise (jitter <1ms from motif to motif) premotor burst of 3-4 spikes at one point during each song motif (see **Figure 2.4** for visual and textual description of a song motif). These

neurons are extremely hard to record from because of their virtual lack of spontaneous activity, despite the fact that they represent 50-80% of all HVC neurons (Fee et al., 2004). A second class of HVC neuron (HVC_X) projects to the avian basal ganglia homologue Area X, and this projection forms the initial part of a highly topographically conserved feed-forward basal ganglia-cortico loop ultimately converging on to RA (and back to Area X as well) (Luo et al., 2001; see **Figure 1.1**). HVC_X neurons fire nearly as precisely and sparsely within a single burst as HVC_{RA} neurons during song production, though they can do so at up to four points during each song motif, and they have a low but measurable spontaneous rate of <1 Hz.

The interneuronal population (HVC_{IN}) , the focus of the recordings described in **Chapter 2**, is the third group of neurons found within HVC. In the song system (Spiro et al., 1999), as in a multitude of other systems (Ferster and Miller, 2000; Merchant et al., 2008; Murayama et al., 2009), interneurons precisely shape the output of projection neurons. In HVC, slice experiments have demonstrated that interneurons reciprocally interact with the two previously described classes of projection neuron (Mooney and Prather, 2005). Despite the fact that they are almost always considered as a single group in physiology studies, HVC_{IN} show a large degree of diversity based on cell morphology, calcium-binding protein profile, and intrinsic firing properties (Mooney, 2000; Nixdorf et al., 1989; Wild et al., 2005). In awake birds, HVC_{IN} have higher spontaneous firing rates than either class of projection neuron (2-40 Hz), which makes it much easier to pick these neurons up than their relative rarity (<10% of all HVC neurons) and small size would suggest. In sharp contrast to the two classes of projection neurons, HVC_{IN} fire tonically

throughout song production and lack extreme stereotypy in their temporal pattern of firing across song renditions. Nonetheless, they still show recognizable patterns of activity from motif to motif and their activity, unlike that of either class of projection neuron, is significantly correlated with song syllable patterns (Kozhevnikov and Fee, 2007).

Section 2. Auditory Responses in HVC

Part 1: Sensitivity to Self Generated Auditory Feedback During Song Production

Birdsong is highly similar to human speech in that both require the guidance of auditory feedback for normal maintenance in adulthood, well after stereotyped motor patterns have been established (Lane and Webster, 1991; Nordeen and Nordeen, 1993; Okanoya and Yamaguchi, 1997; Leonardo and Konishi, 1999; Lombardino and Nottebohm, 2000). In addition, it has been demonstrated that both speech (Howell and Archer, 1984; Howell and Powell, 1987; Houde and Jordan, 1998) and song production (Cynx and von Rad, 2001; Sakata and Brainard, 2006) are sensitive to alteration of auditory feedback in real time. While it would seem logical that motor structures themselves would directly receive instructive signals related to ongoing performance, especially when such signals indicate error, evidence for this is not readily forthcoming from either human functional imaging studies (Hashimoto and Sakai, 2003) or electrophysiology experiments in songbirds (Hessler and Doupe, 1999; Leonardo, 2004; Kozhevnikov and Fee, 2007). In the song system, several studies have looked specifically at whether ongoing singing-related activity in HVC_X (basal ganglia-projecting) neurons is influenced by the presence of

delayed auditory feedback (DAF). In both late juvenile (Kozheznikov and Fee, 2007) and adult (Prather et al., 2008) birds from several songbird species, the highly stereotyped, phasic and precise song premotor activity shown by HVC_X neurons is unchanged in the presence of DAF relative to during interleaved trials with no feedback disruption. In addition, HVC_X neurons that are responsive to the bird's own song (BOS) during passive awake auditory playback (see **Part 2** of this section) are completely insensitive to auditory stimulation during a window of time spanning from 500 ms previous to the onset of production to 500 ms after the offset of song production (Prather et al., 2008). No studies have looked at whether HVC neurons projecting in the primary motor axis to the robust nucleus of the arcopallium (RA) (**see Figure 1.1**) are affected by DAF, though these neurons, unlike HVC_X and HVC_{IN} neurons, do not show passive auditory responses during wakefulness in at least several songbird species (see next sections) (Prather et al., 2008).

In the domesticated Bengalese finch, closely related to the zebra finch, though possessive of a substantially more variable song (Nakamura and Okanoya, 2004; Okanoya, 2004), some sensitivity to perturbed auditory feedback has been demonstrated in putative HVC_{IN} (Sakata and Brainard, 2008). This sensitivity occurs in the form of a decrease in activity over a very short (~10ms) window starting ~50ms after the onset of feedback disruption. This activity modulation, while significant, can be said to be non-specific in several ways. Firstly, the inhibition occurs with equal vigor on trials where feedback disruption causes no ongoing song changes as on trials where ongoing song is altered. Thus, this type of modulation cannot be said to be predictive of real time adaptation to the feedback

disruption. Secondly, the activity decrease is indiscriminate with respect to whether the disruptive signal is a time-delayed version of the ongoing element, the previously discussed DAF, or an entirely different, temporally displaced element. Thus, it seems unlikely that the signal carries specific information regarding the features of the chunk of sound that should be making its way back to the motor system for evaluation at that specific moment. Nevertheless, it will be interesting to know whether these effects are present in zebra finch HVC_{IN}. Because Bengalese finches produce a more variable song and demonstrate more rapid song deterioration after deafening (Woolley and Rubel, 1997, 1999) than do zebra finches, one might expect stronger sensory related signals in Bengalese finch HVC during song production if such signals are in any way related to the subsequent, real-time modulation of singing behavior.

If autogenously generated, instructive auditory signals are not channeled to HVC during song production, it may be directly related to the extreme demands of solving the so-called "temporal credit assignment" problem in real time. The general form of this problem, which has long been appreciated as a major challenge to motor learning and feedback evaluation (Lashley KS, 1951; Troyer and Doupe, 2000), is that circuits moving through a motor production sequence in time have no obvious way to 'tag' elements responsible for previous time steps in the process when feedback related to performance at those previous time steps finds its way back to the production circuit. In the song circuit, the first part of this lag is caused by a premotor delay that has been estimated at 40-50 ms from HVC multiunit and HVC_{IN} recordings (McCasland, 1987; Schmidt, 2003), but may be substantially shorter for at least some neurons (on the order of 15-

20ms) based on estimates derived from recording of single, antidromically verified HVC_{RA} neurons (Hahnloser et al., 2002). The second component of the lag is the delay time for auditory input making it back to the song system after production of a particular element occurs. This lag has been estimated at roughly 20ms for RA (Dave and Margoliash, 2000), which receives putatively monosynaptic auditory input from HVC (Doupe and Konishi, 1991). Because individual song elements tend to be between 50 and 100ms long (mean temporal modulation rate of ~7.5 Hz) (Woolley et al., 2009), with notes evolving on an even shorter timescale, by the time auditory information can get back to neurons involved in motor output, the motor program has likely moved on to representation of a new element or, almost certainly, a new element sub-component. Several sophisticated models have been proposed to account for reafferent auditory lag times by speculating that the basal ganglia pathway is involved in delaying efference copies of song motor commands just long enough to facilitate comparison of these signals with reafferent auditory information reaching the song system (Dave and Margoliash, 2000; Troyer and Doupe, 2000). While long synaptic delays that could potentially support this timing do exist in the basal ganglia pathway (Luo and Perkel, 1999), these models critically require the reentry of auditory information specific to ongoing song activity to the song system. As described earlier in this section, evidence for this type of activity is currently underwhelming, which presents a major challenge to any model in which expected and actual feedback signals are compared in real time within the song system proper.

If the song system is not the primary site of autogenous feedback evaluation during singing, where might this type of processing occur? A recent study in zebra finches during the latter stages of juvenile song learning raises the intriguing possibility that real time auditory feedback evaluation occurs outside of the song system proper, in areas analogous to primary and secondary auditory cortex in mammals. In this study (Keller and Hahnloser, 2009), a small population of neurons in the ascending auditory areas Field L and CLM (see **Figure 1.1**) were found that were virtually silent during ongoing song output except for epochs where a call vocalization was played back as a perturbing stimulus. The properties of these neurons suggest that they are sensitive not to auditory feedback, per se, but to the discrepancy between expected and actual feedback. Some neurons exhibited responses during passive presentation of BOS when the bird wasn't actually singing, but only during epochs where 'errors'(i.e. disruptive calls) had been spliced in to the song. The existence of several flavors of error sensitivity strongly implies that these putatively primary sensory neurons have access to a representation of the expected outcome of song production. Otherwise, there would be no way to generate an error signal when a deviation from the expected outcome arises. Furthermore, in neurons displaying stereotyped, non error-sensitive auditory responses to passive BOS playback, activity during singing reliably precedes that during playback by a few milliseconds. If this activity during song production were purely sensory in nature, it would be expected that it would be delayed relative to that seen during passive presentation by an interval equal to the premotor delay, which is on the order of tens of milliseconds (see previous section on premotor delay and HVC). That it actually occurs *earlier* than activity during passive presentation suggests that there is a premotor and/or

predictive component. In **Section 5** of this Introduction, I describe putatively sensory activity during sleep in RA that similarly shows sensory activity earlier than expected based on assumptions of passive sensory processing (Dave and Margoliash, 2000). That activity has been theorized to be at least partially of an anticipatory motor predictive nature, and that description may just as well be applied to the sensory activity in primary sensory cells described here.

Part 2: Responses to Passively Presented Stimuli

A large number of studies in HVC of anesthetized (Margoliash, 1983; Margoliash and Konishi, 1985; Margoliash, 1986; Sutter and Margoliash, 1994) and sedated (Cardin and Schmidt, 2003, 2004a) birds have demonstrated the presence of robust auditory responses that are highly selective for BOS over other complex stimuli and homogenous across time and recording sites. In one study conducted under urethane anesthesia, intracellular recordings demonstrated that all three classes of HVC neuron in the zebra finch display robust, BOS selective responses at both supra and super threshold levels (Mooney, 2000). It is important to note that the vast majority of studies reporting highly BOS selective responses during anesthesia and sedation have been carried out in only two species, the white-crowned sparrow and zebra finch. These species are non-representative of oscine songbird species in general in that they exhibit only a single, highly stereotyped song type that is virtually unchanged across the adult lifespan. Further, neither species exhibits territorial behavior in which male birds exhibit song matching with encroaching rivals. Such behavior may require song motor areas to show robust sensitivity to a broad range of song features that represent overlap between the bird's own vocal repertoire and that of

other birds (Nealen and Schmidt, 2006; Prather et al., 2008). Perhaps illuminating the problem of making general inferences about tuning from studies limited to a few species is a recent study in the canary, a territorial songbird (Appeltants et al., 2005) with a relatively extensive song repertoire (Leitner and Catchpole, 2004). The results of this study suggest that robust HVC auditory responses under anesthesia can extend to elements and phrases not exhibited by any BOS variants of the subject bird (Lehongre and Del Negro, 2009). Clearly, further studies in oscine species with a diversity of song repertoire and social ecology features will be needed to elucidate the critical variables in determining the degree of BOS selectivity shown by HVC neurons during non-natural states.

Studies of passive auditory response properties in HVC during wakefulness suggest a situation somewhat different from that which occurs during anesthesia and sedation. Multiple studies carried out in zebra finches with low impedance (on the order of 100 kΩ), fixed tungsten wire implants have demonstrated a suppression of auditory response in HVC immediately following arousal at the massively multiunit level (at least tens of neurons simultaneously recorded) (Schmidt and Konishi, 1998; Nick et al., 2001; Cardin and Schmidt, 2003). This arousal suppression has also been seen in smaller multiunit recordings and in recordings from individual putative HVC_{IN} (Cardin and Schmidt, 2004b), and is likely mediated by both direct cholinergic (Shea and Margoliash, 2003) and indirect noradrenergic (Cardin and Schmidt, 2004b) mechanisms. Experiments linking modulatory state to HVC auditory response properties have been carried out only in lightly sedated (Cardin and Schmidt, 2004b) and anesthetized (Shea and Margoliash,

2003) birds. Thus, evidence for relationships between modulatory state, specific awake behavioral characteristic, and auditory response properties has not been directly observed.

Though the studies reporting arousal suppression in HVC leave open the possibility that low impedance wire electrodes are extremely biased toward neurons showing an absence of auditory responses during wakefulness, some studies with identical technology in the zebra finch have demonstrated the existence of auditory responses in HVC during wakefulness (Cardin and Schmidt, 2003; Cardin and Schmidt, 2004a). These responses fluctuate widely in strength across long periods of wakefulness in a non-circadian manner (Cardin and Schmidt, 2004a), though they achieve neither the vigor nor trial-to-trial consistency of responses at the same sites during sedation (Cardin and Schmidt, 2003; Cardin and Schmidt, 2004a). Strikingly, in these studies awake auditory responses were found to be entirely non-selective for BOS over a time-reversed version of BOS (REV). This is in stark contrast to both the same sites during sedation, as well as to the results of anesthesia studies in zebra finches and white-crowned sparrows described at the beginning of this section.

Studies carried out with higher impedance electrodes (on the order of MΩ as opposed to kΩ) during wakefulness on single putative HVC_{IN} or multiunit sites likely to be dominated by HVC_{IN} have yielded somewhat different results from those obtained with fixed wires. Unlike the fixed wire studies in zebra finches, all of these studies have demonstrated at least some degree of selectivity for BOS over REV and/or one or several CON stimuli. These studies have been carried out in multiple species, including the zebra finch (Rauske et al., 2003), white-crowned sparrow (Margoliash and Konishi, 1985),

Bengalese finch (Sakata and Brainard, 2008), and song sparrow (Nealen and Schmidt, 2006). While this is far from an exhaustive sampling of the pool of oscine songbird species, it at least includes several species with non-stereotyped song (Bengalese finch and song sparrow) as well as one territorial bird exhibiting song matching behavior (song sparrow). Only one awake study targeting single HVC_{IN} has been carried out in the zebra finch (Rauske et al., 2003). This study reported auditory responses in single HVC_{IN} that, when present, (two-thirds of cells showed significant awake responses) were uniformly selective for BOS relative to REV and a single CON stimulus. Awake responses in the Rauske et al., study also showed a high degree of stability across time, unlike the responses seen in the fixed implant studies.

It is unclear why Rauske et al. achieved results that were different from the fixed implant studies, both in terms of tuning properties and response strength stability over time. One likely possibility is selection bias; Cardin and Schmidt (2003) hypothesize that their wire recordings may have picked up neuronal types not recorded by Rauske et al. Cardin and Schmidt (2003) speculate that much of this difference may be the result of the presence of many HVC_X neurons in their recordings. They thought it unlikely that HVC_{RA} neurons were contributing because previous work had established that RA neurons themselves, which receive auditory input directly from HVC during anesthesia (Doupe and Konishi, 1991), did not show auditory responses during wakefulness (Dave et al., 1998). Subsequent work has validated that HVC_{RA} neurons in several oscine species do not show passive auditory responses during wakefulness (Prather and Mooney, 2008, 2009). However, recordings from HVC_X neurons in the Prather and Mooney studies suggest that

it is also unlikely that the presence of this class of neuron confers the non-selective, variable response strength properties seen by Cardin and Schmidt. Prather and Mooney found HVC_X responses that were sparse (only a few spikes per song feature), highly phasically precise from trial to trial, and highly BOS-selective (though CON elements bearing extremely high resemblance to BOS elements can receive a response) (Prather and Mooney, 2008, 2009). Intriguingly, these HVC_X responses show the remarkable quality of being highly temporally congruent with song premotor activity recorded in the same basal ganglia-projecting neuron. I will discuss the potential functional significance of this sensory-motor congruence in **Section 3**, which concerns the relation between auditory responses in HVC and perception.

Because neither the properties of HVC_{RA} nor HVC_X neurons appear to explain the difference between the Rauske et al. and Cardin and Schmidt results, it seems likely that the non-selective, response strength-variable responses seen by Cardin and Schmidt were mostly due to recordings of HVC_{IN} subtypes not easily recorded from with relatively high impedance electrodes. It is also worth mentioning that the Rauske et al. study was carried out with a manual drive technology that required frequent interruption of ongoing behavior and no doubt involved stress to birds. While the fixed wire technology used in the Cardin and Schmidt studies precluded electrode movement and single unit isolation, it is possible that birds entered awake behavioral sub-states not attained in the Rauske et al study. In the work described in **Chapter 2**, I recorded from a much larger set of putative single neurons than Rauske et al., and with a remotely controlled microdrive requiring as little manipulation of birds as the fixed wire technology. Thus, if the difference between

the results seen by Cardin and Schmidt and Rauske et al. are partially the result of behavioral variables and/or sampling biases, the recording practices give promise a possible reconciliation of these somewhat conflicting studies.

Section 3: Evidence for a Role for HVC and Associated Song Nuclei in Species-Relevant Perceptual Tasks

Songbirds are not alone in showing sensory responses to passively presented stimuli in high-order cerebral areas associated with motor output. So-called mirror neurons, which are active during both engagement in and observation of goal-oriented mouth and hand movements, have been documented in premotor area F5 (Gallese et al., 1996), primary motor cortical area M1 (Tkach et al., 2007), and inferior parietal cortex (Fogassi et al., 2005) of non-human primates. Their existence in human analogues to these areas, while not documented by electrophysiology, has been inferred by transcranial stimulation (Fadiga et al., 1995; Cattaneo et al., 2009) and functional imaging (Buccino et al., 2004) studies. It has been proposed that mirror neurons underlie something called 'action understanding' (Rizzolatti et al., 2001; Rizzolatti and Craighero, 2004). This term, though inconsistently and somewhat vaguely defined across the literature, can be taken to mean that the basis for interpretation of the goal-directed motor gestures of others lies in one's own motor circuitry for production of similar behaviors. Thus far, however, there is no evidence that mirror neurons serve any role in perception (Hickok, 2009; Lingnau et al., 2009), to say nothing of functional role facilitated by a shared neural code for production and perception.

Unlike mammalian cortical areas containing mirror neurons, HVC has been shown to be necessary for perceptual discriminations involving song stimuli (Brenowitz, 1991; del Negro et al., 1998; Gentner et al., 2000; Halle et al., 2000). In one operant conditioning study in adult male starlings, it was shown that HVC-lesioned birds maintain discriminations between CON stimuli on which they were trained pre-lesion, but they were impaired in their ability to appropriately respond to contingency flips involving these stimuli post-lesion (Gentner et al., 2000). It is not known whether the same is true for discriminations involving the songs of heterospecifics or those from the bird's own repertoire (starlings have large and complex vocal repertoires, unlike zebra finches). HVC lesions also have profound effects on perceptual discriminations in non-singing female birds. Female canaries with bilateral (Brenowitz, 1991; Halle et al., 2002) (but not unilateral) HVC lesions give copulation solicitation displays to both heterospecific and conspecific songs, while control females solicit only to conspecific songs. In addition, even when just considering CON song, females with bilateral HVC lesions display relatively more to stimuli eliciting only very weak responses in intact females (Del Negro et al., 1998).

Lesions to areas of the song system receiving auditory input from HVC also result in impaired performance in perceptual discrimination tasks. Bilateral lesions of Area X and LMAN, two areas of a thalamocortical basal ganglia pathway crucial for normal song learning (Sohrabji et al., 1990; Scharff and Nottebohm, 1991) that receive auditory input from HVC (Doupe and Konishi, 1991; Roy and Mooney, 2009; see **Figure 1.1**), result in significant impairments in the learning of discriminations between BOS and CON stimuli

but not between pairs of CON or heterospecific stimuli (Scharff et al., 1998). Interestingly, this specific type of perceptual deficit may align well with the previously mentioned concept of 'action understanding' from the mammalian mirror neuron literature. Basal ganglia-projecting HVC neurons (HVC_X neurons) exhibit phasic responses to passively presented auditory stimuli during wakefulness that show precise temporal alignment with their own song premotor spiking activity (Prather et al., 2008, 2009). A similar phenomenon may exist in the other class of HVC neurons showing awake auditory responses (HVC_{IN}) , though the relative trial to trial imprecision during song production of these neurons (Hahnloser et al., 2002) may make it difficult to verify this. The extreme sensory-motor temporal congruence shown by HVC_X neurons is far greater than any seen in macaque mirror neurons and suggests that at least one type of response to BOS may be encoded in the language of the motor code. Thus, circuits encoding both production and perception of BOS stimuli may underlie a deeply innate and literal form of 'action understanding' of other song stimuli, and the impairment of these circuits may result in the perceptual deficits seen following lesions to Area X and LMAN. As mentioned previously, it is unknown whether lesions to HVC itself result in discrimination deficits between BOS and CON stimuli, but it seems likely to be so given the reliance of Area X and LMAN on HVC for auditory input, as well as HVC's involvement in discriminations between CON stimuli.

Perceptual discrimination deficits following lesions to areas receiving auditory input from HVC area not restricted to song stimuli alone. RA, the primary target of HVC in the vocal motor pathway (see **Figure 1.1**), receives auditory drive directly from HVC (Doupe

and Konishi, 1991). As with lesions to HVC, lesions to RA result in profound disruption of the production of song (Nottebohm et al., 1976; Simpson and Vicario, 1990; Ashmore et al., 2008) and learned call (Simpson and Vicario, 1990; Vicario et al., 2001) vocalizations. Along with these production deficits, RA lesions cause male birds to shows patterns of response to the contact calls of other birds that bear a strong resemblance to patterns shown by intact female birds (Vicario et al., 2001). Interestingly, RA lesioned males maintain an ability to demonstrate the intact male preference for the features of female distance calls, but they exhibit that preference post-lesion via the duration of their response calls, as do intact females, and not through the number of response calls, as intact males do. This result, while suggestive of a deep connection between mechanisms of perception and production, also highlights the difficulty in delineating between true perceptual deficits and those that fall more in to the domain of sensorimotor transformation. Likewise, for example, the previously described copulation solicitation displays shown by HVC lesioned female canaries to hetereospecific song may be the result of behavioral disinhibition despite intact abilities to distinguish between salient and non-salient stimuli somewhere in the circuits underlying decision making based on perceptual cues. Only with multiple behavioral readouts can the process of disambiguation between perceptual and transformative deficits begin to be gleaned.

Section 4: Known and Possible Sources of Auditory Input to HVC

HVC has been verified via anatomical and functional studies to receive auditory input from two cerebral areas; the nucleus interface of the nidopallium (NIf) and the caudal mesopallium (CM) (see **Figure 1.1**) (Bauer et al., 2008; Cardin et al., 2005; Vates et al.,

1996). Both NIf and CM receive their auditory input from primary auditory forebrain areas (Vates et al., 1996). In NIf, a structure which also shows song premotor activity (Cardin and Schmidt., 2005), auditory responses during anesthesia (Janata and Margoliash, 1999) and sedation (Cardin and Schmidt, 2004a) are highly selective for BOS as compared to REV and CON stimuli. Likewise, responses in the ventromedial portion of CM (CMM) are also highly selective for BOS over other complex stimuli (Bauer et al., 2008). Interestingly, both areas show state-dependent shifts away from extreme BOS selectivity during wakefulness. In NIf, there have been no single unit studies of auditory responses during wakefulness, though a multiunit study demonstrated a lack of BOS-selectivity relative to REV (Cardin and Schmidt, 2004a). In a study of a small number of single neurons during wakefulness in CMM, most cells showed no selectivity for BOS over CON and REV stimuli (Bauer et al., 2008).

The state dependent responses seen in the two areas known to project to HVC are interesting because, as described in **Section 2**, **Part 2** this same phenomenon has also been seen in multiunit recordings in HVC (Cardin and Schmidt, 2003). Nonetheless, as also discussed in **Section 2**, **Part 2**, other studies have, in contrast, seen a predominance of BOS-selective responses in HVC during wakefulness, though with decreased response strength relative to that seen in non-waking states (Rauske et al., 2003; Nealen and Schmidt, 2006). Because neurons in CM and NIf appear to not exhibit BOS-selective auditory activity during wakefulness, it is uncertain where BOS selective auditory responses in HVC during wakefulness arise from. One possibility is that some of this selectivity during wakefulness may arise from intrinsic network dynamics within HVC as

has previously been proposed in anesthetized birds (Coleman and Mooney, 2004). It is also possible that the limited sampling of units in CM during wakefulness and the lack of single unit resolution in the NIf study during wakefulness prevented detection of BOS-selective units.

There are at least several other candidate structures that may provide auditory input to HVC, possibly in a state-dependant fashion. Though anatomical studies have hinted at an anatomical connection between Field L and HVC via a region known as the HVC shelf (Fortune and Margoliash, 1995; Katz and Gurney, 1981), conclusive proof has lacked in this regard. However, a recent study in anesthetized birds has demonstrated functional connectivity between Field L and HVC with Field L with a range of Field L lead times (.5 to 15ms) suggestive of both monosynaptic and polysynaptic connectivity (Shaevitz and Theunissen, 2007). This same study also found that the lateral portion of the secondary-auditory cortical analogue CM (CLM) had similar connectivity patterns with HVC. Though the authors failed to demonstrate functional connectivity between these areas and HVC during auditory presentation, this failure may be a function of the presence of anesthesia. Both Field L and CLM neurons demonstrate a preference for song stimuli over other complex stimuli during anesthesia, but do not display a preference for BOS over other song stimuli (Amin, 2004; Grace et al., 2003; Lewicki and Arthur, 1996). Thus, these areas may mediate non-BOS selective auditory responses reported at the multiunit level previously and in many individual HVC_{IN} I record from in the work described in **Chapter 2** of this thesis. Another candidate for mediation of auditory responses to HVC during wakefulness is nucleus uvaeformus (Uva), a thalamic nucleus

that receives input directly from the ventral lateral lemniscus (LLV) and that sends a robust projection to HVC (Coleman et al., 2007). During anesthesia, neurons in Uva show a mix of BOS selective and non-BOS selective auditory responses. Though it does not appear that Uva sends auditory inputs to HVC during non-waking states (Coleman et al., 2007; Hahnloser et al., 2008), functional auditory connectivity between these areas during wakefulness is completely unexplored.

Section 5: Activity in HVC and RA During Sleep

Part 1: Auditory activity in HVC during sleep

Perhaps as a reaction to the dogma that the rise of thalamocortical burst activity during sleep creates a situation where cortical areas become profoundly isolated from the sensory world and are driven entirely by intrinsic patterns of activity (McCormick DA, 1989; Steriade, 2000), very few studies in any modality or system have evaluated the sensory properties of neurons during sleep. While the truth of such dogma may vary from modality to modality or even between different cortical layers (Livingstone and Hubel, 1981), multiple studies have shown that in the auditory system there is a high degree of diversity on a cell by cell basis in terms of response strength during sleep relative to wakefulness (Edeline et al., 2001; Issa and Wang, 2008; Pena et al., 1999). Recent work has demonstrated that parts of the songbird cerebrum, such as the ectrostriatum (Szymczak et al., 1996) and the visual cortex analogue Wulst (Low et al., 2008) show electroencephalographic (EEG) hallmarks similar to those seen in mammals, including alternation between REM and slow-wave sleep states.

While the non-laminar nature of song system nuclei makes it uncertain that these structures 'cycle' through sleep states in synchrony with the laminar areas, it is clear that song system neurons are highly sensitive to thalamic state much as cortical neurons are in mammals. A shift from a tonic, single spike mode to a low frequency bursting state in the thalamic relay nucleus Uva (see **Figure 1.1**) has previously been associated with increased vigor in BOS responses in putative HVC_{IN} (Coleman et al., 2007; Hahnloser et al., 2008). However, it is critical to note that when such a state is induced via electrical stimulation in the thalamus during anesthesia (Coleman et al., 2007) or during melatonin induced sleep in a head-fixed preparation (Hahnloser et al., 2008), the underlying thalamocortical network dynamics are likely to be much different than during naturally occurring sleep. Support for this notion comes from the fact that it has previously been found that response dynamics in a (very small; n =10 cells) population of single putative HVC_{IN} (Rauske et al., 2003) show a wide range of response strength changes across the wake sleep boundary. While most neurons in the Rauske et al. study did show at least some degree of response strength decrement during sleep relative to wakefulness, another study (Cardin and Schmidt, 2003) found no significant response strength change across the wake-sleep boundary at the multiunit level. This is in contrast to the large increase in response strength seen during the transition between wakefulness and sedation (Cardin and Schmidt, 2003; see **Section 2, Part 3**), and this discrepancy serves to highlight the caveats of extrapolating results from experiments carried out under sedation and anesthesia to those carried out during sleep. See **Chapter 3**, **Section 2** for preliminary evidence from a large collection of putative HVC_{IN} suggesting that response strength across the wake-sleep boundary does indeed vary on a cell by cell basis, and that

response strength changes to BOS may be at least partially independent of changes in response to CON stimuli.

Part 2: Spontaneous activity during sleep may be a key component of 'offline' song learning

The discovery of error sensitive cells in the ascending auditory pathway, as I discuss in **Section 2**, **Part 1,** may provide an answer to the question of where a record of ongoing auditory feedback is registered even as the song circuitry moves forward in time during song production. If it is true that comparison between motor 'expectancy' and reafferent sensory signals takes place outside of the song system proper, this raises the questions of when and how these comparisons are used to update the motor program. Previous work has established that sleep is critical for song learning in juvenile birds; improvements in performance do not occur unless a bird is allowed, in sequence, access to a tutor and autogenous feedback, and then a session of night sleep (Deregnaucourt et al., 2005; Shank and Margoliash, 2009). Thus sleep may serve a consolidating role in song learning analogous to that hypothesized in hippocampal-dependant memory consolidation in mammals (Gais et al., 2002; Marshall and Born, 2007; Ego-Stengel and Wilson, 2009).

One highly striking commonality between hippocampus in mammals and the song system in birds is the existence of spontaneous 'replay' of patterns of activity that were demonstrated during the previous day by the same cells during active task engagement. Just as rat hippocampal cells show spontaneous reinduction of patterns shown in spatial navigation tasks during the previous waking session (Kudrimoti et al., 1999; Nadasdy et

al., 1999), neurons in the song system area RA (see **Figure 1.1**) show patterns of activity during sleep which are (sometimes) temporally congruent with activity demonstrated by the same cells during motor production. While conclusive proof that such activity is critical for learning and maintenance of stable song production is still pending, the onset of such activity is delayed during song development if birds are not allowed access to both a song tutor and autogenous sensory feedback (Shank and Margoliash, 2009). When birds are allowed access to these two sources of auditory input in real time, spontaneous burst structure appears in RA the very next night and song structure begins to move toward tutor song the following day. Because real-time feedback evaluation during song production may occur outside of the song system proper, replay activity in song system neurons may reflect a process critical for song learning and maintenance during which instructive signals are integrated with the current motor program. Many future challenges exist in this line of research, including defining what sleep stages and song system cell types replay occur in, as well as identification of the detailed nature of signals entering the song system during sleep and their specific origin. Furthermore, at least some forms of song updating in the face of feedback perturbation in adult birds appear to occur without an intervening sleep session (Andalman and Fee, 2009; Sober and Brainard, 2009). How these forms of learning differ both mechanistically and in an abstract sense from sleep-dependant forms of learning will sharpen theories about sleep's role in the process of memory consolidation.

Part 3. Do Auditory Responses in song nuclei during sleep provide insight in to motor processing?

In RA, in contrast to HVC, it appears that most or all (putative projection) neurons show no auditory responses during wakefulness, but show vigorous responses to BOS during sleep (Dave and Margoliash, 1998, 2000). As mentioned in the previous section, many of these neurons show temporal congruence between premotor activity and some spontaneous bursts during sleep (Dave and Margoliash, 1998, 2000). Intriguingly, sleep BOS responses in these neurons, in turn, can show strong temporal congruence with both song premotor and sleep spontaneous activity. These auditory responses also show 'predictive' properties (similar to neurons in the ascending auditory system during singing described in **Section 2, Part 1**) in that auditory spikes lag premotor spikes by far less than they should if one adds the premotor lag time of the neuron with the expected delay in an auditory signal returning many synapses to RA. Furthermore, deletion of individual syllables has consequences for auditory responses several elements 'downstream', indicating that responses integrate and encode both local features inherent to an individual element and an expectation of the properties of features to come.

My working hypothesis is that predictive auditory responses in RA during sleep are a proxy for the types of motor program updating and maintenance tasks carried out during spontaneous activity epochs during sleep. Though the RA auditory responses that have been demonstrated during anesthesia and sleep are believed to be mediated solely via HVC (Doupe and Konishi, 1991), no HVC neurons of any of the three classes have been evaluated in terms of the relationships between premotor activity, spontaneous sleep activity, and sleep auditory activity (but see discussion in **Section 2, Part 2** of mirror properties in HVC_X neurons during wakefulness). Unfortunately, unlike RA neurons,

HVC neurons (especially projection neurons) are extremely difficult to hold for the long periods of time necessary to evaluate cross-state activity.

Figure Legends

Figure 1.1. An 'HVC-centric' schematic of auditory and song production circuitry. Caudal mesopallium (CM) and the nucleus interface of the nidopallium (NIf) are the only two structures (red outlines and solid red arrows) known to provide direct auditory input to HVC. Other potential auditory afferents to HVC (dashed red arrows) include the Field L complex and nucleus uveaformis of the thalamus (Uva). HVC projects to RA in the primary motor output axis and to the avian basal ganglia (area X) in a basal ganglia-thalamocortical pathway that is essential for song learning and adult song plasticity, but that only makes subtle contributions to normal adult song production. Reafferent feedback connections (not shown) arising from RA and the VRN make their way back to HVC via the thalamus and may influence ongoing song production. LLV, ventral lateral lemniscus; MLd, mesencephalicus lateralis dorsalis; Ov, nucleus ovoidalis of the thalamus; NCM, nidopallium caudal medial. HVC projects in the vocal-motor stream in two distinct pathways via the dorsal and ventral aspects of the robust nucleus of the arocpallium (dRA and vRA, respectively). $nXII_{ts}$, tracheosyringial portion of the hypoglossal nucleus; VRN; ventral respiratory nuclei.

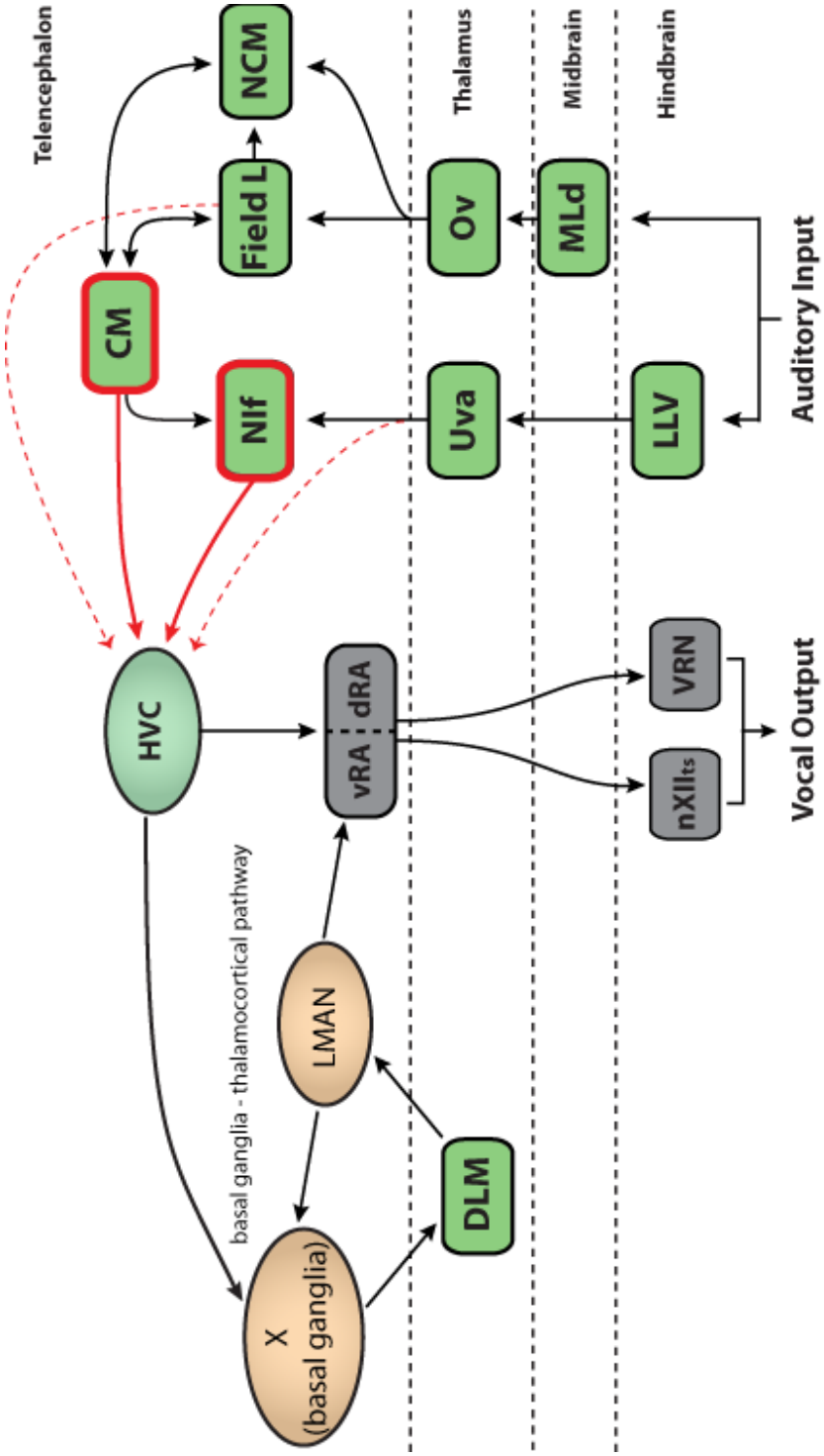
Telencephalon
Thalamus
Midbrain
Hindbrain
NCM
Field L
CM
NIf
Ov
Uva
MLd
LLV
Auditory Input
HVC
vRA
dRA
VRN
nXIIts
Vocal Output
basal ganglia - thalamocortical pathway
LMAN
DLM
X
(basal ganglia)

Figure 1.1

Chapter 2. Linear and Nonlinear Auditory Response Properties of Interneurons in a High Order Avian Vocal Motor Nucleus During Wakefulness

ABSTRACT

Motor-related forebrain areas in higher vertebrates also show responses to passively presented sensory stimuli. Sensory tuning properties in these areas, especially during wakefulness, and their relation to perception, however, are poorly understood. In the avian song system, HVC (proper name) is a vocal-motor structure with auditory responses well defined under anesthesia but poorly characterized during wakefulness. We used a large set of song stimuli including the bird's own song (BOS) and many conspecific stimuli (CON) to characterize auditory tuning properties in putative interneurons (HVC_{IN}) during wakefulness. Our findings suggest that HVC contains a heterogeneity of response types; a third of neurons are either suppressed or show no response to any stimuli and two thirds show excitatory responses to one or more stimuli. A subset of excitatory neurons are tuned exclusively to BOS and show very low linearity as measured by spectrotemporal receptive field analysis (STRF), but many respond well to both BOS and CON stimuli and show response linearity comparable to that previously measured in structures of the ascending auditory pathway. Fourier analysis of the STRFs of linear HVC_{IN} reveals a range of peak spectrotemporal tuning properties, with approximately half of these neurons showing peak sensitivity to modulations occurring with high power in zebra finch song. Previous work has established that HVC lesioned birds are impaired in operant contingency reversals involving CON stimuli and birds with lesions to song nuclei receiving auditory input from HVC are impaired in discriminations

between BOS and CON stimuli. The findings of the present study are consistent with these results and suggest a possible role for HVC in species-relevant auditory tasks.

INTRODUCTION

High order motor areas in humans (Fadiga et al., 2005; Iacobini et al., 2005) and non-human primates (Gallese et al., 1996; Tkach, 2007) show sensory responses during wakefulness. While it has been proposed that such responses facilitate self-referential understanding of the goal-directed motor actions of others (Rizzolatti et al., 2001), no functional evidence exists in support of this notion (Hickock, 2009). The forebrain nucleus HVC forms part of a dedicated neural circuit for vocal production in songbirds (Ashmore et al., 2005; Hahnloser et al., 2002). In addition to its role in motor production, HVC also exhibits auditory responses during wakefulness (Cardin and Schmidt, 2003; Rauske et al., 2003, Sakata and Brainard, 2008). Lesions to HVC in adult male birds, along with disrupting song production (Nottebohm et al., 1976; Thompson et al., 2007a,b), are also associated with perceptual and/or sensorimotor deficits. In adult male starlings, HVC lesions cause deficits in contingency reversals between previously discriminated conspecific (CON) stimuli in an operant task (Gentner et al., 2000). In non-singing female canaries, HVC lesions cause an inability to restrict copulation solicitation displays to conspecifics as compared to hetereospecifics (Brenowitz, 1991; del Negro, 1998; Halle et al., 2002). Lesions to nuclei implicated in song production receiving auditory input from HVC (Doupe and Konishi, 1991) also result in deficits in perceptual and sensorimotor tasks. Destruction of the robust nucleus of the arcopallium (RA), the immediate afferent of HVC in the vocal motor pathway, leads to alteration of the normal

pattern of call responses to male and female contact calls, while lesions of the anterior forebrain structures Area X and the lateral anterior nucleus of the nidopallium (LMAN) result in deficits of discrimination between CON and bird's own song (BOS) stimuli (Scharff et al., 1998). Because auditory processing and perceptual function are co-localized in discrete structures, and disruption of these structures results in deficits in perceptual and sensorimotor tasks, the song system is ideally suited for the study of the specific nature and influence of sensory signals in motor systems.

HVC receives auditory input from two high-order forebrain sources, the caudal mesopallium (CM) and the nucleus interface of the nidopallium (NIf) (Bauer et al., 2008; Cardin et al., 2005; Vates et al., 1996). CM receives auditory input both directly and indirectly from the avian primary auditory cortical analog Field L (Vates et al., 1996), and limited studies of single units during wakefulness suggests a mix of broadly responsive cells, some with modest selectivity for BOS relative to other complex stimuli and others with no BOS selectivity (Bauer et al., 2008). NIf receives auditory input from CM (Vates et al., 1996) and multiunit recordings suggest a lack of selectivity for BOS during wakefulness (Cardin and Schmidt, 2004b). The vast majority of studies in HVC during non-waking states have found reliably present auditory responses highly selective for BOS (Cardin and Schmidt, 2003; Margoliash, 1986; Mooney, 2000; Rauske et al. 2003). During wakefulness, however, some studies across multiple species have found responses that are highly selective for BOS over other complex stimuli (Margoliash and Konishi, 1985; Prather and Mooney, 2008, 2009; Rauske et al., 2003; Sakata and Brainard, 2008), while others have found responses that, though not always present

(Konishi and Schmidt, 1998; Nick and Konishi, 2001), are completely non-selective for BOS (Cardin and Schmidt 2003, 2004b). Factors including extremely limited stimulus sets, response analyses restricted to firing rate metrics, and, with only a few exceptions (Bauer et al., 2008; Prather and Mooney, 2008, 2009), a lack of non-behaviorally disruptive single unit recording techniques has hindered a detailed understanding of awake auditory response properties in both HVC and its known auditory afferents.

Here, we probed the auditory properties of a large population (n = 215 neurons, 17 birds) of putative HVC interneurons (HVC_{IN}) with a large set of CON and BOS stimuli in freely moving, non-behaviorally disrupted adult male zebra finches during wakefulness. Interneurons precisely shape the output of projection neurons in a multitude of systems (Ferster and Miller, 2000; Merchant et al., 2008, Murayama et al., 2009; Spiro et al., 1999). In HVC, interneurons reciprocally interact with neurons projecting to the robust nucleus of the arcopallium (RA) in the primary song production axis as well as with those projecting to the avian basal ganglia (Area X) (Mooney and Prather, 2005). The extremely large population of single units and expansive stimulus set allow the most thorough assay of BOS-selectivity and multiple other basic response features yet carried out in any neural population in the song system during wakefulness. We also quantify linear receptive field properties of single song system neurons for the first time during wakefulness, with the goal of evaluating whether HVC_{IN} are sensitive to features likely to be of use during song-specific perceptual discriminations. To this end, we employ spectrotemporal receptive field (STRF) analysis, a method that has proven successful in capturing linear receptive field features in the ascending auditory pathway (Gill et al.,

2006,2008; Graña et al., 2009; Sen et al., 2001; Theunissen et al., 2000; Woolley et al., 2006,2009).

MATERIALS AND METHODS

Animals. Experimental subjects were adult male zebra finches (Taeniopygia guttata) obtained from a local supplier (Canary Bird Farm; Old Bridge, NJ). All birds were at least 120 days of age at the time of experimentation. Birds were fed ad libitum and kept on a 12:12 light dark cycle in a colony room until several days before implantation of a chronic recording device (see below for details). All procedures documented here were approved by an Institutional Animal Care and Use Committee at the University of Pennsylvania.

Sound recording and presentation. For several days before surgery, the songs of birds were continuously recorded with high quality microphones (Earthworks SRO; NH, USA) in a sound attenuation chamber (Acoustic Systems, Austin, TX) using custom software (Sound Analysis Pro, D. Swigger and O. Tchernichovski). Songs were recorded at a sampling rate of 44.1 kHz and played back at 20 kHz with a peak intensity level of 70 db SPL. A stimulus set consisting of 2-3 motifs of one song from each of ten to twelve (CON) birds, along with a recent version of the bird's own song (BOS), was presented for each site with at least one well isolated neuron. All CON stimuli were unfamiliar to the subject bird previous to the onset of the experiment. Because of concerns related to the challenge of holding single unit recordings in awake birds, our stimulus set was

smaller than that typically used in anesthetized experiments involving spectrotemporal receptive field analysis (STRF) (Theunissen et al., 2000; Woolley et al.,2006) . However, stimuli were chosen such that the range of the spectral and temporal modulations inherent to zebra finch song was well represented (Woolley et al., 2005). To demonstrate the relative spectral and temporal modulation power inherent to our song ensemble, we show a modulation power spectrum (MPS)(**Fig. 2.1D**). This MPS was obtained by first decomposing twelve of the CON songs used in the experiment (not all birds heard the same set of songs) in to their ripple components, which are essentially the acoustic analogue of visual gratings. The power density of each ripple component was then estimated and plotted on a 2-D Cartesian grid (Singh and Theunissen 2003; Theunissen et al., 2004). When recordings were stable, we presented up to 50 repetitions of each stimulus in the ensemble, which guaranteed a robust data set for STRF estimation (Theunissen et al., 2000). Stimuli were presented in pseudorandom order with a random interstimulus interval between 10 and 20 s.

Chronic Recordings. Detailed description of chronic recording device implantation has been previously described (Nealen and Schmidt, 2006). Briefly, birds had food and water removed for 1h before an acute preparatory surgery. They were administered an intramuscular injection of a ketamine (35mg/Kg) /xylazine (7 mg/kg) mixture and placed in a stereotaxic apparatus. Before scalp incision, feathers were removed and a topical anesthetic (1% lidocaine, Copley Pharmaceutical, Canton, MA) was applied along the midline incision site. The scalp was retracted and a custom built (Fred Letterio, INS Machine Shop, U. Pennsylvania), remotely controllable microdrive was implanted on the

skull such that 1-3 tungsten microelectrodes (2-4 MΩ, FHC, Bowdoinham, ME) rested just above the stereotaxic coordinates for HVC. Differential recordings were made between these leads and either a custom ground electrode implanted just outside of HVC (FHC, Bowdoinham, ME) or a silver ground wire implanted between the lower skull layer and the dura. To ensure that the ground wire did not dry out, a mixture of equal parts mineral oil and paraffin was applied. This mixture was also placed in the craniotomy above HVC to prevent the exposed surface of the brain from drying out. Recording locations were verified using multiple methods. These included 1) the presence of characteristic burst activity during initial drive implantation under anesthesia 2) the presence of premotor activity during chronic recording sessions and 3) histological verification of electrode track location and extent within the cresyl violet defined boundaries of HVC (Cardin and Schmidt, 2003).

Immediately following implant surgery, birds were placed on a tether and habituated to the chronic recording apparatus and sound attenuation chamber for 24-48 hrs. Once birds were fully recovered and displayed normal feeding, perching, and vocal behaviors, chronic recordings were initiated. Electrodes were moved remotely with micron resolution using customized hardware and software (RP Metrix, Princeton, NJ). Neurons were not selected based on response to auditory search stimuli, thus reducing bias in terms of response tendencies and potentially allowing for highly heterogeneous sampling (see Results and Discussion). Online unit isolation was achieved using a sound monitor (Grass Telefactor, West Warwick, RI) and oscilloscope mode of custom neural acquisition software (A. Leonardo, Caltech). Further assessment of unit isolation was

performed offline using a template and PCA-based spike sorting algorithm. Spontaneous and auditory evoked neural signals were amplified 100x (custom built headstage) and band-pass filtered between 300 and 5000 Hz (Brownlee 440 Amplifier, Brownlee Precision, San Jose, CA). Signals were then acquired at a sample rate of 25 kHz via the same custom neural acquisition software used for initial unit verification. Auditory presentation always occurred with the cage lights on. A camera was used to verify that birds were awake and active during auditory presentation. Trials were discarded if any of these criteria were met- (1) birds closed their eyes for more than 2s, (2) birds were not in an upright position and assumed one of several characteristic sleep postures (Low et al., 2008) and (3) vocalized within 5 s of an auditory presentation. These criteria are very similar to those previously employed in chronic auditory recording experiments during wakefulness (Cardin and Schmidt, 2003).

Data Analysis

Characterization of single HVC_{IN}. Clustering-based spike sorting was carried out in the Spike 2 programming environment (version 6, CED, Cambridge, UK). Clusters were visually inspected in PCA space, and cluster borders were manually delimited (see **Fig. 2.1S** for example waveform and interspike interval histogram). For each site, clustering was done on a per stimulus basis, with all trials for a given stimulus concatenated in a manner that conserved relative, but not absolute time (see earlier description of pseudorandom presentation). This method, in theory, could lead to different principal components being selected for different stimuli, though spaces were qualitatively identical across stimuli and waveform shape was verified to be identical for a given

cluster across all stimuli. We frequently isolated more than one unit from a given electrode, though we always aimed for one large amplitude waveform per site (**Fig. 2.1A**).

To verify that each cell was an HVC_{IN} we measured the width of the largest positive going spike peak of each isolated waveform at 25% of peak amplitude (**Fig. 2.1B**). Previous work has shown that widths below .35ms were previously uniformly associated with a lack of antidromic activation from the two afferent targets of HVC, Area X and RA (Rauske et al., 2003) (**Fig. 2.1C**). We only accepted neurons with action potential widths that were < 0.35 ms (in practice all were below .3 ms). While electrode impedance can theoretically influence waveform shape, it should be noted that waveform classifications based on the described spike-width parameter were consistent between very low impedance glass- coated metal electrodes (< 1M MΩ) and higher impedance (up to 5 MΩ) glass electrodes (Rauske et al., 2003). Furthermore, HVC_{RA} neurons, the only other class with waveforms relatively close in width to HVC_{IN}, are extremely hard to isolate without antidromic stimultation because of their extremely small size and complete lack of spontaneous activity during wakefulness (Rauske et al., 2003; Fee et al., 2004). HVC_{RA} neurons also do not show auditory responses during wakefulness in several songbird species (Prather et al., 2008, 2009).

Basic auditory response characterization. Spike times were passed back to MATLAB for basic statistical characterization of auditory responsiveness. These methods were previously used to characterize multiunit auditory responses in HVC (Cardin and Schmidt, 2004b). Briefly, on a per stimulus basis, single auditory trial firing rate (FR)

was calculated for two second stretches of immediate pre-stimulus baseline (FR_{BASE}) and stimulus period (FR_{STIM}). We defined whether the response to a given stimulus was significant based on an unpaired t-test (Cardin and Schmidt, 2004b) between FR_{BASE} and FR_{STIM} measurements across all trials. The unpaired test assumes independence of activity during pre-stimulus and stimulus periods and is more conservative than the paired test, though the paired test yields extremely similar results in this particular comparison. For all cells showing a significant response ($p<.01$) to at least one stimulus, we calculated change in mean firing rate (spikes/s) between the pre-stimulus and stimulus periods as defined above. This Response Strength (RS) metric was calculated on a trial by trial basis as $FR_{\mathrm{STIM}} - FR_{\mathrm{BASE}}$, then the average value across trials was taken as $\overline{RS}$ for a given stimulus.

While $\overline{RS}$ is informative in that it reports the raw change in spike rate for a given stimulus between baseline and stimulus periods, we also wanted to report a metric that normalized spike rate in a way that facilitated comparison across cells with different baseline and peak firing rates. The metric we used for this purpose, $\mathrm{RS_{INDEX}}$ was calculated as follows:

$$\mathrm{RS_{INDEX}} = (\overline{FR}_{\mathrm{STIM}} - \overline{FR}_{\mathrm{BASE}})/(\overline{FR}_{\mathrm{STIM}} + \overline{FR}_{\mathrm{BASE}})$$

The advantage of $\mathrm{RS_{INDEX}}$ is that it restricts the dynamic range of response to between -1 and 1 for all cells. An $\mathrm{RS_{INDEX}}$ of 0 indicates no difference in firing rate between pre-stimulus and stimulus periods. A positive $\mathrm{RS_{INDEX}}$ indicates an increase in firing rate during the stimulus period, and a negative $\mathrm{RS_{INDEX}}$ indicates a decrease in firing rate during the stimulus period. We report $\mathrm{RS_{INDEX}}$ for BOS as well as for CON stimuli.

Because many CON stimuli were presented to each cell (between ten and twelve), we represented response strength both for the stimulus that produced the strongest response (best-CON) as well as for the average response for all CON stimuli (mean-CON). The first metric, best-CON, is the response (RS_{INDEX}) for the CON stimulus that produces the strongest response. The second metric, mean-CON, is the average response across the entire set of CON stimuli. Because these measurements are computed differently, the standard error of the mean (SEM) for best- CON represents the variance across trials whereas SEM for mean-CON represents the variance across mean RS_{INDEX} values for each CON stimulus. Along with response strength metrics, we also calculated *d'* values to report selectivity in responsive cells for BOS relative to both the best CON response as well as the mean CON response (Green and Swets, 1966; Theunissen and Doupe, 1998). For each BOS-CON stimulus pair, *d'* was calculated as follows

$$d'_{\mathrm{BOS-CON}} = \frac{2(\overline{RS}_{\mathrm{BOS}} - \overline{RS}_{\mathrm{CON}})}{\sqrt{\sigma^2_{\mathrm{BOS}} + \sigma^2_{\mathrm{CON}}}}$$

Where σ^2_{BOS} and σ^2_{CON} are respectively the variance of RS_{BOS} and RS_{CON} across trials. In describing our findings, we divide responsive cells in to multiple categories and evaluate whether the mean of the *d'* distribution for cells within a given category differs significantly from zero ($H_0: \mu_0 = 0$) (Nealen and Schmidt, 2006). All statistical tests reported in the text were unpaired t-tests assuming equal variance (equality of variance previously verified) unless noted.

STRF Analysis

STRF generation and response prediction For the subset of cells showing significant excitatory responses to a least one auditory stimulus based on the response strength criteria described above, we generated spectrotemporal receptive fields (STRF) in the auditory domain (STRFPAK version 5.3, J. Gallant and F. Theunissen, http://strfpak.berkeley.edu). Briefly, STRF in the auditory domain is the optimal linear filter that transforms a representation of a time-varying stimulus in to a prediction of the firing rate as estimated by the PSTH of the neuron (Theunissen et al., 2000). Auditory STRF methodology is well described elsewhere (deCharms et al., 1998; Hsu et al., 2004b; Sen et al., 2001; Theunissen et al., 2000, 2004; Woolley et al., 2006, 2009). STRF generation, briefly, includes three steps: 1) generation of a spike-triggered average (STA) via cross-correlation between log spectrograms of sound (here CON song stimuli) and averaged time-varying spiking response 2) removal of stimulus autocorrelations from the STA, and 3) a regularization – cross validation step to effectively reduce the number of parameters used to estimate the STRF (i.e. to avoid over-fitting of the data). For the initial spectrographic representation of song, we chose spectral and temporal filter widths of 125 Hz (from 250 Hz to 8kHz, which is the audible range for zebra finch hearing) and 1.27ms, respectively, because these values have previously yielded good predictions in auditory midbrain and forebrain neurons of anesthetized birds (Singh and Theunissen, 2003; Woolley et al., 2006).

Validation of the STRF involves a jack-knife procedure wherein the model is tested on untouched data. One point with critical relevance to our analyses is that the jack-knife procedure used to generate predicted responses to individual stimuli always

leaves the specific stimulus being predicted on out of the STRF used for prediction of its response. Thus, though we use CON-derived STRFs to predict responses to BOS stimuli (see next section), this prediction is an equally valid and no more stringent a test of linearity than is using CON-derived STRF to predict response to a novel CON stimulus. The noise-corrected (Gill et al., 2006) mean correlation value between the predicted and actual PSTHs in response to the set of CON stimuli is the mean CC ratio, which we commonly refer to as response linearity. We also report non-noise corrected CC ratios (raw CC values) for evaluation of how well the STRF model predicts responses to novel CON and BOS stimuli (see next section). We chose a Hanning window width of 21ms for smoothing actual PSTHs, a value which has been used in previous studies with which we compare our results (Gill et al., 2006; Woolley et al., 2006).

To evaluate how well novel BOS responses were predicted by CON-derived STRF relative to novel CON responses, we calculated a Z-score metric for the raw CC value (BOS CC-Z) to indicate the number of standard deviations (i.e Z's) that separate the average CON raw CC value from the BOS raw CC value. This provides a normalized statistic to evaluate whether CON-derived STRF predict novel BOS responses as well as they predict novel CON responses across our population of recorded neurons. Negative values indicate BOS predictions that were lower than the average CON prediction, while positive values indicate BOS predictions that were higher than the average CON prediction.

$$\text{BOS CC} - \text{Z} = \frac{(\overline{\text{CON raw CC}} - \text{BOS raw CC})}{\sigma_{\text{CON raw CC}}}$$

Where CON and BOS raw CC are the raw cross- correlation values between predicted and actual PSTHs for individual stimuli and $\sigma_{\text{CON raw CC}}$ is the standard deviation of the individual CON raw CC values.

STRF Feature Extraction

STRF provides a powerful tool for measuring a host of temporal, spectral, and spectrotemporal receptive field features in response to complex stimuli (Theunissen et al., 2004). As detailed in the next few sections, we measured excitatory and inhibitory latencies, best inhibitory and excitatory frequencies, and temporal and spectral response bandwidths. In addition to these temporal and spectral parameters, we also measured joint spectrotemporal response properties, including best temporal and spectral modulation frequencies. We chose to measure spectral and temporal receptive field properties only from cells showing mean CC ratios that were greater than .3; which is slightly more conservative and less inclusive than a low-end linearity criterion previously used in the context of feature extraction in the auditory forebrain of anesthetized birds (Woolley et al., 2009). Overall, 49/82 cells showing significant responses to both BOS and CON stimuli reached this criterion, though we excluded nine cells from this analysis because the complexity of STRF shapes precluded measurement of one or more of the parameters described in detail below. All feature measurements we made from STRFs are represented in **Figures 2.8E and F**. Green areas on the STRF represent mean firing rate. Red and blue areas represent increases and decreases, respectively, in firing rate relative to the mean firing rate. Increasing color intensity indicates greater change in firing rate from baseline values.

Temporal feature extraction Excitatory and inhibitory latencies describe the amount of time between the presence of a stimulus feature (excitatory) or the absence of a stimulus feature (inhibitory) most reliably associated with a spike (Woolley et al., 2005). Excitatory latency was taken as the time of maximum amplitude in the STRF and, likewise, inhibitory latency was taken as the time of minimum amplitude in the STRF. Temporal bandwidth relates the temporal precision between the occurrences of specific frequencies and changes in firing rate. We defined temporal bandwidth as the full width at 50% peak amplitude of the peak excitatory and inhibitory regions in a 2-D temporal profile of the STRF at best frequency (Nagel and Doupe, 2008). When these regions did not overlap in time (as in **Fig. 2.8F**), this measurement reflected the time from the onset of the first peak component, be it excitation or inhibition, to the offset of the second component (Woolley et al., 2006). In the small subset of cells where there was partial temporal overlap between peak excitation and inhibition, the measurement reflected the time from onset of the first peak component to the offset of the second, minus the region of temporal overlap. Finally, because excitatory and inhibitory best frequencies were nearly always offset (as in **Fig. 2.8E**), temporal widths were measured separately for excitatory and inhibitory response components at their respective best frequencies (see next section for description of best frequency measurement).

Spectral feature extraction Excitatory and inhibitory best frequency describe the sound frequencies most likely to elicit a spike based on their presence (excitatory) or absence (inhibitory) prior to a spike. Excitatory best frequency was defined as the point of peak amplitude in a frequency profile of the STRF at the time of peak excitation. Inhibitory

best frequency was defined as the point of minimum amplitude in a frequency profile of the STRF at the time of peak inhibition. Spectral bandwidth defines the range of frequencies that are reliably associated with increases, in the case of excitation, or decreases, in the case of inhibition, of spike rate relative to mean firing rate. We measured spectral bandwidth separately for excitation and inhibition and defined it as the full width at half of peak amplitude in a frequency profile of the STRF at the time of peak excitation or inhibition, respectively (Nagel and Doupe, 2008; Sen et al., 2001).

Spectrotemporal feature extraction We carried out 2-D Fourier transform of the best STRF for linear neurons in order to obtain their modulation transfer functions (MTFs). MTFs show the range of temporal modulations, such as peaks and troughs in the song amplitude envelope (measured in Hz), and spectral modulations, such as harmonic elements (measured in cycles/kHz) to which neurons are sensitive (Theunissen et al., 2004). The temporal and spectral modulations corresponding to the peak amplitude of the MTF were defined as the best temporal and spectral modulation frequencies. MTFs are plotted on the same scale as the modulation power spectrum (MPS) of song (see above and **Figure 2.1D**), and can thus be used to evaluate whether the modulation power of a given neuron falls within the region well represented in the stimulus ensemble. Though spectral and temporal tuning properties can also be calculated fitting each best STRF with a product of Gabor functions (Qiu et al., 2003; Woolley et al., 2009), many of our STRFs violated separability requirements of this method. Nonetheless, estimates of temporal and spectral STRF parameters between the two methods are quite similar (Theunissen et al., 2004). From the MTF, we measured a symmetry index by dividing the modulation

spectrum in to left (M_{left}) and right (M_{right}) halves (Miller et al., 2002; Nagel and Doupe, 2008):

$$\frac{\sum M_{right} - \sum M_{left}}{\sum M_{right} + \sum M_{left}}$$

The symmetry index, as the RS_{INDEX} described above, ranges from -1 to 1. Large negative values indicate strong sensitivity to upwardly modulated frequency sweeps, while large positive values indicate strong sensitivity to downwardly modulated frequency sweeps.

RESULTS

HVC interneurons in awake birds show a hetereogeneity of auditory responses

The high degree of auditory selectivity to the bird's own song (BOS) and the virtual omnipresence of stereotyped auditory responses in the zebra finch song system during non-waking states is extremely well established (Margoliash, 1986 ; Mooney, 2000; Sutter and Margoliash, 1994). While it is also well established that auditory responses in the zebra finch are suppressed for some time upon arousal (Cardin and Schmidt, 2003; Nick and Konishi, 2001; Schmidt and Konishi, 1998), there are conflicting reports concerning the degree of BOS- selectivity, consistency and vigor of responses when present during wakefulness (Cardin and Schmidt, 2003; Rauske et al., 2003). Previous studies have been limited in terms of stimuli presented (usually just BOS and one or two other complex stimuli), small numbers of single units that, when present,

were usually recorded with techniques highly disruptive to ongoing behavior, and analysis of responses limited to spike-rate derived measures.

In an effort to provide a rigorous characterization of awake auditory response properties in zebra finch HVC at the single neuron level, we sampled from a large number of neurons (n = 215 single units in 17 birds) with a non-disruptive motorized microdrive and used a comprehensive stimulus set for each recorded neuron that consisted of 10-12 conspecific song (CON) stimuli and 1 BOS stimulus. Recordings in HVC focused entirely on responses in neurons that were defined as putative interneurons, a class of neuron well known to shape the output of projection neurons across many neural systems. All neurons in the present study had waveform widths at 25% peak amplitude that were smaller than 0.35 ms (.18 $\pm$ .001 ms) (**Fig. 2.1C**). Based on a previous study, this cutoff is sufficient to provide a clear separation from antidromically identified projection neurons, which have much wider waveforms (Rauske et al.,2003). **Figure 2.1C** shows the complete lack of overlap between the distribution of spike widths for the cells included in the present study and those obtained in the Rauske et al. study for both types of HVC projection neurons. From here forward, we refer to these neurons as HVC interneurons or HVC_{IN}.

We found that neurons could be classified into three broad classes based on their auditory responsiveness: (1) excitatory responses to one or more stimuli (n = 146 cells; 67.9% of total cells), (2) suppressive responses to one or more stimuli with no excitatory responses to any stimuli (n = 30 cells; 14% of total cells) and (3) no significant excitatory or inhibitory responses to any stimuli (n = 39 cells; 18.1% of total cells). BOS responses

of a representative cell from each of the three broad classes are shown in the top panel of **Figure 2.2**. The excitatory neuron (top right panel) was obtained simultaneously from the same electrode as the neuron showing the suppressive response (top left panel). It was not uncommon for us to simultaneously record cells from different classes at the same electrode site, highlighting the heterogeneity of auditory response types in HVC during wakefulness suggested in a previous study (Rauske et al., 2003). Additional examples of paired recordings highlighting simultaneous recordings of cells with particularly striking differences in response properties, are found in **Figures 2.2S** and **2.3S**. To quantify and compare response strengths in the population of HVC_{IN}, we calculated a normalized response strength, RS_{INDEX} , for each cell. Because all excitatory neurons responded to BOS but not necessarily to CON (see next section), we only plot the distribution of RS_{INDEX} in response to BOS. The wide distribution of BOS RS_{INDEX} values from moderately negative to highly positive reinforces the notion of a range of response types in our population of HVC_{IN} (**Fig. 2.2**, bottom panel). To test whether putative HVC_{IN} exhibiting these different response properties might be distinguished by other physiological attributes, we compared both action potential waveform as well as spontaneous activity across these different populations of neurons. No difference was observed for either spike waveform ($p>.05$, one-way ANOVA) or spontaneous activity ($p>.05$, one-way ANOVA). Thus, it appears that HVC_{IN} with similar spike morphology and baseline firing properties can respond differently to auditory stimuli.

Auditory properties of HVC_{IN} showing suppressive responses to auditory stimuli

While the remainder of this study focuses on the attributes of cells demonstrating excitatory responses to one or more BOS and CON stimuli, neurons with suppressive auditory responses merit a quantitative description of their properties in terms of possible biases in suppression for BOS over CON stimuli. In a previous study recording from a small number of auditory responsive HVC_{IN} (n= 21 cells), it was found that a subset of neurons (n = 4) showed suppressive auditory responses to song stimuli. A few of these cells showed less suppression to BOS than they did to CON stimuli or to BOS stimuli presented in reverse (Rauske et al., 2003). In the present study, neurons showing only suppressive responses to one or more stimuli (n =30 cells) tended to have RS_{INDEX} values that indicated less suppression to BOS $(-.2 \pm .03)$ than to CON stimuli (mean CON response: $-.28 \pm .03$; $p<.05$). Nonetheless, the *d'* value comparing the response to BOS and the mean CON response was low for these cells $(.14 \pm .09)$, indicating a lack of strong selectivity for BOS in this group of neurons. The suppressive example shown in **Figure 2.2** (top right panel) exemplifies this relative lack of selectivity (response to non-BOS stimuli not shown)..

Auditory properties of HVC_{IN} showing excitatory responses to auditory stimuli

The majority of HVC_{IN} (146/215) showed excitatory auditory responses to one or more stimuli. To test for the possible bias these neurons might have had for BOS, we presented each neuron with BOS as well as a large set of CON stimuli (n =10-12 stims) that well represented the richness (e.g the range of temporal and spectral modulations) inherent to zebra finch song (**Fig. 2.1D**; Woolley et al., 2005). We used this stimulus set to establish rigorous criteria for BOS selectivity and divided cells into those that showed

excitatory responses exclusively to BOS (BOS-ONLY cells) and those that showed excitatory responses to both BOS and CON stimuli (BOS-CON cells). Even with the extensive CON stimulus set, we observed a remarkably large number of BOS-ONLY cells (n = 64/146 excitatory cells). Multiple lines of evidence suggest that there were fundamental differences between the BOS-ONLY and BOS-CON cells at the population level. Firstly, BOS-CON cells (n = 82/146 excitatory cells) tended to show excitatory responses to many of the presented CON stimuli
($60 \pm .04$ percent of presented CON stims) (**Fig. 2.3A**) with a distribution mode of 100 percent of presented CON stims. The tendency to respond to many CON stimuli indicates that BOS-CON cells were quite different as a population than the BOS-ONLY cells, which by definition showed excitatory responses to not a single CON stimulus. Secondly, the strength of response to BOS, the one stimulus that both cell types responded to, was significantly greater in BOS-CON cells. **Figure 2.3B** shows the strong tendency for BOS RS (spikes/s above baseline) to be higher in BOS-CON cells (white bars; $6.69 \pm .66$ spikes/s) than in BOS-ONLY cells (black bars; $2.07 \pm .27$ spikes/s) ($p<.001$).

Characterization of auditory properties of BOS-ONLY Neurons

The typical response properties of BOS-ONLY cells are well represented by the example in **Figure 2.4**. This cell had relatively modest, phasic excitatory peaks in response to BOS ($RS_{INDEX} = .12$) that were reliably present from trial to trial at specific time points throughout the stimulus. These phasic excitatory peaks were sometimes followed by transient suppression below baseline levels, a common response property of

cells in this class. This example cell also clearly showed response peaks during the second and third motifs (M2 and M3 in the top panel of **Fig. 2.4**) that were larger than during the first motif (M1). This increase in response magnitude across motifs was a response feature that we sometimes observed in BOS-ONLY cells. In contrast to its response to BOS, this cell showed no response peaks to any of the representative CON. Rather, the cell showed a tendency toward weak suppression in response to CON stimuli (mean $RS_{INDEX} = -.05 \pm .02$), which is highly representative of responses to CON stimuli in BOS-ONLY cells (see **Fig. 2.3C**).

As described earlier, BOS-ONLY cells showed a relatively modest average increase in spike rate during BOS stimulation (range: .05 to 11.2 spikes/s above baseline firing rate). By definition, cells in this group did not show significant responses to CON stimuli. Quantitative confirmation of these properties is shown in **Figure 2.3C**, where RS_{INDEX} to BOS is greater than the best (i.e. most positive) CON response $(-.08 \pm .03)$($p<.001$)(**Fig. 2.3C**, left of dashed line), as well as greater than the mean RS_{INDEX} for all CON stimuli $(\text{BOS: } .17 \pm .02; \text{CON: } -.17 \pm .02)(p < .001)$. As a population, we found that the distribution of best CON responses in these cells was significantly smaller than zero ($p<.002$; $H_0: \mu_0 = 0$), indicating that CON responses in BOS-ONLY cells were suppressed below baseline firing rates. As a comparison point for many other studies, we also computed the selectivity metric *d'* for neurons in this group. For the BOS vs. mean CON response comparison, mean *d'* was highly significant $(.91 \pm .02)$ ($H_0: \mu_0 = 0$; $p <.001$). When compared to the best CON response, *d'* was

lower ($.60 \pm .08$) than for mean CON but nevertheless still highly significant ($H_0: \mu_0 = 0$; $p < .001$).

Characterization of auditory properties in BOS-CON neurons

Beyond response to BOS and at least one CON stimulus, response properties of BOS-CON neurons tended to be diverse. To capture the range of responses observed in these neurons, we depict two examples in **Figures 2.5 and 2.6** that represent most of the response features observed in this class of HVC_{IN}. Both cells showed BOS RS values (4.36 and 11.32, respectively) that were substantially higher than the typical BOS-ONLY cell (see previous section). The cell depicted in **Figure 2.5** showed reliable phasic response peaks to both BOS (**Fig. 2.5B** top panel, black PSTH) as well as CON stimuli (bottom two panels, black PSTHs). This particular cell did not show a strong preference for BOS as compared to CON stimuli (*d'* = 0.01; BOS vs. best-CON). The cell depicted in **Figure 2.6** had somewhat different, yet still common to the BOS-CON class, response characteristics. While responses to CON stimuli (**Fig.2.6B**, bottom two panels, black PSTHs) were well above baseline, responses were substantially weaker than those elicited by BOS (**Fig. 2.6B** top panel, black PSTH).This selectivity for BOS is supported by a moderately high *d'* value relative to the best CON response (*d'* = .34). Finally, while there were clearly consistent response peaks to both BOS and CON stimuli, this cell had higher background activity and slightly less precision than the cell shown in **Figure 2.5**. As will be discussed later in the context of temporal precision of STRF-derived linear response, the population of BOS-CON cells showed a range of phasic and tonic response properties.

As a population, BOS-CON neurons showed a diversity of response characteristics both in terms of the degree of BOS selectivity as well as the overall strength of response. The response strength to BOS ranged from .28 to 31.6 spikes/s with a mean RS_{INDEX} $(.33 \pm .02)$ that was significantly greater than that calculated for the mean response to all CON stimuli $(.17 \pm .02)$ ($p<.001$) as well as for the CON stimulus that elicited the strongest response $(.22 \pm .02)$ ($p<.001$)(**Fig. 2.3C**; right of dashed line). BOS selectivity at the population level for BOS-CON cells was verified by measurement of *d'*, which was significant when compared to both the mean CON response $(.63 \pm .06)$ ($p<.001$), as well as to the best CON response $(.28 \pm .06)$($H_0: \mu_0 = 0$; $p < .001$).

While BOS selectivity was evident at the population mean level, we found that over half of BOS-CON cells (42/82) showed *d'* values of below .5 relative to mean CON response. The number of cells with *d'* less than .5 increased to 57/82 when BOS responses were compared to best CON response. In previous studies, cells with *d'* below .5 were deemed to be non-selective for BOS (Cardin and Schmidt, 2003; Solis and Doupe, 1997). **Figure 2.5** exemplifies the relative lack of BOS selectivity exhibited by many BOS-CON cells. Because many neurons responded equally well to BOS and CON stimuli, we decided to investigate whether established linear analysis methods could be used to characterize spectral, temporal and spectrotemporal receptive field properties in these neurons.

A subpopulation of BOS-CON neurons showed responses well predicted by linear STRF

Spectrotemporal receptive field analysis (STRF) is a method by which the linear portion of responses to complex, time-varying stimuli, such as songs and other natural sounds, can be estimated and used to predict responses to other such stimuli. Introduction of static nonlinearities in the initial spectrographic representation of song has aided response prediction in areas of the songbird auditory forebrain where neurons are tuned to features inherent to CON song as compared to complex modulated noise stimuli (Grace et al., 2003; Theunissen et al., 2000). However, because auditory responses in HVC under anesthesia are highly biased toward the bird's own song (BOS), and thus show an extreme degree of nonlinearity, CON-based STRF has not previously been used to analyze auditory responses in this area (Theunissen and Doupe, 1998). The existence of a relatively large population of HVC_{IN}, the BOS-CON cells, which respond both to BOS and CON stimuli in awake birds motivated us to employ STRF based methods to describe the linear tuning properties of these cells. We measured mean CC ratio (response linearity) as the normalized (see Materials and Methods for details) average cross correlation between the actual time-varying response of neurons to CON stimuli and the response predicted by STRF generated from responses to other CON stimuli.

Figure 2.7A shows the distribution of response linearities across the population of BOS-CON cells. The population of BOS-CON cells showed mean response linearity $(.32 \pm .02)$ similar to that measured in various areas of the ascending auditory pathway in anesthetized birds using similar CON stimulus sets, spectrogram time-frequency parameters, and STRF smoothing parameters (Gill et al., 2006; Sen et al., 2001). In contrast to BOS-CON neurons, it is not surprising that BOS-ONLY cells

showed very low linearity in response to CON stimuli ($.18 \pm .02$) given their extreme nonlinearity and resemblance to HVC responses under anesthesia. Because of their lack of significant excitatory response to the CON stimuli we used to generate our STRFs, BOS-ONLY cells are not included in the distribution depicted in **Figure 2.7A** or in any further STRF-based analyses.

To extract spectral and temporal response parameters from individual neuron STRF, we chose to focus on neurons whose response linearity scores were at least .3. This criterion is similar to that previously used in a study of neural properties under anesthesia in the ascending auditory pathway (Woolley et al., 2009). Using this criterion, we were left with a subgroup of cells (n = 49/82 BOS-CON cells) that we refer to as linear neurons from here forward.

STRFs and response prediction in the subpopulation of BOS-CON linear neurons

As stated in the Materials and Methods, the jack-knife procedure used to validate the STRF allows prediction of responses to 'novel' (e.g. not used in generation of their own prediction) stimuli. We wanted to know whether STRFs generated based on the responses to the set of CON stimuli were as effective at predicting responses to novel BOS stimuli as they were at predicting responses to novel CON stimuli. Within the population of linear neurons, we found a strong positive correlation between response linearity (i.e. the ability of STRF to predict responses to novel CON stimuli) (**Fig. 2.7B**, vertical axis) and the degree to which individual novel CON and BOS responses could be well predicted (horizontal axis) ($r = .57$; $p < .001$). In other words, the cells showing the

highest average response linearity to the ensemble of CON stimuli also had BOS responses well predicted by CON-derived STRF. In contrast, neurons showing low linearity scores had BOS responses that were much more poorly predicted than CON responses. We represent the quality of BOS predictions with Z-scores to facilitate comparison across neurons. A BOS CC-Z score of -1 indicates that prediction of BOS response by CON-derived STRF was one standard deviation lower than the mean prediction of response to all individual CON stimuli. Cells within the range of -1 to +1 Z-score (shaded grey area in **Fig. 2.7B**) were defined as having well-predicted BOS responses, while those with a Z score lower than -1 were defined as having poorly predicted BOS responses.

Mean linearity for cells within the well- predicted BOS response range $(.53 \pm .02; n = 19)$ was significantly higher than the mean linearity for all BOS-CON cells ($p<.001$). The cell depicted in **Figure 2.5** (circled and labeled in **Fig. 2.7B**) is a representative example of the group with well- predicted BOS responses and illustrates nicely how well the measured PSTH (black PSTH) can follow the predicted (red PSTH) response (**Figure 2.5B**). This neuron showed a high linearity value (mean CC ratio: .57) and had a well predicted BOS response (BOS raw CC: .55) (open symbol in **Fig. 2.5C**) that was comparable to the mean raw response predictions to individual CON stimuli (mean raw CON CC: $.57 \pm .02$) (closed symbols). The BOS CC-Z score for this neuron (-.30) (see **Fig. 2.7B**) is highly representative of that shown by neurons in the well-predicted BOS response group. **Figure 2.4S** profiles an additional cell in this response

group, and **Figure 2.6S** profiles an unusual case of a neuron with a very high mean CC ratio to CON stimuli but a relatively poorly predicted BOS response.

In contrast to the well- predicted BOS response group, cells in the poorly predicted BOS response group showed lower linearity values in response to CON stimuli. Mean linearity for the poorly predicted BOS response group ($.38 \pm .01$) was significantly lower than for cells in the well- predicted BOS response group ($p<.001$). The cell depicted in **Figure 2.6** (circled and labeled in **Figure 2.7B**) is a representative example of the poorly predicted BOS response group. The linearity of this cell (mean CC ratio: .41) was high relative to mean linearity in all BOS-CON cells, but substantially lower than that seen in most cells in the well- predicted BOS response group. As shown in the figure, the predicted responses to CON stimuli (red PSTHs in bottom two panels of **Fig. 2.6B**) closely follow the measured PSTHs for these stimuli (black lines). In contrast, the predicted response to BOS (red PSTH in top panel) provides a relatively poor prediction of the actual PSTH obtained for BOS (black line) across the entire stimulus. Neural response to BOS in this cell was poorly predicted (BOS raw CC: .22) (open symbol in **Fig. 2.6C**) compared to individual CON responses (mean raw CON CC: $.42 \pm .03$) (closed symbols). This neuron was associated with a very large negative BOS CC-Z score (-2.59) (see Fig. 7B). **Figure 2.5S** profiles another cell from the poorly predicted BOS response group, though one with very different STRF characteristics than those of the cell depicted in **Figure 2.6**.

To make sure that lower response linearity values measured in the poorly predicted BOS response group were not simply due to lower response strength values to

CON stimuli, we compared response strength values between this group and the well-predicted BOS response group. We found that RS_{INDEX} in response to CON stimuli did not differ between groups (**Fig. 2.7C, left**), although there was a non-significant trend toward weaker CON responses in the well-predicted BOS response group ($p = .09$). This suggests that the lower mean linearity seen in the poorly predicted BOS response group is not likely the result of weaker responses to CON stimuli. Response strength to BOS, however, was significantly greater for cells in the poorly predicted BOS response group (BOS RS_{INDEX}: $.43 \pm .03$) than for those in the well predicted BOS response group (BOS RS_{INDEX}: $.29 \pm .04$) ($p<.001$) (**Fig. 2.7C, right**). These results, when considered with the linearity scores detailed in the previous section, indicate that cells in the poorly predicted BOS response group receive strong excitatory drive to both BOS and CON stimuli and that this drive is BOS-biased and only partially linear. The nonlinearity of these responses is highlighted by the poorly predicted large response peaks in the example in **Figure 2.6B** (middle panel and indicated by dashed arrows in top inset). Because cells in the poorly predicted BOS response group showed strong, partially linear CON responses and stronger, highly nonlinear BOS responses we refer to them as "hybrid cells" (i.e. exhibiting properties that are observed in both highly linear BOS-CON cells and nonlinear BOS-ONLY cells) in the legends for **Figures 2.6 and 2.7**, as well as in the Discussion .

STRFs and Receptive Field Feature Extraction

Prediction of response linearity exemplifies only one small facet of the power of the STRF approach. Analysis of two-dimensional temporal and spectral slices through the

STRF allow extraction of 'classical' receptive field properties including, but not limited to, spike latencies, precision of the relationship between specific stimulus features and modulation of spike rate, and the spectral frequencies that a neuron is reliably sensitive to. Moreover, deconstruction of the STRF in to its fundamental ripple components via 2-D Fourier analysis reveals the joint spectral and temporal (i.e. spectrotemporal) sensitivities of the neuron. Such analysis is especially informative because it is carried out in the same parameter space as analysis of the power density of zebra finch song (see **Fig. 2.1D**), allowing a direct assessment of whether and to what extent neurons are sensitive to features common to song stimuli. We obtained receptive field features from a large subset of linear neurons (40/49 neurons with mean CC ratios >.3) from which we could unambiguously extract all measured features from the best STRF.

Spectral receptive field features in BOS-CON linear neurons

We found that the population of linear neurons from which we could unambiguously extract features (n = 40) showed best excitatory (range: .263 kHz to 6.44 kHz) and inhibitory (range: .656 kHz to 7.49 kHz) frequencies that nearly spanned the entire range of frequencies represented in our STRF analysis (.250 kHz to 8 kHz). This range of best frequencies also covered the range of frequencies audible to the zebra finch (.05 kHz to 7 kHz) (Okanoya and Dooling, 1987). Excitatory and inhibitory best frequencies were observed across the entire STRF frequency range (**Fig. 2.8A**) and there was a significant tendency for best excitatory frequencies $(2045 \pm 263.91 \text{ Hz})$ to be lower than best inhibitory frequencies $(3844 \pm 277.29 \text{ Hz})(\text{paired } t-\text{test}; p < .001)$. The STRFs in **Fig. 2.5B** and **Fig**. **2.8E** are representative of this trend in the population.

Individual neurons tended to show broadband frequency sensitivity. For comparison, we include the estimated inter-quartile range of frequency bandwidth measured in a previous study (Woolley et al., 2009) from the auditory forebrain area Field L in anesthetized birds (dashed grey box in Fig. **2.8B**). Though Woolley et al. considered inhibitory and excitatory bandwidth concurrently, the majority of their values fell over a considerably more restricted range than ours. This testifies to the relatively broadband nature of responses in our population. Furthermore, the Field L population included many cells with extremely narrow frequency bandwidths (< 1kHz) that were not represented at all in our population. As with best frequency, mean spectral bandwidth in linear HVC_{IN} differed significantly between excitation $(2631 \pm 230$ Hz) and inhibition $(3425 \pm 235$ Hz)(p<.001). The tendency for inhibition to have wider spectral bandwidth than excitation is well illustrated by the STRF shown in **Fig. 2.8E**.

Temporal receptive field features in BOS-CON linear neurons

Along with the spectral parameters described above, we extracted two types of temporal parameters from the STRFs of linear neurons. First, we extracted excitatory and inhibitory spike latencies. This measure indicates the most reliable time interval between the presence (excitation) or absence (inhibition) of a given frequency in the song stimulus and a neural spike. We found that minimum excitatory $(15.80 \pm 1.26$ ms) and inhibitory $(16.85 \pm .95$ ms) latencies were not significantly different at the population level$(\text{paired } t-\text{test}; p = .52)$. The vertical black arrows on the STRF in **Figure 2.8F** depict the measurement of excitatory and inhibitory spike latency. Although population latencies were similar, at the single cell level, as is well represented by the STRF in

Figure 2.5D, peak inhibition and excitation tended to be offset in time. The scatter plot in **Figure 2.8C** shows the trend for temporal offset of excitation and inhibition and illustrates clearly that there was a near equal probability for each response component to lead the other (peak excitation led peak inhibition in 24/40 cells).

A second temporal feature that we extracted from STRFs of linear neurons is the temporal bandwidth (**Fig. 2.8D**). This measure indicates the precision of the temporal relationship between specific spectral frequencies in the song stimuli and neural spiking. Lower temporal bandwidths indicate a temporally precise relationship (i.e. low jitter) between a neuron's response and the presence of a specific spectral frequency. Because peak excitatory and inhibitory STRF components were always offset in time, the overall measurement of temporal bandwidth extended from the onset of the first component (here inhibition) to the end of the second component. The population of neurons recorded in the current study showed a broad range of temporal bandwidths, 10-52 ms, with a mean value of 20 ± 1.51 msec. For comparison, we provide the estimated inter-quartile range of temporal bandwidths obtained from primary auditory forebrain area Field L responses in a previous study (grey dashed box in **Fig. 2.8D**; Woolley et al., 2009). As with spectral bandwidth, temporal bandwidth for BOS-CON linear neurons was much broader than for Field L neurons, with Field L containing many values below 10ms. Such low values were never observed in BOS-CON neurons and indicates strong coherence and especially precise phase locking between stimulus and response in Field L that is not observed in HVC_{IN}. The STRF of the cell profiled in **Figure 2.5** exhibits a narrow temporal bandwidth (12ms) at the low end of the range observed in our population of BOS-CON

linear neurons. This is typical for cells with a sharp relationship between stimulus and spiking response. In contrast, the STRF of the cell profiled in **Figure 2.6** shows a relatively wide temporal bandwidth (28ms) (see also **Fig. 2.7S** for another example), which is typical for cells that have a relatively imprecise temporal relationship between stimulus features and spiking response.

Consideration of joint spectral and temporal properties in BOS-CON linear neurons

Simultaneous consideration of joint spectral and temporal properties facilitates a deeper understanding of the specific stimulus features that drive responses in linear HVC_{IN}. **Figure 2.9A** shows a scatter plot of the temporal and spectral bandwidth properties described in the previous sections, though here they are plotted against each other. This representation illustrates clearly the relatively broadband temporal and spectral properties measured in this group of BOS-CON neurons. As a point of comparison, the estimated joint inter-quartile range of temporal and spectral bandwidths in the population of Field L neurons obtained in a previous study is plotted as well (grey dashed box; Woolley et al., 2009). Though the joint sensitivities of the two populations overlap to some degree, the Field L population contains many more cells with narrow spectral and temporal bandwidths.

Fourier analysis of STRFs reveals spectral and temporal modulation sensitivity

Two-dimensional (2-D) Fourier analysis of STRFs yields the modulation transfer function (MTF), which provides a map of the spectral and temporal modulation sensitivities of neurons in the same space as the modulation power spectrum of the CON

song ensemble (MPS; see **Fig. 2.1D**). **Figure 2.9B** shows several prominent features of the population of BOS-CON linear neurons in terms of their modulation sensitivities. Cells showed peak sensitivity to a relatively broad range of temporal modulation frequencies (8-57Hz; range). This range of best temporal modulation frequencies largely overlaps the range of temporal modulations commonly seen in our CON song ensemble (the inner and outer red contour lines represent the 50% and 80% modulation power density boundaries, respectively, of our ensemble MPS). The average temporal modulation frequency of zebra finch song syllables has been estimated at ~7.5 Hz, and rapid song transients, such as note and syllable boundaries, occur in the 50 Hz range (Woolley et al., 2009). Thus, the population of HVC_{IN} may be sensitive to the broad range of timescales inherent to zebra finch song. The cell described in **Figure 2.5** showed peak temporal modulation sensitivity (45 Hz) near the high end of the observed range, indicating a peak sensitivity to rapid transients that is consistent with the strong onset characteristics evident in the STRF. For a cell with similar transient sensitivity, but with clear offset, as opposed to onset, characteristics, see **Figure 2.6S**. In contrast, the cell described in **Figure 2.6** showed relatively low peak temporal modulation sensitivity (12 Hz). This feature, coupled with the complex STRF shape, indicates that the cell may be sensitive to spectrotemporal features varying on a longer timescale than transient features such as onsets and offsets (see also the cell depicted in **Figure 2.7S**). For comparison, we plot the estimated inter-quartile range of peak temporal modulation sensitivities previously observed in Field L (grey dashed box along x-axis; Woolley et al., 2009).

The majority of BOS-CON linear neurons showed peak sensitivity to relatively low spectral modulations, indicating limited sensitivity to spectral content in the CON song stimuli. Three quarters (30/40) of cells had a peak spectral modulation sensitivity of below .5 cyc./kHz, which corresponds to a peak spectral pitch sensitivity of 500 Hz. This fundamental frequency corresponds to the lowest commonly seen in zebra finch song (Hsu et al., 2004a ; Zann, 1993). The neurons depicted in **Figures 2.5, 2.4S, and 2.6S** show the population-typical peak sensitivity to low spectral modulations. Nonetheless, the remaining 10/40 cells showed peak spectral modulation sensitivities above .5 cyc./kHz, ranging up to as high as 1.11 cyc./Hz. While the CON ensemble MPS contained substantial power in spectral modulation frequencies well above 1 cyc./kHz, most cells in our population with high peak spectral modulation sensitivity showed relatively high peak temporal modulation sensitivities (> 10 Hz) as well. Because most power in zebra finch song occurring at high spectral modulation frequencies occurs at low temporal modulation frequencies (see **Fig. 2.9B**), these cells do not respond optimally to the most common joint spectrotemporal features seen in CON song. See **Figures 2.6** and **2.5S** for examples of cells with peak sensitivity to relatively high spectral modulations. As previously mentioned, the cell depicted in **Figure 2.6** (see also the cell depicted in **Figure 2.7C**) has, along with a relatively high peak spectral modulation sensitivity (.91 cyc./kHz), a relatively low peak temporal modulation frequency (12 Hz), which makes it a strong candidate for sensitivity to the complex spectrotemporal information inherent to the non-transient parts of many song elements. It is clear from the MTF of this cell that there is sensitivity to various parts of the modulation spectrum in zebra finch song containing high power. Many cells in Field L

(inter-quartile range shown in grey dashed box along y-axis) show peak spectral sensitivity above .5 cyc./kHz, and many of these cells are similar to those with high spectral modulation sensitivity in our study in that they showed peak sensitivity to relatively high temporal modulations.

Evidence for frequency modulation sensitivity in the population of BOS-CON linear neurons

The existence of a small, yet substantial, minority of linear BOS-CON neurons showing peak sensitivity to relatively high spectral modulation frequencies opens the possibility that at least a subset of HVC_{IN} are involved in the analysis of the complex spectral structure of song, such as harmonic composition. Furthermore, many neurons with low peak spectral modulation sensitivity were nevertheless sensitive to higher spectral modulation frequencies (see **Figs. 2.5E**, **2.4SE**, and **2.6SE**). Figure **2.10A** shows the distribution of symmetry indices in the population of linear cells. This index is derived from comparison of the relative power in the left and right halves of the MTF for a given cell; a negative index indicates a cell with relatively more sensitivity to downwardly modulated frequency sweeps, while a positive index indicates a cell with relatively more sensitivity to upwardly modulated frequency sweeps. The population of BOS-CON linear neurons recorded in the present study showed a significant bias toward a negative symmetry index ($-.052 \pm .02$ ms)($H_0: \mu_0 = 0$; $p < .01$). Along with the information derived from the MTFs, the structures of most of the STRFs of linear neurons suggest sensitivity to frequency modulation. Figure **2.10B** shows a scatter plot of the absolute value of the difference in excitatory and inhibitory spike latencies (horizontal

axis) against the absolute value of the difference in excitatory and inhibitory best spectral frequency (vertical axis). Because the majority of values (30/40 cells) fall in the upper right quadrant delimited by the dashed lines, this indicates that most of our cells had peak excitation and inhibition offset in both time and frequency (see **Figs. 2.8A & C** and previous section for quantitative description of mean differences between excitation and inhibition in both the frequency and time domains). This type of STRF shape (represented well by the canonical STRF in **Figure 2.10C**), has previously been associated with sensitivity to oriented frequency sweeps in bats (Andoni et al., 2007).

DISCUSSION

Heterogeneity of auditory response properties in HVC of awake songbirds

The present study is the first to record from a large number of single units in a song vocal motor nucleus during presentation of a comprehensive set of complex, natural stimuli in awake, freely behaving birds. The heterogeneity in response properties we observed in the population of HVC_{IN} stands in sharp contrast to the vast majority of studies of HVC auditory responses in non-waking birds, which have shown vigorous, excitatory, BOS-selective responses that are highly homogenous in their responses properties across time and (at least in species with highly stereotyped songs) recording sites (Cardin and Schmidt, 2003; Rauske et al., 2003; Sutter and Margoliash, 1994). Furthermore, the wide range of response properties shown by HVC_{IN} in the present study provides a possible functional correlate to the diversity previously described for this cell

type based on morphology, calcium-binding protein profile, and intrinsic firing properties (Mooney, 2000; Nixdorf et al., 1989; Wild et al., 2005).

The results of some previous studies have opened the possibility that factors such as repertoire sharing (Lehongre et al., 2009) and territorial interactions requiring rapid song matching of neighboring birds (Margoliash and Konishi, 1985; Prather and Mooney, 2008, 2009) may be positively correlated with responses extending beyond the bird's own song (BOS) in HVC during wakefulness. The results of the present study, however, support previous multiunit studies suggesting that broad and non BOS-selective responses also occur in the zebra finch (Cardin and Schmidt, 2003, 2004b), a species with a highly stereotyped song and no overt repertoire sharing or territorial behavior (Zann, 1993). Nonetheless, we also recorded from many cells showing a high degree of BOS-selectivity, and this corroborates the results of multiple previous studies in species with diverse social ecology and repertoire sizes (Margoliash and Konishi, 1985; Nealen and Schmidt, 2006; Rauske et al., 2003; Sakata and Brainard, 2008). Only a few studies previous to the present one have involved single unit recordings with techniques not highly disruptive to ongoing behavior (Prather and Mooney, 2008, 2009), and these studies focused on responses in basal ganglia-projecting neurons (HVC_X) in the swamp sparrow, an uncommonly studied species. Thus, further studies will be needed to elucidate cell type, behavioral niche, and species specific correlates of BOS- selectivity in HVC during wakefulness.

In addition to the two-thirds of HVC_{IN} showing excitatory responses to song stimuli, a third of cells showed either only suppressive responses or were completely

unresponsive. The finding of many suppressive $HVC_{IN,}$ in both BOS-selective and non BOS-selective varieties, corroborates hints of their existence from a highly limited population recorded in a previous study (Rauske et al. 2003). The song evoked suppression of HVC_{IN} may promote auditory responses in HVC_X neurons, a class of cell which shows precise, phasic responses to BOS and BOS-like stimuli during wakefulness (Prather and Mooney, 2008, 2009). In anesthetized birds, a decrease in HVC_{IN} spiking activity during song playback is associated with less hyperpolarization in HVC_X neurons (Mooney, 2000). The existence of HVC_{IN} showing no auditory responses during wakefulness may be related to previous findings showing a complete suppression of responsiveness in HVC following arousal (Cardin and Schmidt 2003, 2004a; Nick and Konishi, 2001; Schmidt and Konishi, 1998). Many non-responsive $HVC_{IN,}$ however, retained this property stably across many hours of wakefulness. Previous multiunit studies showing slow oscillation from non-responsive to vigorous responsiveness in HVC during wakefulness (Cardin and Schmidt 2003, 2004b) would certainly have missed individual persistently non-responsive cells among those that did become active during 'up' states.

Possible sources of auditory input to HVC_{IN} during wakefulness

The results of the present study imply that HVC_{IN}, as a population, receive auditory inputs exhibiting a combination of linear and nonlinear response properties. HVC receives direct auditory input from two cerebral areas, NIf (Coleman and Mooney, 2004; Cardin et al., 2005) and CM (Bauer et al., 2008), that receive input from the primary auditory forebrain (Vates et al., 1996) (see **Fig. 2.1B**). Data obtained from

multiunit recordings in awake birds suggests that neurons in NIf, whose projection neurons drive all three classes of HVC neuron (Hahnloser and Fee, 2007), lack BOS selectivity (Cardin and Schmidt, 2003). A limited amount of single unit data obtained in CM during wakefulness suggests a mix of broadly responsive cells, some with modest selectivity for the bird's own song (BOS) relative to other complex stimuli and others with no BOS- selectivity. Thus, it appears that these structures are unlikely sources for the extremely BOS-selective excitatory responses shown by approximately one-third of auditory responsive HVC_{IN} (BOS-ONLY cells). Nevertheless, the limited scope of these studies does not preclude that there may exist specific subpopulations of neurons in these areas that might provide BOS-selective input during wakefulness, especially considering that auditory activity in non-waking states is dominated by BOS-selective responses in both areas (Bauer et al., 2008; Cardin and Schmidt, 2004b; Janata and Margoliash, 1999). Alternatively, or in addition, intrinsic network dynamics within HVC may shape less BOS-selective inputs, as has been suggested by simultaneous recordings in NIf and HVC projection neurons during anesthesia (Coleman and Mooney, 2004).

The basic response properties of CM and NIf neurons do not account for the extreme BOS-selectivity seen in many HVC_{IN} during wakefulness. Nevertheless, these properties are consistent with these areas providing most or all input to the highly linear, non-BOS selective neurons as well as to the moderately linear "hybrid" neurons that show robust responses to CON stimuli and exhibit a degree of BOS selectivity. Somewhat paradoxically, spike latencies derived from STRF analysis indicate that many of these BOS-CON linear neurons have input latencies similar to those obtained in

primary and secondary auditory forebrain structures (Sen et al., 2001). Though these auditory forebrain values were obtained in anesthetized birds and anesthesia is known to significantly alter auditory spike latencies and other receptive field properties (Populin et al., 2005; Wang et al., 2005), the shortest excitatory latencies observed in the current study (8 ms) are only a few milliseconds longer than the mean of those recorded in nucleus MLd of the auditory midbrain (Woolley et al., 2006). While no evidence exists for direct auditory connectivity between MLd and HVC, HVC does receive a robust input from nucleus uvaeformis (Uva), a thalamic nucleus that receives input directly from the ventral lateral lemniscus (LLV) in the auditory hindbrain (Coleman et al., 2007). Neurons in Uva show both BOS selective and non-BOS selective auditory responses during anesthesia, and may therefore be a source of short latency auditory inputs to HVC. Unfortunately, nothing is known about awake auditory properties in this structure. Another possible contributor of short latency auditory input to HVC is the primary auditory cortical analogue Field L, which has recently been shown to have direct functional connectivity with HVC under anesthesia (Shaevitz and Theunissen, 2007).

HVC interneurons exhibit a range of linear and nonlinear response properties and may subserve perceptual discrimination of song

To evaluate the possible link between auditory response properties in HVC and the song-related perceptual processes in which this structure is involved (Gentner et al., 2000) it is crucial to understand the nature of the song features that best drive neurons in HVC. One class of HVC_{IN} we recorded from (BOS-ONLY cells) demonstrated the remarkable property of showing excitatory response only to BOS and not a single

stimulus from the large ensemble of CON stimuli. The low overall linearity of these responses supports previous work in anesthetized birds showing that these responses are exclusively driven by nonlinear inputs (Theunissen and Doupe, 1998). The second class of neurons (BOS-CON cells) were responsive to both BOS and CON stimuli. Within this group of neurons, a substantial number of cells (approximately 10% of all auditory responsive HVC_{IN}) showed excitatory responses that had mean linearity values as high as those observed in Field L (Gill et al., 2006) and MLd (Gill et al., 2006; Woolley et al., 2006), an area where neurons respond with high precision to the temporal features of sound (Woolley and Casseday, 2004, 2005). These results imply that response linearity can propagate many synapses from the auditory periphery to the highest levels of the auditory system. The high degree of temporal precision exhibited by many highly linear HVC_{IN} (see **Fig. 2.5**) is consistent with earlier work showing that relative time-varying phase across frequency bands of complex stimuli is preserved in HVC at the millisecond timescale (Theunissen and Doupe, 1998). Interestingly, many cells in areas closer to the auditory periphery exhibit response linearity as low as that seen in BOS-ONLY interneurons (Sen et al., 2001; Woolley et al., 2006). Thus, it is likely that linearity is established early in some auditory processing streams and is preserved to the highest levels of the system, while in other processing streams linearity is either rapidly lost or simply never established.

We described one prevalent group of BOS-CON cells as hybrid because they had vigorous excitatory responses to CON stimuli but showed responses to BOS that were both substantially more vigorous than their CON responses and poorly predicted by

STRF. These neurons tended to have linearity scores in response to CON stimuli similar to the mean linearity value observed in CM of anesthetized birds (Gill et al., 2006) but nevertheless lower than the highly linear BOS-CON neurons. We propose that hybrid neurons receive a combination of linear (making them respond reliably to time-frequency features common to many or all song stimuli) and non-linear (biasing them toward responding more strongly to BOS) inputs. **Figure 2.11** depicts plausible ways in which these neurons may acquire their response properties and serves to summarize how the different response types may emerge in HVC_{IN}.

Hybrid neurons, possessive of strong yet well differentiated response properties to both CON and BOS stimuli, may be particularly well suited to participate in perceptual discrimination between these song types given the evidence that lesions to song nuclei (Scharff et al., 1998) receiving auditory input from HVC (Doupe and Konishi, 1991) significantly affect this specific type of discrimination. HVC-lesioned birds have not been explicitly tested for deficits in BOS vs. CON discriminations, though they show deficits in contingency reversals during perceptual discrimination tasks involving CON stimuli with previously defined operational salience (Gentner et al., 2000). Nonetheless, auditory responses during wakefulness in basal ganglia -projecting HVC neurons (Prather et al., 2008, 2009) show a remarkable temporal concordance with motor activity in the same neurons. Thus, BOS responses may function as 'self' in a motor-based comparison with 'other' (CON responses), in a similar manner to what has been proposed for mirror neurons in primate and human premotor cortex (Rizzolatti et al., 2001). In this regard, it will be interesting to know how well aligned auditory and motor activity are in BOS-

ONLY HVC_{IN}, though such comparison may be complicated by the relative variability of song premotor activity shown by this class of neuron (Hahnloser et al., 2002; Kozhevnikov and Fee, 2007).

A population of HVC interneurons specializes in temporal coding on timescales common in song

Few studies in vertebrates have focused on the spectrotemporal properties of single sensorimotor neurons in awake behaving animals (David et al., 2009; Elhilali et al., 2007) and ours is the first to do so in the songbird (but see Graña et al., 2009). In non-awake birds, many neurons in MLd (Woolley et al., 2006) and Field L (Nagel and Doupe, 2008; Woolley et al., 2009) are tuned to temporal modulation frequencies between 50-100 Hz and therefore fall above the range that is typically observed in zebra finch song. Most linear HVC_{IN}, in contrast, showed peak sensitivity to temporal modulation frequencies (range; 8-57 Hz) falling within the range common in zebra finch song, suggesting that these neurons might be specialized toward the analysis of temporal features inherent to species-specific vocal output. These might include the onsets (high end of the range; see **Fig. 2.5**) and offsets (see **Fig. 2.6S**) of syllables, as well as whole syllables and gaps (low end of the range; see **Fig. 2.6**).

Relatively few linear BOS-CON cells showed peak sensitivity to high spectral modulation. In this regard, our population is more similar to that previously documented (in anesthetised birds) in MLd as compared to Field L (Woolley et al., 2009) and suggests a relative insensitivity to frequency characteristics such as spectral pitch and harmonic

structure commonly seen in species song elements. Our finding is consistent with the previous suggestion that HVC neurons, at least in anesthetized birds, are more sensitive to the temporal features of songs than to their spectral features (Theunissen and Doupe, 1998). Nonetheless, one-quarter (10/40) of the population of linear BOS-CON HVC_{IN} showed peak spectral modulation sensitivity above .5 cyc./kHz, which corresponds to a spectral frequency (500 Hz), close to the low end typically found in zebra finch call and song elements (Vicario, 2004; Zann, 1993). Interestingly, it was recently found that peak spectral modulation sensitivities of a population of songbird auditory forebrain neurons during anesthesia were consistently higher than their STRF-derived best spectral frequencies (Woolley et al., 2009). Because the majority of power in zebra finch song lies above 1.5 kHz (albeit at lower temporal modulation frequencies), it is possible that cells tuned to especially high spectral modulation frequencies, and/or with STRFs showing harmonic structure (see **Fig. 2.7C**) may be beneficial in extracting salient spectral content from complex stimuli. In this regard, six of our cells showed peak spectral modulation sensitivity of .8 or higher (spectral frequency of 750 Hz and above), and may therefore be involved in extraction of spectral information from power-laden song components that are nonetheless well above typical fundamental frequencies. Other pieces of evidence suggesting some degree of spectral sensitivity in our population include a significant population preference for downward, as opposed to upward, frequency modulations and a tendency for peak inhibitory and excitatory STRF components to be offset in both time and frequency. Interestingly, previous work indicated neither spectrotemporally oriented STRFs nor modulation sensitivity at the population level in neurons of the ascending auditory system in non-anesthetised birds (Nagel and Doupe, 2008).

The ability to record from a large number of single units while presenting a wide range of ethologically relevant auditory stimuli has allowed a characterization of the heterogeneity of auditory response properties in HVC during wakefulness. Our findings reveal that HVC_{IN} exhibit auditory tuning properties that include feature-based linearity and robust selectivity for BOS. A significant future challenge will be to understand how these linear and nonlinear, BOS-selective response properties are integrated to subserve perceptual discrimination. Recent evidence in secondary auditory forebrain suggest that these areas can encode the recent exposure history (Gill et al., 2008; Terlaph et al., 2008), ethological relevance (George et al., 2008) and behavioral salience (Gentner and Margoliash, 2003) of complex acoustic stimuli. If HVC neurons are sensitive to these or related contextual stimulus features, it will provide strong evidence that the auditory forebrain and the song system constitute a unified network that functions in high-order, behaviorally relevant perception.

Acknowledgements

We thank Frederic Theunissen and Patrick Gill for technical assistance, Dan Margoliash and Pete Rauske for raw spike waveform data, Richard Hahnloser and Christopher Glaze for critical reading of the manuscript, and members of the Schmidt Lab and JNR thesis committee for helpful discussion and critique.

Figure Legends

Figure 2.1. Neural recordings from putative single HVC interneurons (HVC_{IN}).

(A), Representative raw trace with a well isolated single unit (top panel) during the presentation of conspecific (CON) song (bottom panel). Song is represented as a spectral derivative, with time on the x-axis and frequency on the y-axis. (B) A schematic of verified and potential auditory afferents to HVC. Caudal mesopallium (CM) and the nucleus interface of the nidopallium (NIf) are the only two structures (red outlines and arrows) known to provide direct auditory input to HVC. Other potential auditory afferents to HVC (dashed red arrows) include the Field L complex and nucleus uvaeformis of the thalamus (Uva). LLV, ventral lateral lemniscus; MLd, mesencephalicus lateralis dorsalis; Ov, nucleus ovoidalis of the thalamus; NCM, nidopallium caudal medial. HVC projects in the vocal-motor stream in two distinct pathways via the dorsal and ventral aspects of the robust nucleus of the arcopallium (dRA and vRA, respectively). $nXII_{ts}$, tracheosyringial portion of the hypoglossal nucleus; VRN; ventral respiratory nuclei. (C) Spike width characteristics were typical of HVC interneurons. All recorded neurons in the present study (n = 215; left most distribution) had spike widths at 25% of maximal value that were < .3ms. This width was narrower than those of any antidromically verified projection neurons (HVC_{RA} and HVC_X) recorded in a previous study by Rauske et al. (shown in the shaded grey area. (D) Modulation Power Spectrum (MPS) of 12 CON zebra finch songs used in the experiment. Not all songs used in generating this MPS were presented to any given neuron. The inner and outer black contour lines denote 50% and 80%, respectively, of the total modulation

power in the CON song ensemble. Green indicates areas of low power density on the MPS, while red indicates areas of high power density.

Figure 2.2. HVC interneurons exhibited three general classes of responses to song stimuli.

The top two panels represent the raster plot (top) and PSTH (middle) for each of three example neurons to illustrate the general types of responses obtained from HVC_{IN} during the presentation of a song stimulus. In all three examples, the stimulus was the BOS. The left most example ("suppressed") represents neurons showing suppressive responses to song stimuli. This response type was observed in 30/215 cells (14%). These neurons showed suppressive responses to one or more stimuli and failed to show excitatory responses to any CON or BOS stimuli. The center example ("Non-responsive") represents neurons showing a lack of response to BOS or any other song stimuli. This response type was observed in 39/215 cells (18.1%). These cells showed no significant suppressive or excitatory responses to any CON or BOS stimuli. The example to the right ("Excitatory") represents neurons showing excitatory responses to at least one song stimulus and made up the majority of neurons recorded in this study (146/215; 67.9%). The bottom row shows the distribution of RS_{INDEX} values following presentation of BOS for all 215 neurons recorded in this study. The arrows illustrate the RS_{INDEX} values for the three example cells. These values were respectively, -0.51, 0.07 and 0.42 for the suppressed, non-responding and excitatory neurons. The suppressive cell in the top left panel and the excitatory cell in top right panel were recorded simultaneously from the same electrode.

Figure 2.3. Response characteristics of HVC interneurons showing excitatory responses to one or more song stimuli.

(A) BOS-CON cells responded to multiple CON stimuli. The distribution of all recorded BOS-CON neurons shows the tendency for these cells to exhibit excitatory responses to multiple CON stimuli. This feature strongly distinguished them from BOS-ONLY cells, which showed excitatory responses only to BOS. Arrow represents the mean percentage of CON stimuli capable of eliciting an excitatory response. (B) Response strength in HVC interneurons. BOS-ONLY (black bars) and BOS-CON (white bars) cells both showed excitatory responses to BOS stimuli but response strength tended to be more robust in BOS-CON cells. Arrows in A and B denote mean response strength values. (C) Comparison of response strength characteristics in BOS-ONLY and BOS-CON cells. BOS-ONLY cells (n = 64, left of dashed line) had a positive mean RS_{INDEX} in response to BOS and a suppressive mean RS_{INDEX} in response to the CON stimulus eliciting the most positive response (best- CON). BOS-CON cells (n =82; right of dashed line) had a strongly positive mean RS_{INDEX} in response to BOS but, unlike BOS-ONLY cells, also showed an excitatory mean RS_{INDEX} to best- CON. Mean BOS RS_{INDEX} was nevertheless significantly greater for BOS than for best CON. (*** = $p<.001$).

Figure 2.4. Auditory Response Profile of a typical BOS-ONLY neuron.

Like the majority of BOS-ONLY neurons, this exemplar shows a modest, phasic excitatory response to BOS (RS_{INDEX} = .12; top half). The BOS stimulus used in this experiment was made up of three individual motifs (top panel, M1-M3). The BOS

response of this neuron was stronger for M2 and M3 than M1, a feature sometimes observed in BOS-ONLY neurons. Response to CON stimuli (mean RS_{INDEX} = $-.05 \pm .02$; bottom half) tended to be slightly suppressed relative to baseline. Moderate suppression to CON stimuli was common in BOS-ONLY neurons.

Figure 2.5. Response profile of a highly linear BOS-CON neuron.

(A) Neural response to CON. This neuron had phasic, precise response peaks reliably present across trials. The top panel depicts the song spectral derivatives (Sound Analysis Pro, O. Tchernichovski, D. Swigger), the middle panel the raster plot and the bottom panel the PSTH (red dashed line denotes baseline firing rate). (B and C) This neuron showed high linearity in response to CON stimuli (mean CC ratio: .57). The neural response to BOS (black PSTH in top panel of B) was well predicted by CON-derived STRF (red PSTH in top panel of B, open symbol in C). Neural responses to CON (black PSTHs in bottom two panels of B) were also well predicted (red PSTHs in bottom two panels of B, closed symbols in C). The insets in B highlight how well large response peaks could be modeled by CON-derived STRF for both BOS (top inset) and CON (middle and bottom insets) stimuli. (D) Best STRF for the neuron. The rapid succession from peak excitation (red) to peak inhibition (blue) and broadband frequency sensitivity in this neuron are characteristic of a cell with strong sensitivity to the onsets of sounds. (E) Modulation Transfer Function (MTF). This example neuron showed peak sensitivity to relatively high temporal (45 Hz) and low spectral (.12 cycles/kHz) modulations, reinforcing the notion that this cell was sensitive to rapid changes in song amplitude. Red regions of the MTF have relatively high power density, bluer regions have relatively little

power density. The inner and outer black contour lines represent the 50 and 80% power density inherent to the song MPS. The peak modulation sensitivities of this neuron, like many linear cells in our population, fell within the range of modulations common to zebra finch song.

Figure 2.6. Response profile of a moderately linear "hybrid" BOS-CON neuron.

(A) Response to a CON stimulus. This neuron, like the neuron depicted in Figure 5, showed consistent phasic response peaks, but with more tonic background activity in both pre-stimulus and stimulus periods. (B & C) This neuron type showed moderate linearity (mean CC ratio: .41) to CON stimuli. The neural response to BOS (black PSTH in top panel of B) was poorly predicted by CON-derived STRF (red PSTH in top panel of B, open symbol in C). In contrast, neural responses to CON (black PSTHs in bottom two panels of B) were relatively well predicted (red PSTHs in bottom two panels of B, closed symbols in C). The insets in B highlight how many of the peaks could be well modeled by CON-derived STRF (bottom inset panel). In contrast to highly linear cells, many of the larger response peaks during the presentation of CON stimuli (dashed arrows, top inset panel) were as poorly predicted as the responses recorded during the presentation of BOS. (D) Best STRF for the neuron. The long integration time dominated by inhibition is indicative of a neuron optimally sensitive to the presence of gaps between song elements. (E) Modulation Transfer Function. This example neuron showed peak sensitivity to both low temporal (14 Hz) and spectral modulations (.02 cycles/kHz). These peak sensitivities overlap with the high modulation power density area of the

ensemble MPS, indicating strong sensitivity to common features in zebra finch song. Figure conventions are identical to those in **Figure 2.5**.

Figure 2.7. BOS-CON neurons exhibit a wide range of STRF-derived linearity values.

(A) Linearity distribution for BOS-CON cells. Linearity scores (mean CC ratio) ranged from 0.03 to 0.64 with a mean linearity score for the population (n = 146) of $.32 \pm .02$. (B) Linearity correlates with the ability to predict responses to BOS. In cells with high linearity (mean CC ratio >.3; n = 49 cells) there was a strong positive correlation between prediction of BOS response and linearity values obtained from the CON stimulus set (r = .57, p<.001). Neurons showing high linearity in response to CON stimuli (mean CC ratio >.45, y-axis) tended to have relatively well predicted BOS responses (BOS CC-Z score, x-axis) whereas cells with moderate linearity (mean CC ratio between 0.3 and 0.45) tended to have poorly predicted BOS responses. The grey shaded area delimits the range of Z- scores between -1 and +1 and highlights neurons whose responses can be well predicted to both BOS and CON stimuli. Points to the left of this area (e.g BOS CC-Z score more than one Z below mean raw CC) represent cells in the poorly predicted BOS response group. The two small circles in the distribution identify the two neurons we highlight in **Figures 2.5** and **2.6**. (C) Response strength does not correlate with response linearity. RS_{INDEX} values to CON stimuli did not differ between the poorly predicted and well predicted BOS response groups, indicating that the lower mean linearity seen in the poorly predicted BOS response group was not the result of weaker responses to CON stimuli. In contrast, RS_{INDEX} values to BOS were stronger in the poorly predicted

neurons, suggesting that this group actually received greater overall excitatory drive relative to the well- predicted BOS response group. *** = p<.001

Figure 2.8. STRF-derived spectral and temporal features of BOS-CON linear neurons.

(A) Distribution of best spectral frequencies. Neurons subject to feature extraction (n = 40 cells) showed a broad distribution of best spectral frequencies. Population mean best excitatory frequency (red bars) was significantly lower than best inhibitory frequency (blue bars). Blue and red colored arrows denote, respectively, the mean best spectral frequency for inhibition and excitation. (B) Spectral Bandwidth. The majority of cells showed spectrally broadband excitation (red bars) and inhibition (blue bars), with a significant difference in mean spectral bandwidth between inhibition and excitation. Blue and red colored arrows represent, respectively, the mean excitatory and inhibitory spectral bandwidth. Field L (grey box) shows a narrower range that is skewed toward extremely sharp spectral tuning, which is rarely observed in HVC_{IN}. (C) Temporal Bandwidth. Most cells in the population showed temporal separation of peak excitation and inhibition. The dashed line denotes simultaneous peak inhibition and excitation. (D) Distribution of temporal bandwidths. Temporal bandwidths were distributed over a broad range (10 to 52 ms) but were never observed below 10 msec. Field L (grey box) shows a range that is skewed to the left and narrower than for HVC_{IN}. This suggests that Field L neurons show greater relative precision between stimulus features and neural responses. (E & F) STRF of a representative cell indicating spectral (E) and temporal (F) feature measurements. Temporal bandwidth, as measured in D, represents time from the onset of

the first STRF component (here inhibition) to the offset of the second component (here excitation). The grey dashed boxes in B & D show the estimated inter-quartile range of spectral (B) and temporal (D) bandwidth seen in Field L of anesthetized birds (Woolley et al., 2009).

Figure 2.9. Spectrotemporal properties of BOS-CON linear neurons.

(A**)** Linear neurons lacked temporal bandwidths in the 5 – 10 msec range and showed temporal bandwidths that were consistently broader than those measured in Field L (shaded box). Spectral bandwidth for excitatory frequencies (Y-axis) was also much broader than in Field L (note the log scale) with the large majority of neurons having frequency bandwidth greater that 1 KHz. (B) Best spectral and temporal modulation frequencies were obtained via 2-D Fourier analysis of STRFs, a process that generates a modulation transfer function (MTF) for a neuron (see **Figs. 2.5E and 2.6E**). Approximately half of all BOS-CON linear cells showed joint peak spectral and temporal modulation sensitivity that fell within the 80% power density of the CON song ensemble (outer red contour line). The Field L population (grey box), in contrast, showed a much broader range of peak sensitivities. The grey dashed boxes in A & B show the estimated inter-quartile range of spectral and temporal bandwidths (A) and best spectral and temporal modulation frequencies (B) seen in Field L of anesthetized birds (Woolley et al., 2009).

Figure 2.10. Evidence for modulation sensitivity in BOS-CON linear neurons.

(A) Linear neurons are preferentially biased toward oriented frequency sweeps. The symmetry index compares total power in the left and right halves of the modulation transfer function. HVC_{IN} showed a moderate but significant bias toward downward frequency sweeps (mean symmetry index: $-.052 \pm .02$) ($p < .01$). (B) The majority of linear cells showed peak inhibition and excitation separated in both time and frequency. Three quarters of neurons (30/40 BOS-CON linear cells) fell in the upper right quadrant delimited by the dashed lines, which indicates that they showed a difference of at least 1 kHz in best excitatory and inhibitory spectral frequency and 5ms in excitatory and inhibitory latency. (C) The offset between excitation and inhibition may increase sensitivity in the direction of offset between the two STRF components (white arrow), much as inhibitory regions in classical receptive fields increase sharpness of tuning in their preferred dimension.

Figure 2.11. Hypothetical model of how auditory inputs might shape response characteristics of HVC_{IN} during wakefulness.

Neurons showing excitatory responses to auditory stimuli fall in to two broad categories: BOS-ONLY neurons respond selectively to BOS and often show response suppression to CON. BOS-CON neurons show excitatory responses to BOS as well as CON. Within this category, some neurons have highly linear STRFs that predict responses well to both BOS and CON stimuli ("highly linear neurons"). Other neurons have STRFs that predict responses to CON stimuli well but predict BOS responses poorly. Because these neurons respond more vigorously to BOS than they do to CON, these "hybrid" neurons are hypothesized to receive a linear input that drives the CON response and a nonlinear input

that acts to boost the response to BOS. This scheme predicts that CON responses in hybrid neurons should be weaker than those in highly linear neurons. This trend is present in the data, but does not achieve statistical significance ($p = .09$). Likely input sources are shown to the right. It should be noted that further response shaping is likely to take place within the HVC network itself, where HVC_{IN} interact closely and reciprocally with other interneurons and both types of projection neurons (Prather and Mooney, 2005). Plus symbols (+) denote gain estimates based on BOS and CON response strengths for each of the three classes of excitatory inputs. Red circles represent inputs that are functionally inhibitory. Relative size of symbols is scaled to input strength.

Supplementary Figure Legends

Figure 2.1S. Action potential characteristics of HVC_{IN}.

An averaged waveform of a putative HVC_{IN} shows a characteristic narrow positive peak (top panel). The duration indicated by the horizontal arrow indicates the spike width at 25% of positive going peak amplitude. Single units were verified by relative suppression of inter-spike intervals (ISI) below 1 ms (indicated by arrowhead) (bottom panel).

Figure 2.2S. Paired Recording Example I

(A) Responses to BOS and a representative CON stimulus for a BOS-ONLY (Cell 1; top panels with PSTH in blue) and BOS-CON cell (Cell 2; bottom panels with PSTH in blue) simultaneously recorded on the same electrode. Black dashed lines in PSTH denote baseline firing rate. (B) Averaged raw waveforms (left panel) and PCA space (right panel) for this simultaneously recorded pair.

Figure 2.3S. Paired Recording Example II

(A) Responses to BOS and a representative CON stimulus for a BOS-CON cell showing some degree of BOS selectivity(Cell 1; top panels with PSTH in blue) and a BOS-CON cell (Cell 2; bottom panels with PSTH in blue) showing no preference for BOS relative to CON stimuli. Black dashed lines in PSTH denote baseline firing rate. (B) Averaged raw waveforms (left panel) and PCA space (right panel) for this simultaneously recorded pair.

Figure 2.4S Response profile of a highly linear BOS-CON neuron.

(A) Response to a CON stimulus. This neuron had phasic response peaks reliably present across trials, though it also showed a substantially higher tonic firing rate than the highly linear example shown in **Figure 2.5**. (B and C) As was typical of neurons showing high linearity in response to CON stimuli (mean CC ratio: .59), actual BOS response (black PSTH in top panel of B) was well predicted by CON-derived STRF (red PSTH in top panel of B, open symbol in C). Actual CON responses (black PSTHs in bottom two panels of B) were also well predicted (red PSTHs in bottom two panels of B, closed symbols in C). The inset in B highlights how well modeled large response peaks were in response to both BOS and CON stimuli for this cell. (D) Best STRF for the neuron. The rapid succession from peak excitation (red) to peak inhibition (blue) and broadband frequency sensitivity are characteristic of a cell with strong sensitivity to the onsets of sounds. (E) the Modulation Transfer Function (MTF) of the neuron. The neuron showed peak sensitivity to relatively high temporal (48 Hz) and low spectral (.13 cycles/kHz) modulations, reinforcing the notion that the cell was sensitive to rapid changes in song

amplitude. The peak modulation sensitivities of this neuron, like many linear cells in our population, fell within the range of modulations common found in zebra finch song. Figure conventions are identical to those in **Figures 2.5 and 2.6**.

Figure 2.5S Response profile of a moderately linear BOS-CON neuron.

(A) Response to a CON stimulus. This neuron showed consistent response peaks across trials and a relatively low baseline firing rate. (B and C) As was typical of neurons showing moderate linearity (mean CC ratio: .37), actual BOS response (black PSTH in top panel of B) was poorly predicted by CON-derived STRF (red PSTH in top panel of B, open symbol in C). In contrast, actual CON responses (black PSTHs in bottom two panels of B) were relatively well predicted (red PSTHs in bottom two panels of B, closed symbols in C). The insets in B highlight another typical property of moderately linear cells; many fluctuations in CON response were well modeled (bottom inset panel) but some larger peaks in response to CON were as poorly predicted as large peaks in the BOS response (dashed arrows in middle inset panel). (D) best STRF for the neuron. The rapid succession from peak excitation (red) to peak inhibition (blue) and broadband frequency sensitivity are characteristic of a cell with strong sensitivity to the onsets of sounds. (E) the Modulation Transfer Function of the neuron. This neuron had a high best spectral modulation frequency (.64 cycles/kHz) relative to most neurons in our population (see **Fig. 2.9B**). Best temporal modulation frequency (37 Hz) was also relatively high. These peak sensitivities are indicative of a neuron sensitive to both transient changes in the amplitude envelope (in this case sound onsets) and to some degree of spectral structure as well. Though the peak spectral modulation sensitivity of

this neuron was high relative to that shown by most cells in our population, both it and peak temporal modulation sensitivity fell within the range of modulations commonly found in zebra finch song. Figure conventions are identical to those in **Figures 2.5, 2.6**, and **Figure 2.4S**.

Figure 2.6S Response profile of a highly linear BOS-CON neuron with relatively low BOS response linearity.

(A) Response to a CON stimulus. This neuron had phasic response peaks reliably present across trials. (B and C) In a slightly atypical manner for neurons showing high linearity in response to CON stimuli (mean CC ratio: .61), actual BOS response (black PSTH in top panel of B) was relatively poorly predicted by CON-derived STRF (red PSTH in top panel of B, open symbol in C). Actual CON responses (black PSTHs in bottom two panels of B) were well predicted (red PSTHs in bottom two panels of B, closed symbols in C). The top inset in B highlights how some response peaks to BOS were largely under-predicted while most response peaks to CON stimuli were very well predicted (middle and bottom insets). (D) Best STRF for the neuron. The rapid succession from peak inhibition (blue) to peak excitation (red) and broadband frequency sensitivity are characteristic of a cell with strong sensitivity to the offsets of sounds. (E) the Modulation Transfer Function (MTF) of the neuron. The neuron showed peak sensitivity to relatively high temporal (37 Hz) and low spectral (.11 cycles/kHz) modulations, reinforcing the notion that the cell was sensitive to rapid changes in song amplitude. The peak modulation sensitivities of this neuron, like many linear cells in our population, fell

within the range of modulations common found in zebra finch song. Figure conventions are identical to those in **Figures 2.5, 2.6, 2.4S, and 2.5S**.

Figure 2.7S Response profile of a moderately linear BOS-CON neuron with high best spectral modulation frequency sensitivity.

(A) Response to a CON stimulus. This neuron had an extremely low spontaneous firing rate (dashed red line in PSTH) and a response profile characterized by relatively precise peaks and some epochs of near complete suppression. (B) As was typical of neurons showing moderate linearity (mean CC ratio: .44), many large response peaks to both BOS (black PSTH in top panel of B) and CON (black PSTHs in middle and bottom panels of B) were poorly predicted. (C) quality of individual CON predictions varied widely (open symbols) and prediction of BOS response (closed symbol) was not as relatively poor as was typical of the moderately linear BOS-CON cell group. (D) Best STRF for the neuron. Relative to the population of linear BOS-CON neurons, this cell showed a high degree of 'spectral' orientation; a restricted frequency domain and an extended temporal domain. (E) the Modulation Transfer Function (MTF) of the neuron. As anticipated from the STRF shape, this cell showed peak sensitivity to low temporal (8.45 Hz) and high spectral (1.1 cycles/kHz) modulations. This combination of peak sensitivities falls within the 80% power bound of the ensemble modulation power spectrum (MPS), and therefore this neuron may be sensitive to spectrotemporal content commonly found in zebra finch song.

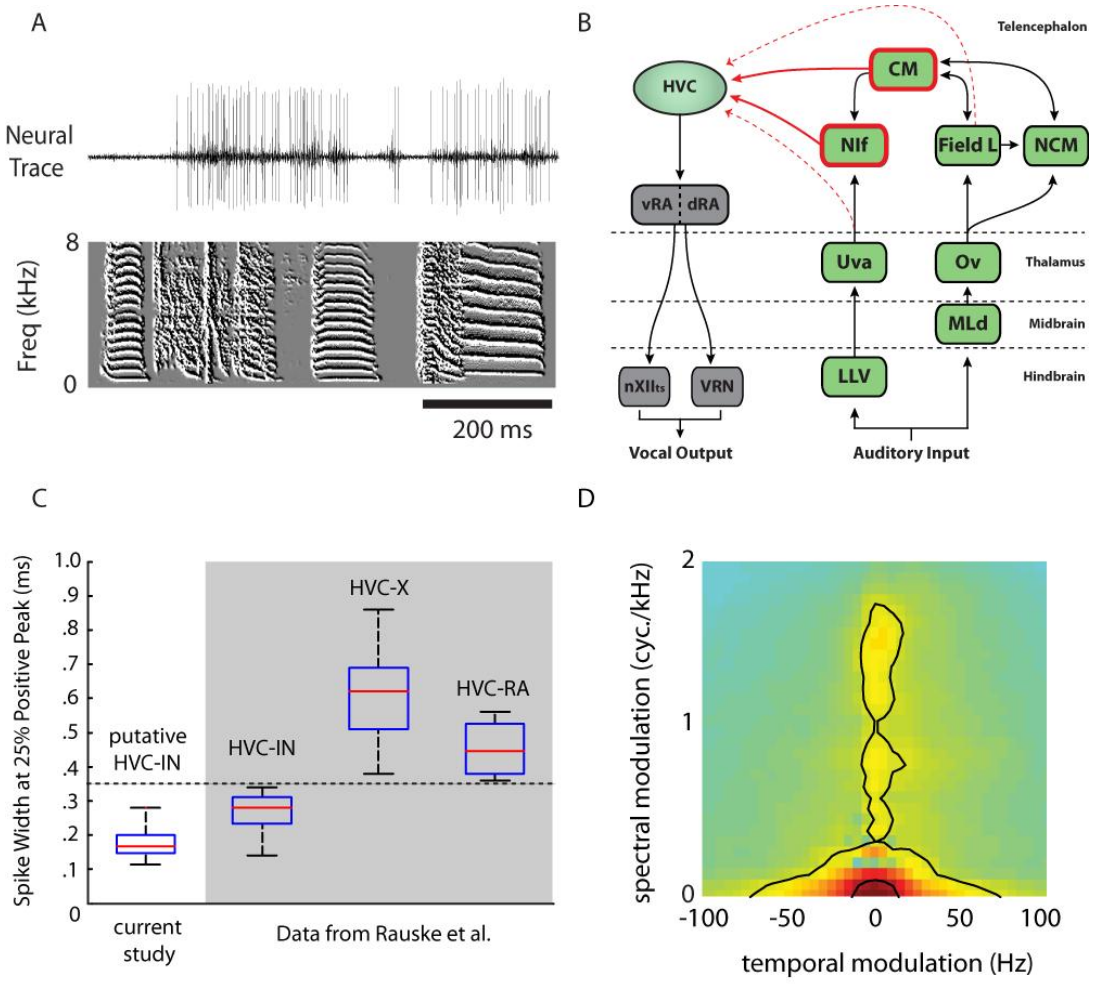
A
Neural Trace
Freq (kHz)
8
0
200 ms
B
Telencephalon
HVC
CM
NIf
Field L
NCM
vRA
dRA
Uva
Ov
Thalamus
MLd
Midbrain
Hindbrain
nXIIts
VRN
LLV
Vocal Output
Auditory Input
C
Spike Width at 25% Positive Peak (ms)
1.0
.9
.8
.7
.6
.5
.4
.3
.2
.1
0
putative HVC-IN
HVC-IN
HVC-X
HVC-RA
current study
Data from Rauske et al.
D
spectral modulation (cyc./kHz)
2
1
0
-100
-50
0
50
100
temporal modulation (Hz)

Figure 2.1

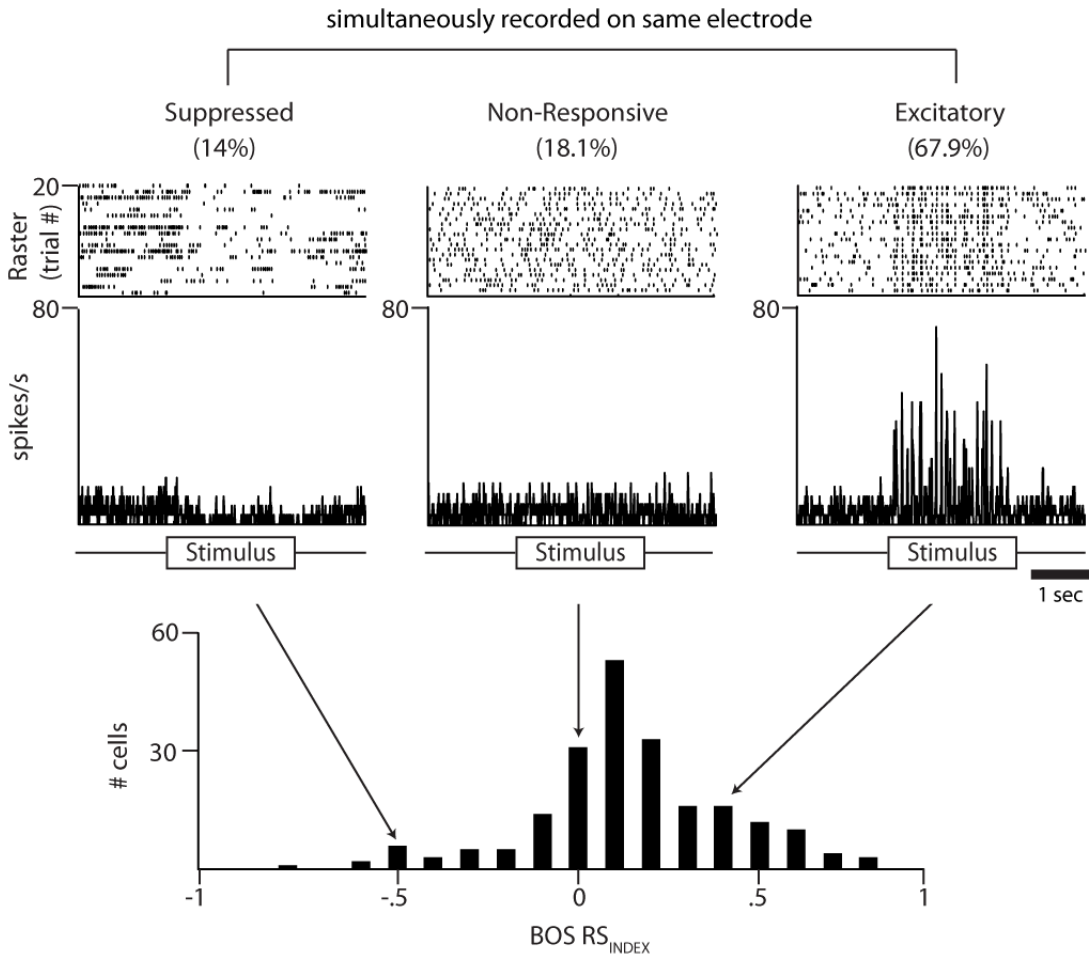
simultaneously recorded on same electrode
Suppressed
(14%)
Non-Responsive
(18.1%)
Excitatory
(67.9%)
Raster
(trial #)
20
80
80
80
spikes/s
Stimulus
Stimulus
Stimulus
1 sec
60
30
cells
-1
-.5
0
.5
1
BOS RS INDEX

Figure 2.2

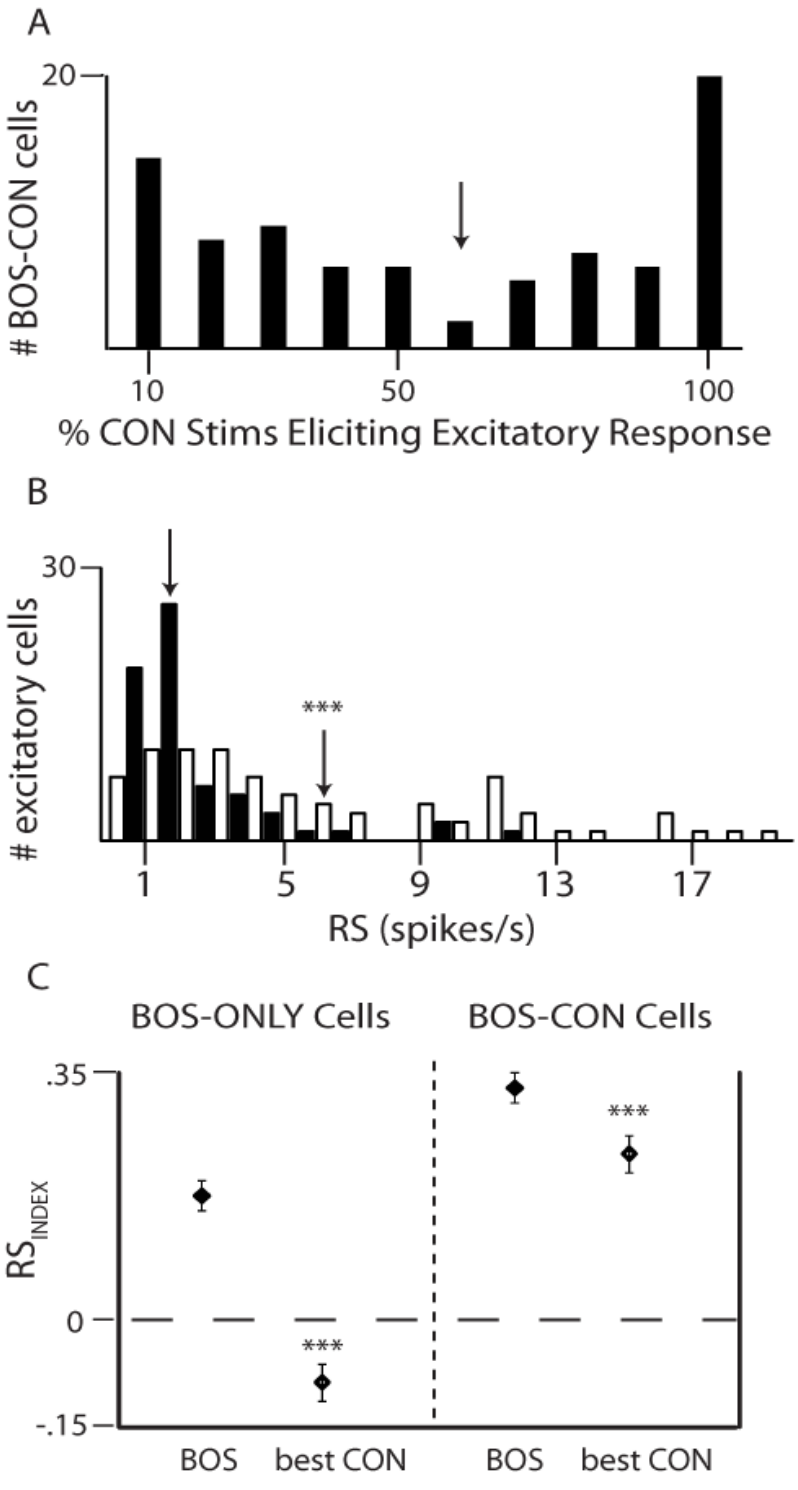
A
20
BOS-CON cells
10
50
100
% CON Stims Eliciting Excitatory Response
B
30
excitatory cells
***
1
5
9
13
17
RS (spikes/s)
C
BOS-ONLY Cells
BOS-CON Cells
.35
RS INDEX
0
-.15
***
***
BOS
best CON
BOS
best CON

Figure 2.3

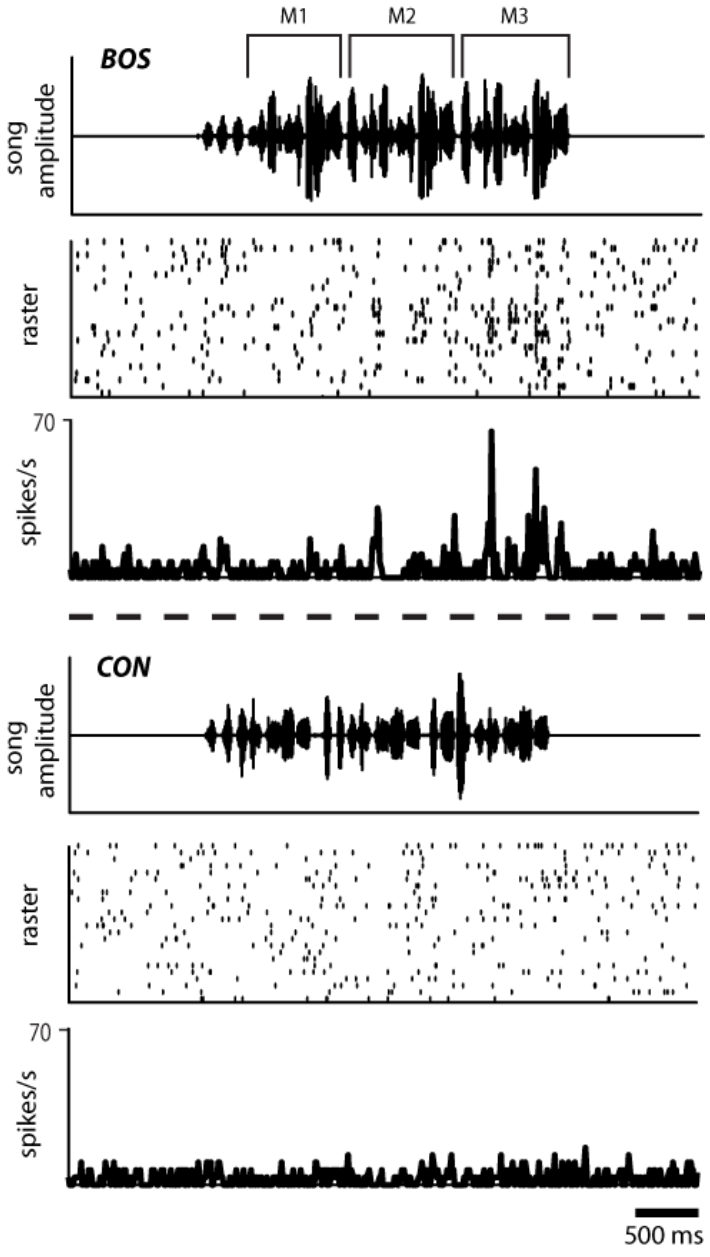
M1
M2
M3
BOS
song amplitude
raster
70
spikes/s
CON
song amplitude
raster
70
spikes/s
500 ms

Figure 2.4

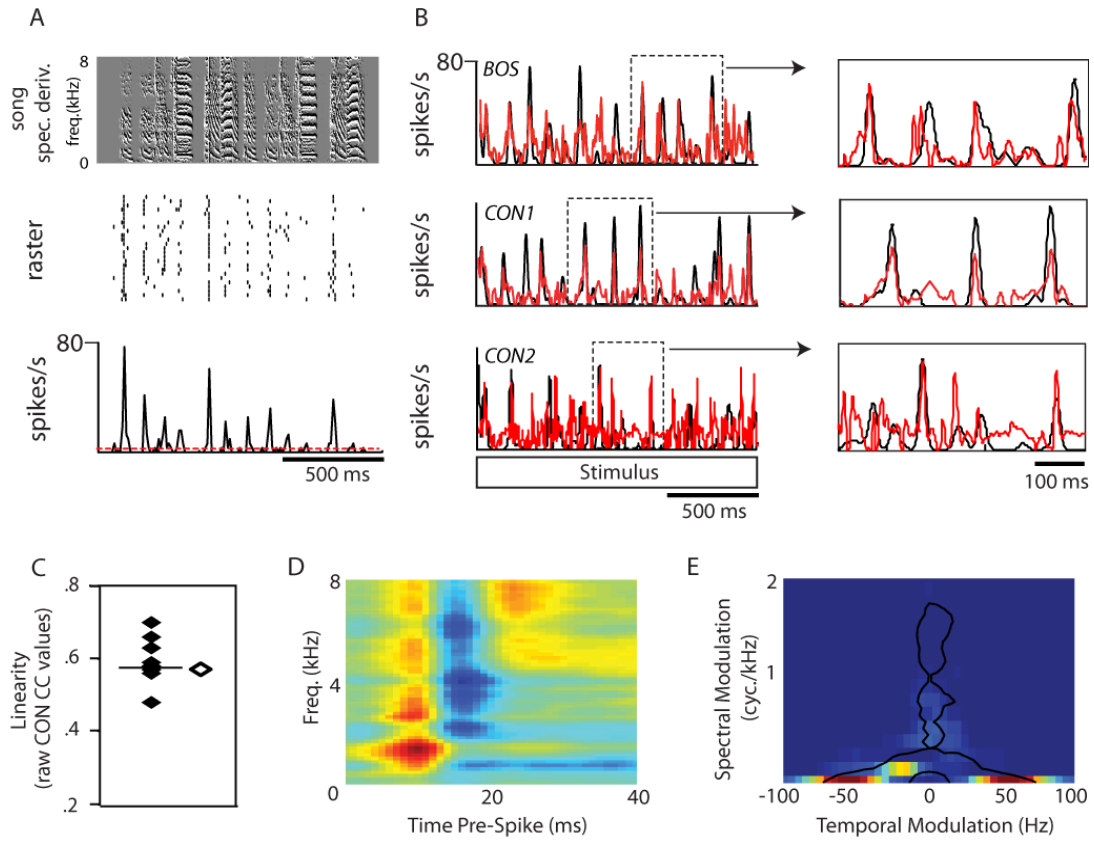
A
B
song
spec. deriv.
freq.(kHz)
8
0
raster
spikes/s
80
500 ms
BOS
CON1
CON2
Stimulus
500 ms
100 ms
C
Linearity
(raw CON CC values)
.8
.6
.4
.2
D
Freq. (kHz)
8
4
0
20
40
Time Pre-Spike (ms)
E
Spectral Modulation
(cyc./kHz)
2
1
-100
-50
0
50
100
Temporal Modulation (Hz)

Figure 2.5

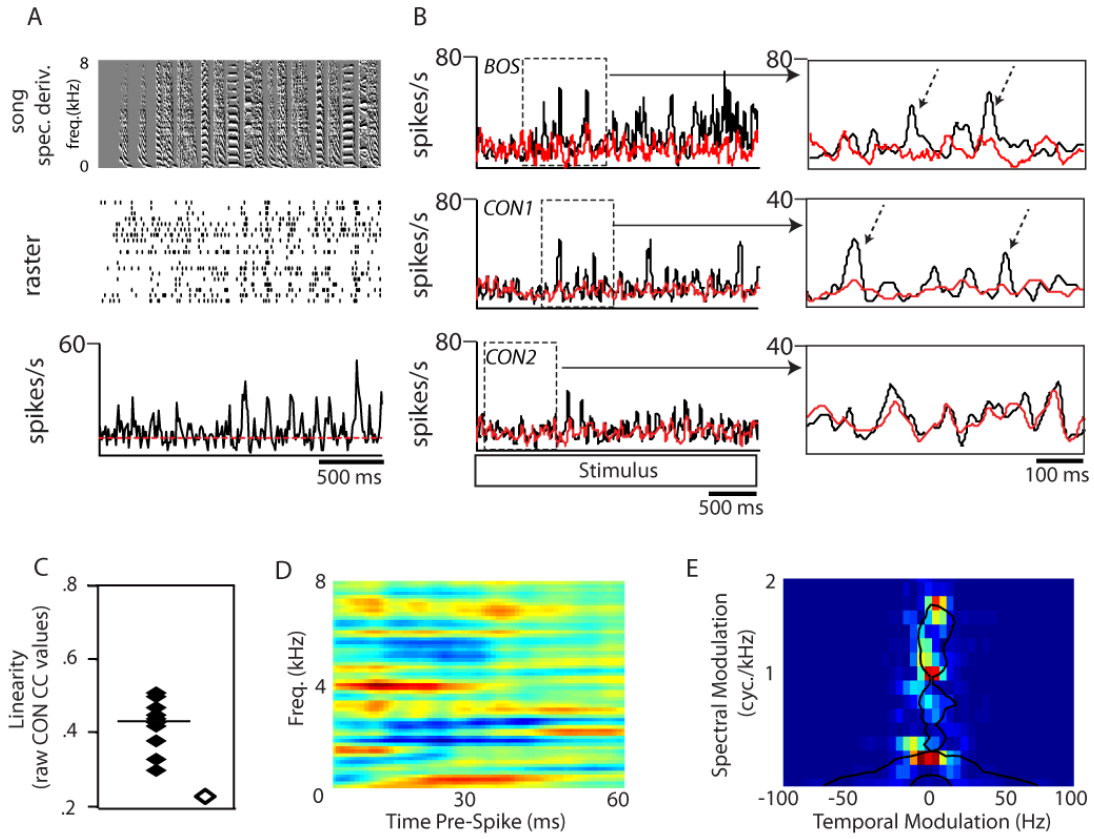
A
B
song
spec. deriv.
freq.(kHz)
8
0
raster
spikes/s
60
500 ms
BOS
CON1
CON2
80
40
Stimulus
500 ms
100 ms
C
Linearity
(raw CON CC values)
.8
.6
.4
.2
D
Freq. (kHz)
8
4
0
30
60
Time Pre-Spike (ms)
E
Spectral Modulation
(cyc./kHz)
2
1
-100
-50
0
50
100
Temporal Modulation (Hz)

Figure 2.6

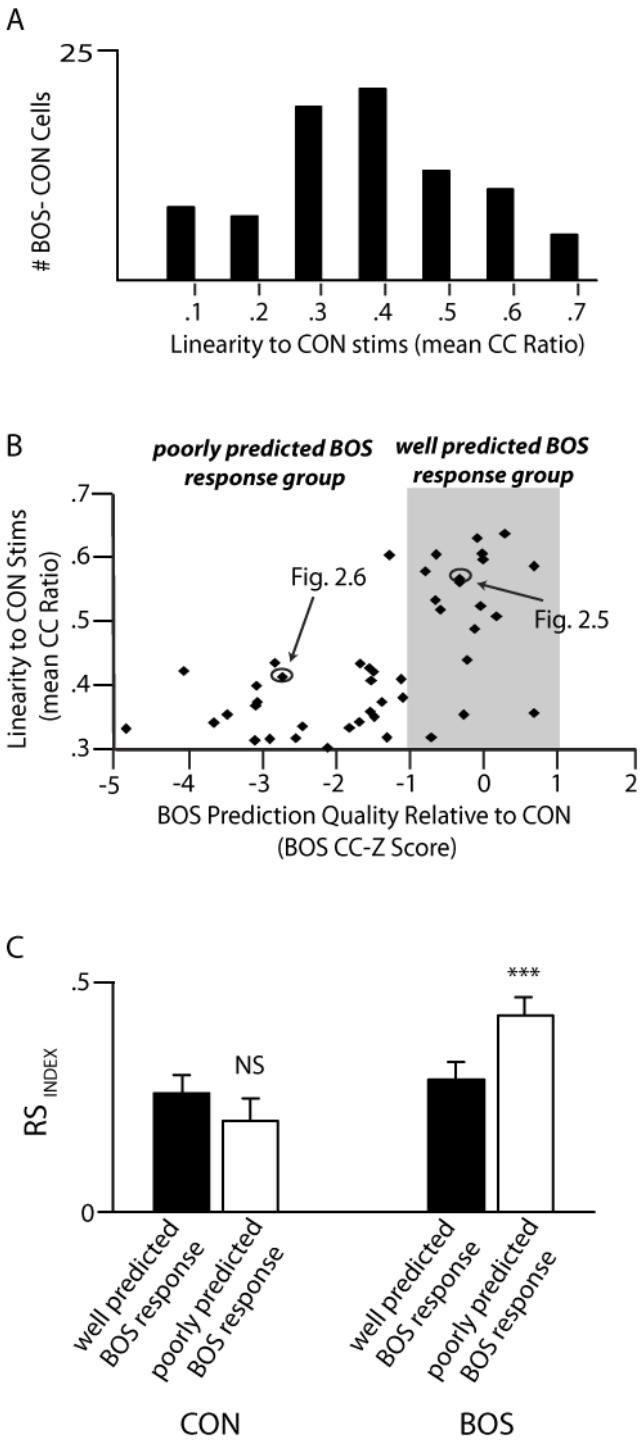
A
25
BOS- CON Cells
.1
.2
.3
.4
.5
.6
.7
Linearity to CON stims (mean CC Ratio)
B
poorly predicted BOS response group
well predicted BOS response group
Fig. 2.6
Fig. 2.5
Linearity to CON Stims (mean CC Ratio)
.7
.6
.5
.4
.3
-5
-4
-3
-2
-1
0
1
2
BOS Prediction Quality Relative to CON (BOS CC-Z Score)
C
.5
0
RS INDEX
NS
***
well predicted BOS response
poorly predicted BOS response
well predicted BOS response
poorly predicted BOS response
CON
BOS

Figure 2.7

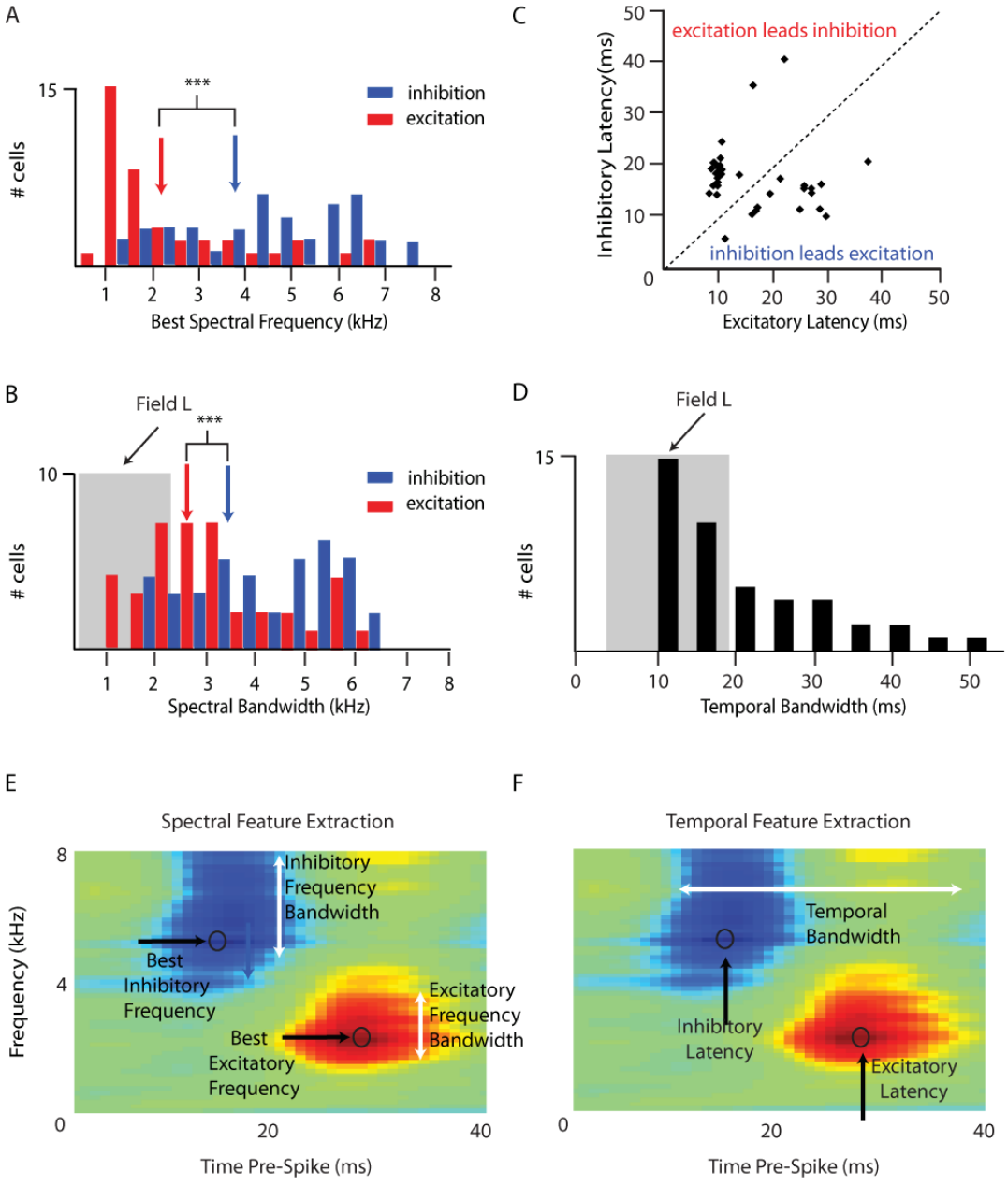
A
15
***
inhibition
excitation
cells
1 2 3 4 5 6 7 8
Best Spectral Frequency (kHz)
C
50
40
30
20
10
0
excitation leads inhibition
inhibition leads excitation
Inhibitory Latency(ms)
10 20 30 40 50
Excitatory Latency (ms)
B
Field L
***
10
inhibition
excitation
cells
1 2 3 4 5 6 7 8
Spectral Bandwidth (kHz)
D
Field L
15
cells
0 10 20 30 40 50
Temporal Bandwidth (ms)
E
Spectral Feature Extraction
8
4
0
Frequency (kHz)
Inhibitory
Frequency
Bandwidth
Best
Inhibitory
Frequency
Excitatory
Frequency
Bandwidth
Best
Excitatory
Frequency
20
40
Time Pre-Spike (ms)
F
Temporal Feature Extraction
Temporal
Bandwidth
Inhibitory
Latency
Excitatory
Latency
0
20
40
Time Pre-Spike (ms)

Figure 2.8

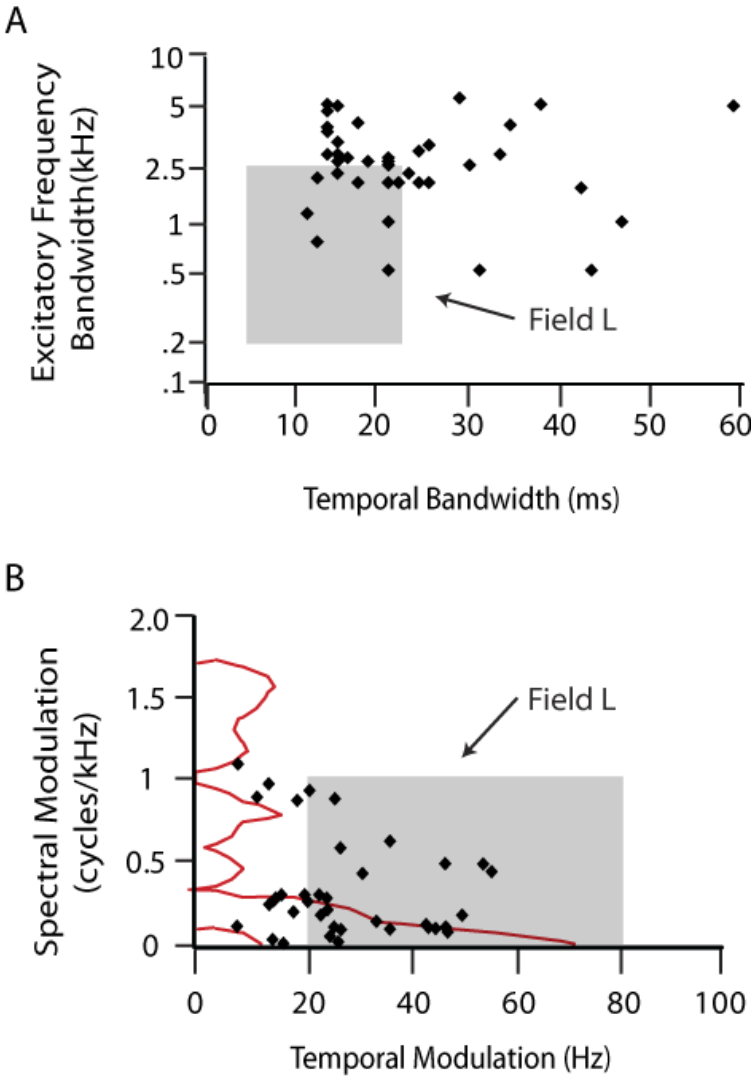
A
Excitatory Frequency Bandwidth(kHz)
10
5
2.5
1
.5
.2
.1
Field L
0
10
20
30
40
50
60
Temporal Bandwidth (ms)
B
Spectral Modulation (cycles/kHz)
2.0
1.5
1
0.5
0
Field L
0
20
40
60
80
100
Temporal Modulation (Hz)

Figure 2.9

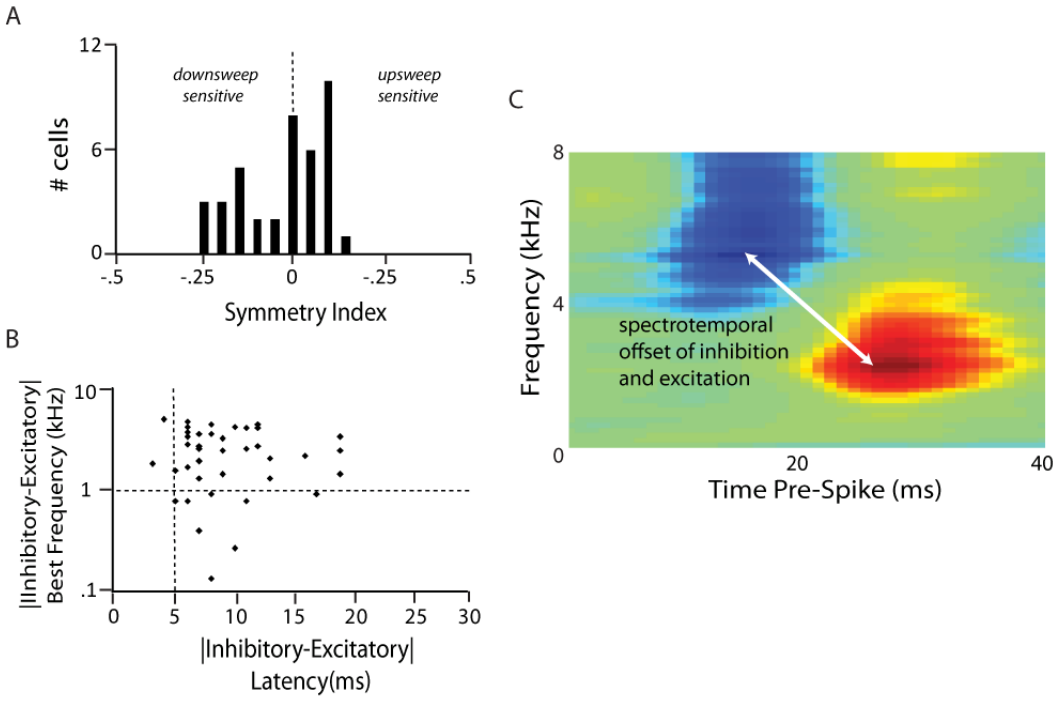
A
12
6
0
cells
downsweep sensitive
upsweep sensitive
-.5
-.25
0
-.25
.5
Symmetry Index
B
|Inhibitory-Excitatory| Best Frequency (kHz)
10
1
.1
0
5
10
15
20
25
30
|Inhibitory-Excitatory| Latency(ms)
C
8
4
0
Frequency (kHz)
spectrotemporal offset of inhibition and excitation
20
40
Time Pre-Spike (ms)

Figure 2.10

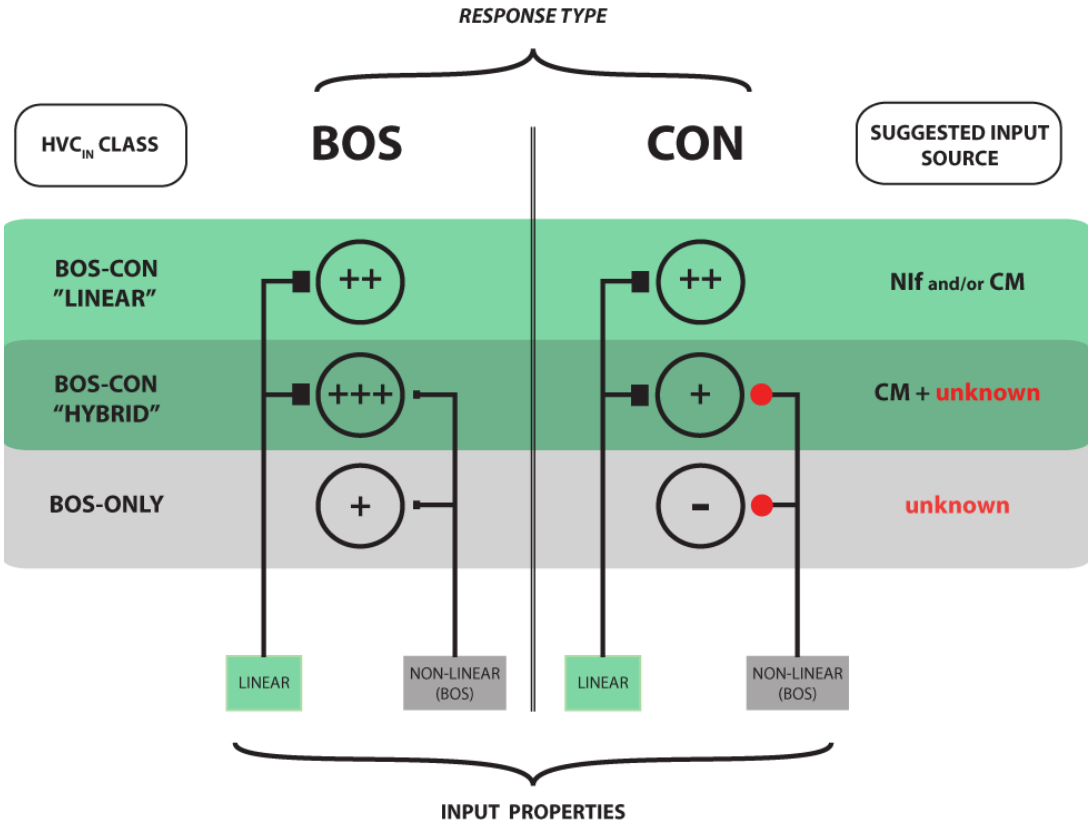
RESPONSE TYPE
HVC$_{IN}$ CLASS
BOS
CON
SUGGESTED INPUT SOURCE
BOS-CON "LINEAR"
++
++
NIf and/or CM
BOS-CON "HYBRID"
+++
+
CM + unknown
BOS-ONLY
+
-
unknown
LINEAR
NON-LINEAR (BOS)
LINEAR
NON-LINEAR (BOS)
INPUT PROPERTIES

Figure 2.11

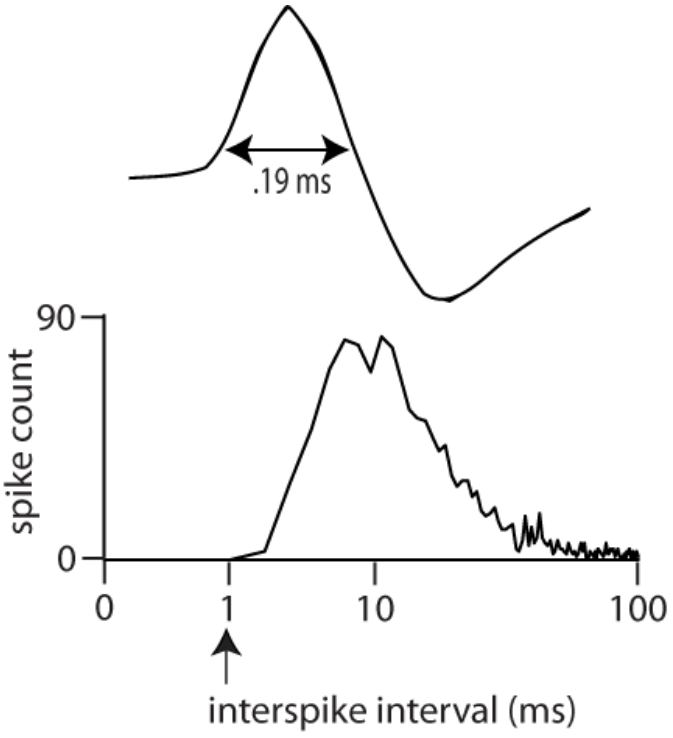

Figure 2.1S

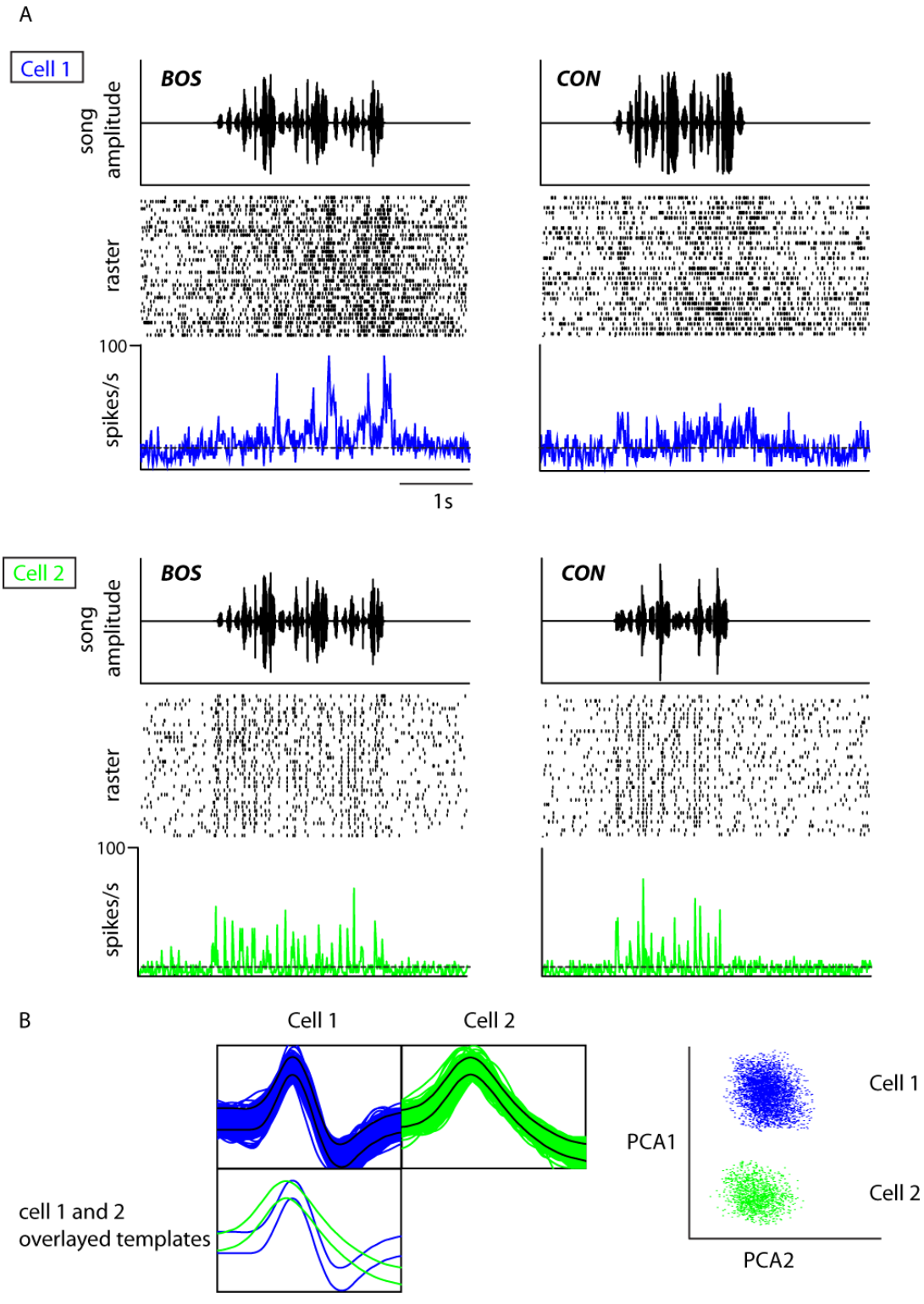
A
Cell 1
BOS
CON
song amplitude
raster
100
spikes/s
1s
Cell 2
BOS
CON
song amplitude
raster
100
spikes/s
B
Cell 1
Cell 2
cell 1 and 2
overlayed templates
PCA1
PCA2
Cell 1
Cell 2

Figure 2.2S

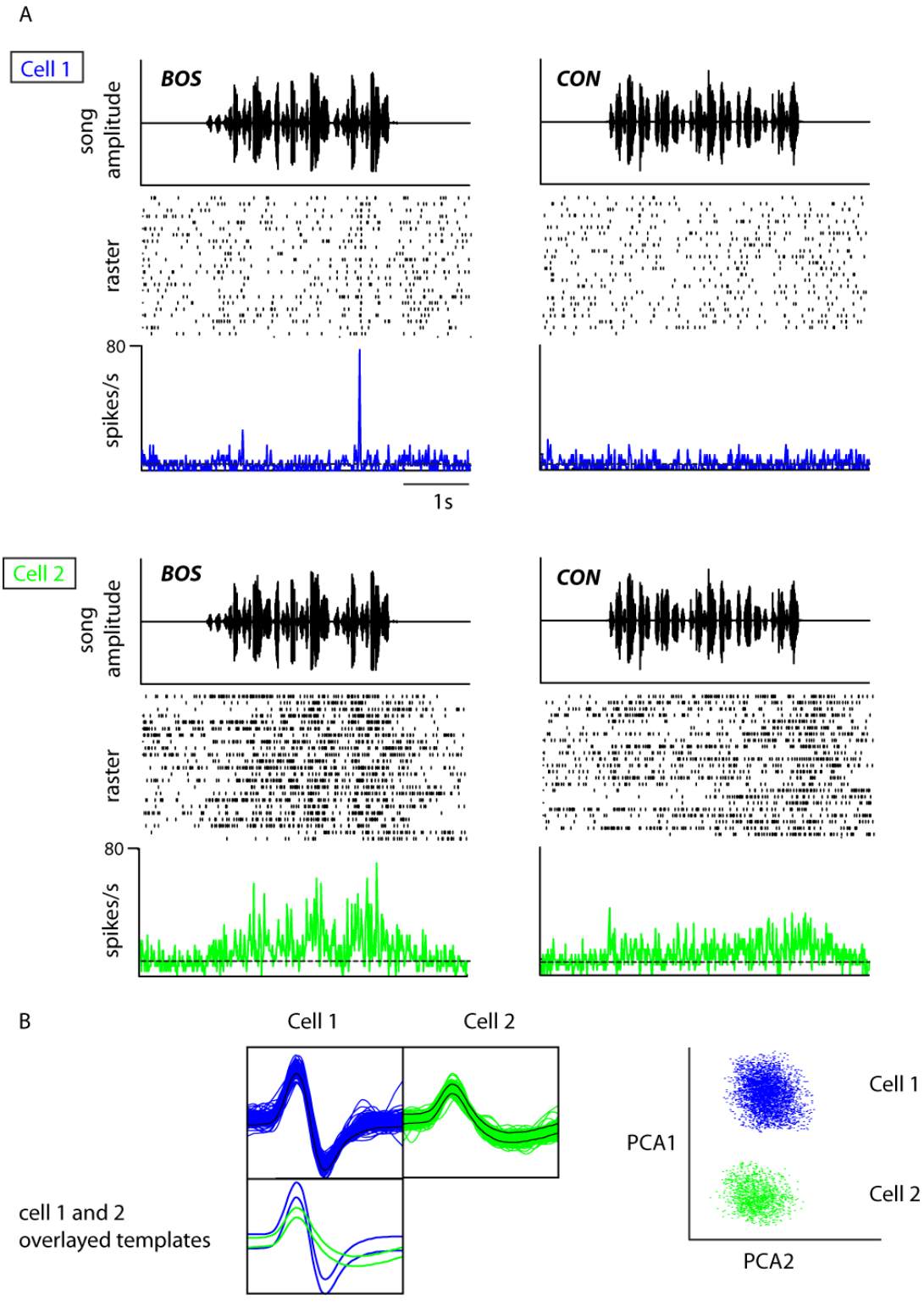
A
Cell 1
BOS
CON
song amplitude
raster
80
spikes/s
1s
Cell 2
BOS
CON
song amplitude
raster
80
spikes/s
B
Cell 1
Cell 2
cell 1 and 2
overlayed templates
PCA1
PCA2
Cell 1
Cell 2

Figure 2.3S

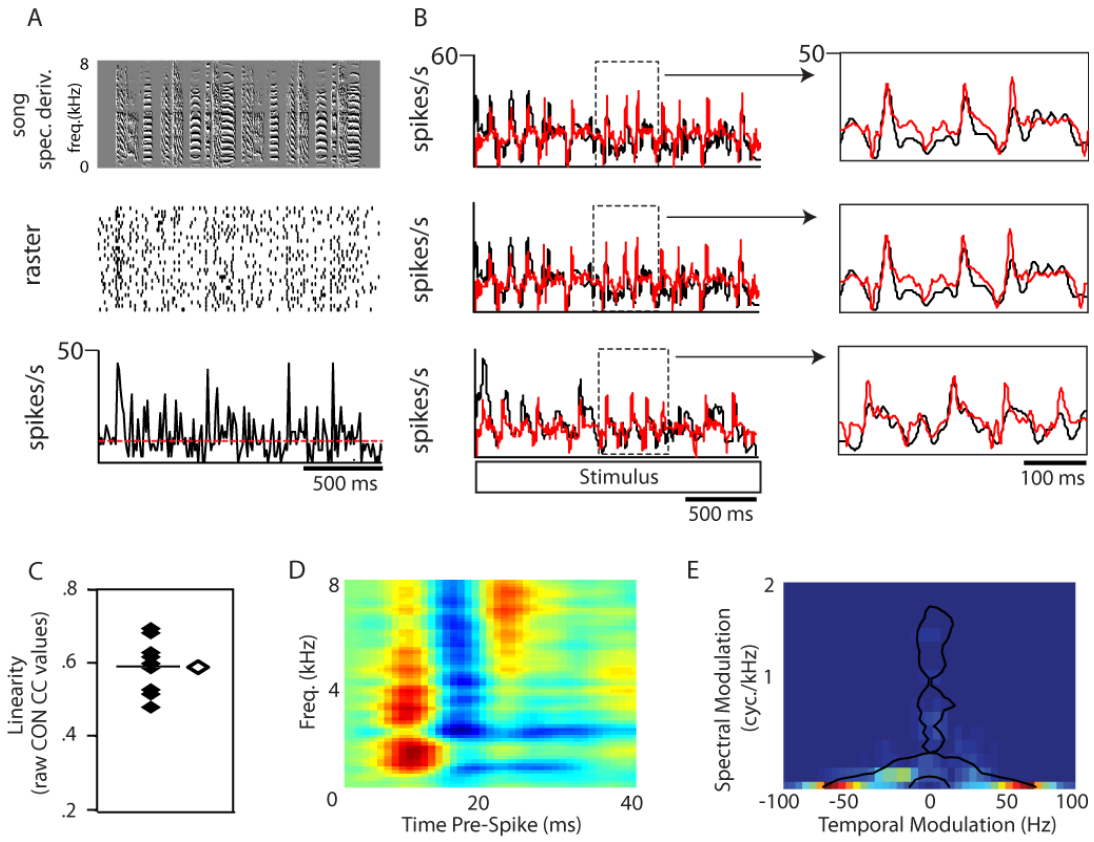
A
B
song
spec. deriv.
freq.(kHz)
8
0
raster
spikes/s
50
500 ms
60
50
Stimulus
500 ms
100 ms
C
Linearity
(raw CON CC values)
.8
.6
.4
.2
D
Freq. (kHz)
8
4
0
20
40
Time Pre-Spike (ms)
E
Spectral Modulation
(cyc./kHz)
2
1
-100
-50
0
50
100
Temporal Modulation (Hz)

Figure 2.4S

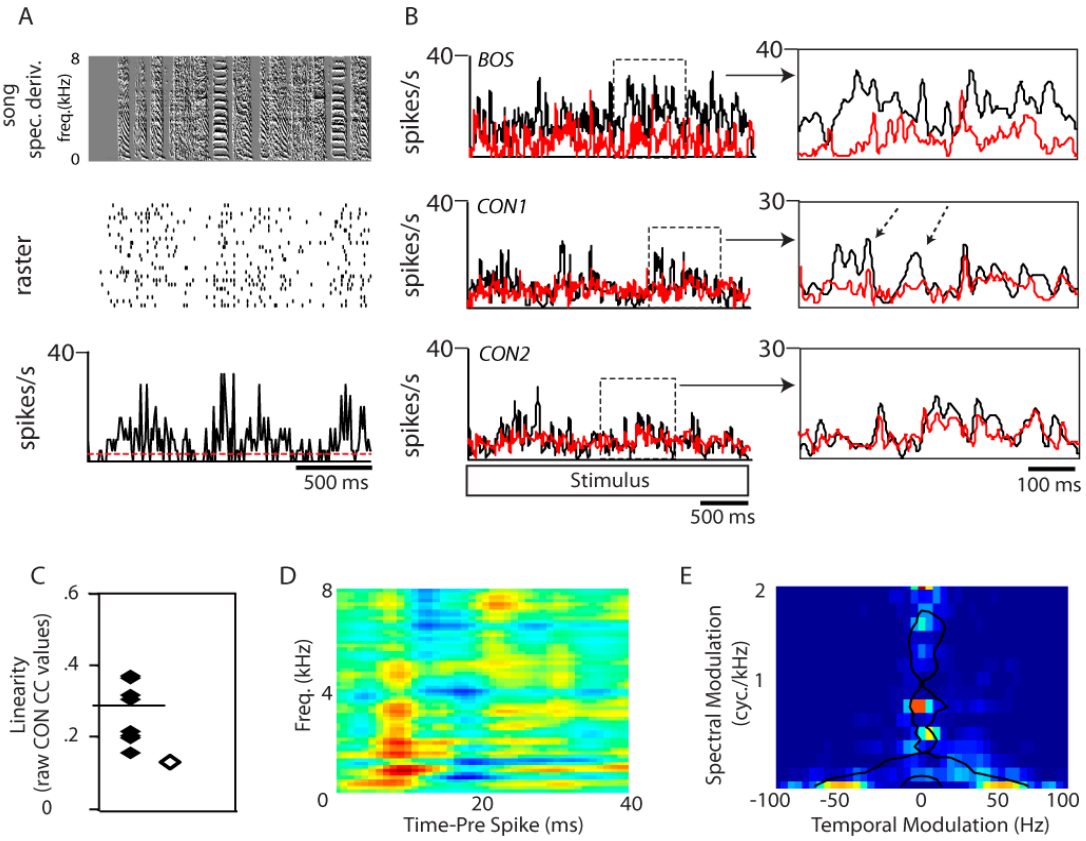
A
B
song
spec. deriv.
freq.(kHz)
8
0
raster
spikes/s
40
500 ms
BOS
CON1
CON2
30
Stimulus
100 ms
C
Linearity
(raw CON CC values)
.6
.4
.2
0
D
Freq. (kHz)
8
4
0
20
40
Time-Pre Spike (ms)
E
Spectral Modulation
(cyc./kHz)
2
1
-100
-50
0
50
100
Temporal Modulation (Hz)

Figure 2.5S

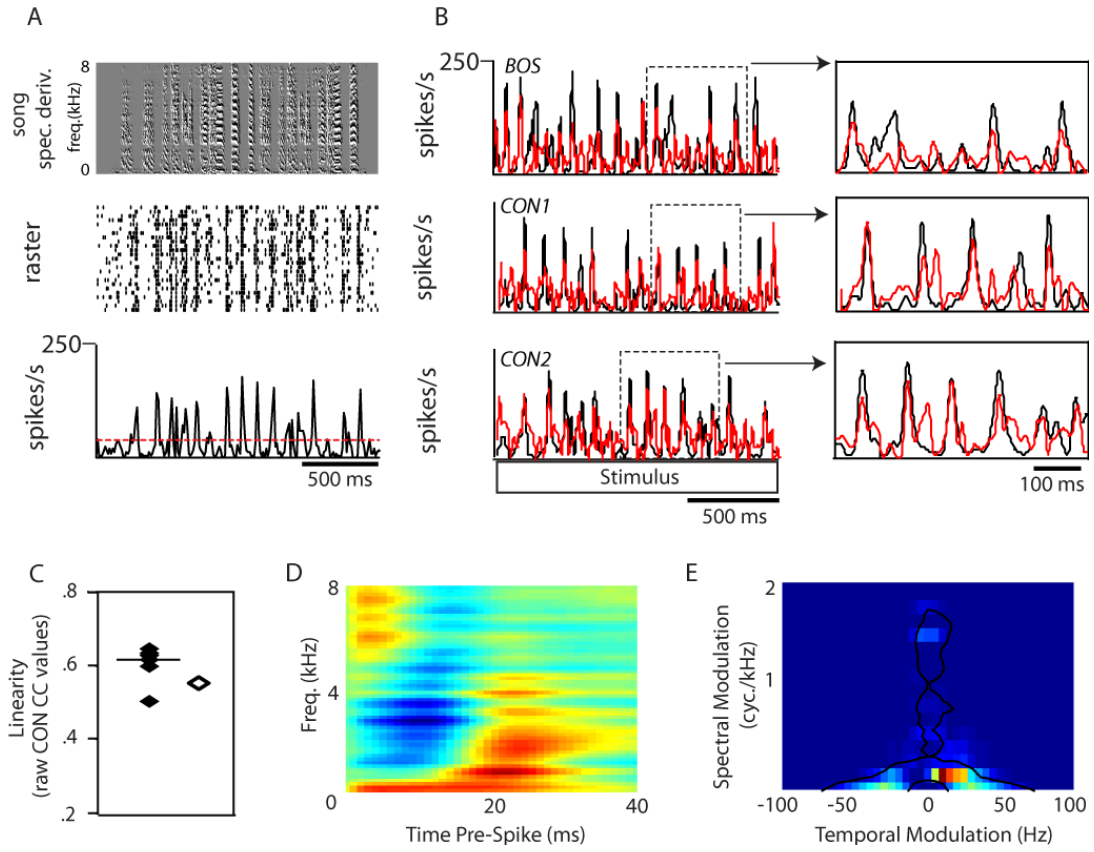
A
B
song
spec. deriv.
freq.(kHz)
8
0
raster
250
spikes/s
500 ms
BOS
CON1
CON2
Stimulus
100 ms
C
Linearity
(raw CON CC values)
.8
.6
.4
.2
D
Freq. (kHz)
8
4
0
20
40
Time Pre-Spike (ms)
E
Spectral Modulation
(cyc./kHz)
2
1
-100
-50
0
50
100
Temporal Modulation (Hz)

Figure 2.6S

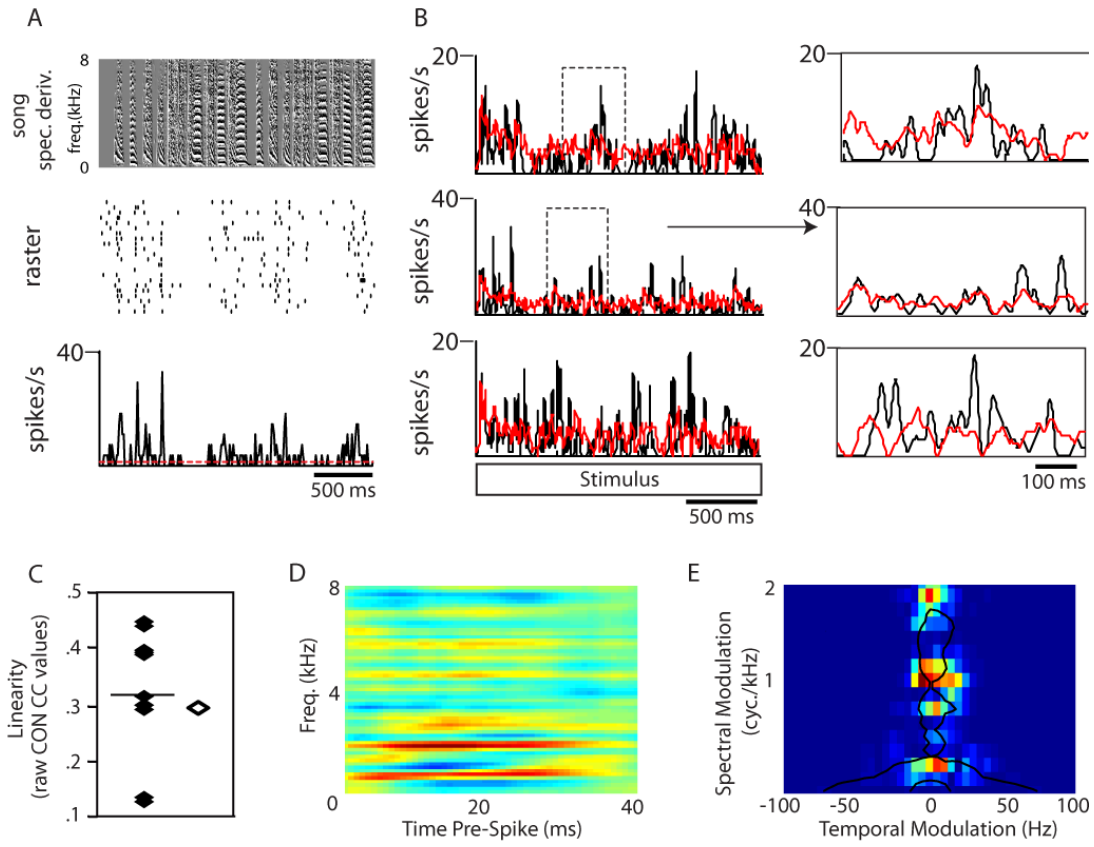
A
B
song
spec. deriv.
freq.(kHz)
8
0
raster
spikes/s
40
500 ms
20
40
20
Stimulus
500 ms
100 ms
C
D
E
Linearity
(raw CON CC values)
.5
.4
.3
.2
.1
Freq. (kHz)
8
4
0
20
40
Time Pre-Spike (ms)
Spectral Modulation
(cyc./kHz)
2
1
-100
-50
0
50
100
Temporal Modulation (Hz)

Figure 2.7S

Chapter 3. Conclusions and Future Directions

Section 1. Heterogeneity of Auditory Responses in Putative HVC_{IN} During Wakefulness

In **Chapter 2**, I demonstrate that a large population (n = 215 cells) of putative HVC interneurons (HVC_{IN}) show a wide array of response properties to bird's own song (BOS) and conspecific (CON) stimuli. Two-thirds of cells showed excitatory responses to one or more BOS and CON stimuli, and nearly half of these cells showed excitatory responses to both types of stimuli. Of the neurons showing excitatory responses to both BOS and CON stimuli, nearly half showed a degree of response linearity, as measured by spectrotemporal receptive field analysis (STRF), comparable to that deemed to be substantial in previous studies in the ascending auditory system (Gill et al., 2008; Woolley et al., 2006). Fourier analysis of STRFs revealed a range of temporal and spectral sensitivities that overlaps substantially with the range of such modulations occurring with high power in the species song (Hsu et al., 2004a). Thus, while the population as a whole is less sensitive to extremely rapid spectral and temporal modulations than the population of cells in the avian auditory cortical analogue Field L (Nagel and Doupe, 2008; Woolley et al., 2009), it may still be well poised to participate in perceptual discriminations tasks in which HVC has previously been demonstrated to be a necessary player (Brenowitz, 1991; Gentner et al., 2000).

The most pressing issue in regard to solidifying this work is to reanalyze all spike data using a sophisticated, automated, Bayesian clustering algorithm (C. Glaze, custom in

MATLAB 7.0). As described in **Chapter 2 (Materials and Methods)**, all spike clustering was carried out in the Spike 2 (version 6, CED, Cambridge, UK) programming environment on a stimulus by stimulus basis. The main weakness of the previous approach is that it is theoretically possible that different principal components were used to generate cluster maps for different stimuli. This new method should yield more accurate results, despite the fact that with the previous method the same template width and amplitude thresholding parameters were used for each stimulus, maps were qualitatively similar across all stimuli for a given cell, and averaged waveforms were verified to be identical for a given putative unit across all stimuli. An additional benefit to the new methodology is that data are analyzed in a completely time-sequential manner. Previously, all trials for a given stimulus were concatenated before analysis; while the pseudo-random presentation paradigm ensured that not very much time elapsed between any two presentations of the same stimulus (see **Chapter 2**, **Materials and Methods**) the several minute gaps between trials may have, in some cases, caused temporal discontinuities between trials that could make it more difficult to track gradual shifts in spike shapes. Finally, the new method has quantitative criteria (the exact details are still pending) for determining whether clusters are sufficiently separated to deem them single units, whereas in the previous methodology such determinations were made on a strictly qualitative basis.

Assuming the results after reanalysis are similar to those obtained with the previous method, there are many possible lines of experimental inquiry to follow up the results. Many of these lines are considered in the **Chapter 2 Discussion**. To my mind, the

most intriguing line of further exploration would be to link HVC auditory responses to functional roles in perceptual discrimination tasks. Gentner et al., 2000 showed that starlings previously trained to distinguish between conspecific (CON) stimuli in a GO/NO GO operant task were impaired in contingency flips in the wake of HVC lesions. Cells and circuits involved in discriminations between stimuli with previously established operationally defined salience would need to carry signals sufficient to not just distinguish the features of these stimuli (as I may have recorded in the experiments described in **Chapter 2**), but also, critically, to link these features to a particular contingency.

Previously, cells in the caudal mesopallium (CM), an area known to send auditory information to HVC (Bauer et al., 2008; Roy and Mooney, 2009), have been shown to respond (at least under anesthesia) to the salience of complex auditory objects. Neurons in this area have been shown to be sensitive both to the prior probability of recent presentations of CON stimuli (Gill et al., 2008), as well as to the previously defined operational salience of CON songs (Gentner and Margoliash, 2003). Results from a single study of auditory responsiveness in CM during wakefulness under salience neutral conditions similar to those under which I recorded in **Chapter 2** (Bauer et al., 2008) suggest a mix of responses with no BOS selectivity and moderate BOS selectivity. Given this profile, it is likely that at least some BOS-CON cells in HVC receive auditory inputs from CM during wakefulness. Based on this logic, it would be interesting (but far from easy) to train birds on an operant task similar to that employed by Gentner and Margoliash (2003) with a set of song stimuli, some with and some without pre-defined

operational salience and then record from individual BOS-CON neurons in HVC during wakefulness. One question would be whether CON stimuli with operational salience showed response properties, including STRF properties, clearly different from those shown by CON stimuli without operational salience (or perhaps those with operational salience but on trials with no operational context).

If BOS-CON neurons in HVC were to show task-related modulation, a logical second order experiment would be to transiently inactivate CM in order to evaluate whether this had effects of feature based and/or task related response properties in HVC. Perhaps perturbation of the activity of single BOS-CON cells within HVC would have detectable effects on perceptual discrimination behavior as well, though effects may only be seen if the functional network for auditory object/operational salience representation is relatively non-distributed (Houweling and Brecht, 2008; Voigt et al., 2008). Gentner et al., 2000 did not evaluate whether HVC is necessary for discrimination behavior involving BOS stimuli. Our discovery of 'hybrid' cells, with partially linear responses to CON stimuli and larger, non-linear responses to BOS stimuli, raises the possibility that at least some BOS-CON cells in HVC are sensitive to differences between BOS and CON stimuli. Given that anterior forebrain vocal motor structures receiving auditory input from HVC (Doupe and Konishi, 1991) have been show to be important for perceptual discriminations involving BOS and CON stimuli, it is likely that HVC is involved as well.

Section 2. Future Directions

Part 1. Overview: Toward Understanding of BOS Selective Auditory Responses

In the remainder of this chapter, I describe preliminary work in which I focus on the properties of BOS-selective neurons in HVC. Most of this work was carried out during sleep, where it has previously been shown in both HVC (Chi et al., 2003; Hahnloser et al., 2008; Rauske et al., 2003) and its immediate afferent in the vocal motor pathway, the robust nucleus of the arcopallium (RA) (Dave and Margoliash, 1998, 2000), that BOS responses are more vigorous than during wakefulness. As I discuss in **Chapter 1, Section 5**, mounting evidence suggests that BOS auditory responses during sleep may provide deep insights in to motor production in the song system. Auditory responses of putative projection neurons in RA during sleep show high temporal alignment with both their own premotor activity and spontaneous activity during non-auditory sleep epochs (Dave and Margoliash, 2000). Likewise, 'mirroring' responses recorded in response to BOS during wakefulness in basal ganglia-projecting HVC neurons (HVC_X) show a high degree of temporal alignment with their own premotor activity (Prather et al., 2008,2009). My own experiments focus on responses in HVC_{IN}, which may lack as a population (but see examples like **Figure 2.5**) the temporal sparseness and precision to facilitate alignments between different activity modes such as have been performed in RA and HVC_X neurons. Nonetheless, as I detail in the final section, their responses can still be probed from the perspective of what they may tell us about motor function in the song system.

Part 2. Auditory Responses of Putative HVC_{IN} Across the Wake-Sleep Boundary

Though it is often assumed that the transition from wakefulness to non-REM sleep is associated with a closing of the forebrain to sensory signals (Steriade et al., 1993; McCormick and Bal, 1997), few studies have looked at cross-state response dynamics in single cortical neurons. Studies in the visual (Evarts, 1963; Livingstone and Hubel, 1981), somatosensory (Gùcer, 1979) and auditory (Edeline et al., 2001) cortices have indeed demonstrated decreased neural responsiveness at the population level during non-REM sleep. However, several studies in the auditory cortex (Edeline et al., 2001; Issa and Wang, 2008; Pena et al., 1999) have demonstrated that many individual cells either maintain or increase their responsiveness during non-REM sleep. It is not known whether cross-state response strength heterogeneity generalizes beyond mammalian primary sensory cortex.

In songbirds, as in mammals, loop circuitry reciprocally connects thalamic and forebrain structures (Striedter and Vu, 1998; Vates et al., 1997) and the forebrain shows the electroencephalographic hallmarks of REM and non-REM sleep (Szymczak et al., 1996; Low and Margoliash, 2008). The forebrain song nucleus HVC (proper name) receives input from a polymodal thalamic relay (nucleus uvaeformis, Uva) (Streidter and Vu, 1998; Wild, 1994). As with thalamic relay activity in mammals (Glenn and Steriade, 1982; Swadlow et al., 2002), sleep bursting in Uva is associated with a transition from single spike to burst mode in HVC interneurons (HVC_{IN}) (Hahnloser et al., 2008). The transition from wakefulness to sleep is associated with a large increase in auditory response strength to the bird's own song (BOS) in single neurons of the main afferent of HVC in the vocal motor pathway (the robust nucleus of the acropallium, RA) (Dave et

al., 1998; Dave and Margoliash, 2000). In HVC itself, however, which appears to provide all auditory drive to RA (Doupe and Konishi, 1991), there have been very few recordings of auditory responses in single neurons across the wake-sleep boundary (Hahnloser et al., 2008; Rauske and Margoliash, 2003), and the few studies that have been carried out have looked at responses to only BOS and one or several other stimuli.

I have recorded from a fairly large population (n = ~70) of HVC_{IN} (see **Chapter 2** for criteria for identifying single HVC_{IN}) across the wake-sleep boundary while presenting BOS and a large ensemble (10-12) CON stimuli. Preliminary results suggest that the transition from wakefulness to sleep is not accompanied by a uniform change in response patterns across all single units, which corroborates the findings of a previous cross-state study of a very small population (n =10 cells) of single putative HVC_{IN} in which the ratio of response strengths to BOS in waking vs. sleeping birds ranged widely (Rauske et al., 2003). Cases where BOS and CON response strengths are modulated in different directions (see **Figure 3.2 and Figure 3.5A**) across the wake-sleep boundary challenge simple models in which changes in thalamic firing properties control the gain of HVC auditory response properties in a simple linear manner (Hahnloser et al., 2008). Despite the heterogeneity on a cell by cell basis, I have found that the general trend is for an increase in responsiveness to BOS stimuli across the wake-sleep boundary (see **Figure 3.5 A,B**), which was also a significant trend in the Rauske et al. study despite the aforementioned cell to cell variability in modulation of response strength. Interestingly, Cardin and Schmidt (2003) found no significant difference in BOS response strength across the wake-sleep boundary at the massively multiunit level. This is yet another

difference between the findings of Rauske et al., 2003 and Cardin and Schmidt, 2003 (discussed at length in **Chapter 1, Section 2**) and likely primarily reflects (as discussed in **Chapter 1**) a difference in the types of neurons recorded from with the two very different techniques.

Figures 3.1-3.4 provide a qualitative description of the various response transition flavors I encountered in my recordings. If I were to proceed with this data set, one of the principle challenges would be to come up with a prudent way to delineate when response changes across states were significant. A particular complication in this regard is that only a single BOS stimulus was presented while a large set (10-12) of CON stimuli were presented. Thus, it would be more likely that small response strength changes in response to one or more CON stimuli would be picked up as significant as opposed to equal-sized changes in response to the single BOS stimulus. A second challenge would be to figure out a way to incorporate spectrotemporal receptive field analysis (STRF) to evaluate whether linear receptive field properties change across defined natural states. Such a study would be informative, since only a single study I am aware of (in the auditory cortex of marmosets; Issa and Wang, 2008) has looked at receptive field dynamics across the wake-sleep boundary in response to ethologically relevant stimuli. However, many of the neurons I managed to hold across the wake-sleep boundary showed relatively weak responses to CON stimuli during wakefulness and these responses were often further attenuated during sleep (see **Figure 3.5**). Thus, while I have preliminarily employed a well established method for comparing STRFs across states (SI Index; Escabi and Schreiner, 2002; Woolley et al., 2006) there are major questions surrounding the validity

of this approach when the responses being measured, at least during sleep, have very low response strengths associated with them.

Part 3. BOS Responses During Sleep in the Wake of Peripheral Song Production Disruption

In **Part 2** of the **Future Directions** chapter, I describe preliminary evidence corroborating earlier work (Rauske et al., 2003) suggesting that the responses of single units to the bird's own song (BOS) increase in their vigor across the transition from wakefulness to sleep. I also report that, for the most part, responses to non-BOS stimuli are attenuated during sleep relative to wakefulness in putative HVC interneurons (HVC_{IN}). The functional significance of auditory responses highly selective for BOS remains one of the most enigmatic questions associated with the song system. During wakefulness, highly BOS selective responses occur in basal ganglia-projecting neurons (HVC_X), and these responses demonstrate high temporal congruity with the premotor song activity shown by the same neurons during song production (Prather et al., 2008; Prather et al., 2009). While such activity suggests a deep linkage between auditory and motor function (indeed, the authors dub these to be 'mirroring' responses), there have been no attempts to either provide a functional significance to them or to enact a manipulation to attempt to dissociate sensory and motor properties.

So how might one challenge the system to evaluate the specific relationship between sensory and motor representations? One approach is to manipulate motor output in the periphery such that central motor commands result in unexpected feedback.

Transection of the tracheosyringial nerve (ts transection) causes an immediate disruption of spectral, but not temporal, features of song production in the zebra finch (Williams et al., 1992; Williams and McKibben, 1992). Bilateral ts transections, among other effects, remove all learned frequency components from song (and distance call) output. Unilateral ts transections, especially right side transections, greatly reduce the amount of frequency complexity in song output without causing the breathing distress induced by bilateral transections. In a subset of birds, ts transections induce changes to song syntax, which, as opposed to the immediate disruption of spectral content, manifest days to weeks after transection. These temporal disruptions, which can include stuttering of pre-existing or novel elements, and additions and deletions of elements, have been shown to be centrally mediated. These changes, but not spectral changes, do not occur if nerve injury is induced after disruption of LMAN (Williams and Mehta, 1999), which provides the output of a thalamocortical basal ganglia pathway critical for vocal learning (Aronov et al., 2008; Scharff and Nottebohm, 1991) on to the primary vocal motor axis.

Because ts transection causes immediate and permanent (I remove the distal stump to prevent regrowth) spectral changes in all birds, and later temporal changes in a subset of birds (the exact proportion varies widely from study to study and seems to be highly sensitive to song analysis methodology), it is a useful tool for evaluating the properties of BOS responses in sensorimotor neurons. I have recorded from >20 birds during sleep at various time points following ts transection. The study is not truly longitudinal, in that recording of a given bird has been restricted to a narrow time window (no longer than four days) due to technical concerns. The basic question I have

begun to ask is whether neurons continue to favor the version of BOS that pre-existed the transection, i.e. the version presumably intended by the central motor program, or do they begin to show preference for the spectrally disrupted version that comes back to the sensory and sensorimotor systems each time the bird sings in the wake of ts transection. A second-order question is whether relative preference for pre vs. post ts transection song is in any way related to the central commitment to change the motor program (syntax plasticity) shown by a proportion of the birds with some delay relative to the immediate spectral effects.

A range of outcomes are clearly possible; a 'motor template' hypothesis might suggest that neurons remain highly tuned to the original song no matter the spectral and/or subsequent temporal consequences of ts transection. Such an outcome would strongly suggest that the sensory response is immutably imprinted during the initial learning of song. A 'sensory' hypothesis might suggest that neurons rapidly come to prefer the spectrally degraded version of song induced immediately upon ts transection. This outcome would imply that these responses are truly sensory in nature, and that they align with the motor representation of song in adult birds because of the tight correspondence between intended and actual output. A 'sensorimotor' hypothesis would suggest that relative preference may be contingent on whether the system has made the commitment to change the temporal pattern of song in the days to weeks following ts transection.

My preliminary results rule out the extreme 'motor template' hypothesis and lean toward a hybrid of the 'sensory' and 'sensorimotor' type hypotheses. **Figures 3.6** and **3.7**

depict neurons from two different birds highly representative of those recorded (n = 5 birds) during the first week post right ts transection. Even though all birds have heard themselves produce numerous renditions (usually hundreds of motifs) of spectrally degraded songs by the time of neural recording, neurons remain highly preferential for the features of pre ts transection BOS. In these two birds, as in the other three first week birds, the temporal pattern of song was highly conserved at the time of neural recording. Thus, it is clear that temporal song characteristics alone do not dictate responses in these neurons; otherwise, the pre and post ts transection versions would show similar responses.

In the second and third weeks post ts transection (n = 8 birds), the story begins to get more complicated. **Figure 3.8** depicts a cell recorded in the second week post ts transection (I should add here that all cells recorded in a given bird at a given time point tended to have at least qualitatively similar preferences) that showed a strong preference for the pre ts transection song and virtually no responsiveness to features of the post transection song, like that shown by all cells in the first week post ts transection. In some birds during the second week post ts transection (represented by **Figure 3.9**), however, responses to at least some features of post transection song began to show some vigor, despite the fact that these elements were spectrally quite different that those of the identical elements in pre transection song. The bird depicted in **Figure 3.9** is notable in that he showed syntax changes starting late in the first week post ts transection. Interestingly, a response peak during the latter half of the element 'D' was stronger when preceded by its normal 'C' as opposed to by the novel element 'X'. Novel and non-

stereotyped elements appear to generally be associated with weak responses (see also **Figure 3.13**) and this phenomenon may be related to the consequences of violating sensorimotor prediction previously shown during sleep by auditory units in RA (see **Section 5** of **Introduction** for details).

Three birds recorded in the second and third weeks post ts transection had cells with properties similar to those depicted in **Figure 3.10**. These cells showed a near complete reversal of the situation from first week birds; cells showed relatively strong preference for post ts transection song and a near absence of response to pre transection song. Though the bird depicted in **Figure 3.10** showed no overt syntax change at all at the time of recording, he and two others with cells showing strong preference for post ts transection song during weeks two and three post ts transection went on to show syntax changes within several weeks after these recordings were made. Thus, the intriguing possibility exists that preference for the spectrally degraded song in the wake of ts transection is in some way predictive (if not a precondition) of subsequent syntax changes. Such anticipatory tuning shifts have recently been seen in the second and third weeks post ts transection in urethane anesthetized birds in LMAN (Roy and Mooney, 2009). Nonetheless, data from more birds during this interesting period, ideally with diverse syntax change outcomes in terms of both type and timing, is needed before conclusions can be made about the factors critical for dictating whether tuning shifts will occur.

Results from birds recorded more than one month post ts transection (n = 12 birds) bolster the notion that the sleep BOS responses of HVC neurons show a mix of

sensory and sensorimotor properties. Regardless of syntax status, all cells from birds recorded more than a month post ts transection showed bias toward the current version of the song. The cells depicted in **Figures 3.11** and **3.13** share a common thread in that both birds showed song largely conserved from pre ts transection versions, though with the addition of a novel element outside of the core motif. Both depicted cells showed preference for the current post ts transection song, though the cell depicted in **Figure 3.13** showed a substantially higher degree of selectivity. The cell depicted in **Figure 3.12,** like the one shown in **Figure 3.13**, had a very high degree of selectivity for the current post ts transection song. However, this bird had a song motif that, save for the first element, was completely different from the original motif. While long term restabilization with a new motif has been reported in the literature as a fairly common phenomenon (Williams and Mehta, 1999) this bird is my only example that I have recorded sleep auditory responses from. Thus, it is impossible at this point to know whether the most radical syntax changes are reliably associated with the strongest post ts transection tuning.

Figure Legends

Figure 3.1. Examples of three variants of BOS selective neuron across the wake-sleep boundary. (A) This neuron showed a significant excitatory response to BOS during wakefulness (green on raster and PSTH) and a larger excitatory response during sleep (red on raster and PSTH). In contrast, CON responses (representative example shown) were either suppressive or non-significant during wakefulness and more strongly suppressive during sleep. (B) This neuron showed no significant response during wakefulness to BOS but had a significant response during sleep. CON responses, when present, were suppressive, when present, during wakefulness and remained similar during sleep. (C) This neuron showed no detectable activity, spontaneous or otherwise, during wakefulness but had a strong BOS response during sleep. CON responses during sleep were suppressive to all presented stimuli.

Figure 3.2. Examples of BOS-CON cells showing bi-directional modulation of auditory responses across the wake-sleep boundary. (A) This cell showed a relatively strong excitatory response to BOS during wakefulness and a substantially increased response strength during sleep. In contrast, significant excitatory responses to CON stimuli were seen during wakefulness, but there was a dramatic shift during sleep, when almost all CON stimuli elicited suppressive responses. (B) This cell showed response trends during sleep similar to those seen in the cell depicted in A, though responses during wakefulness and sleep were more phasic and the degree of change in response to both BOS and CON stimuli across states was more modest.

Figure 3.3. **A simultaneous recording on the same electrode of two very different response types.** The cell depicted in (A) was one of the few highly linear cells I held across the wake-sleep transition. It showed an uncommon decrement in response strength to both BOS and CON stimuli during sleep (and subsequent recovery during wakefulness). In contrast, the BOS response in (B) goes from weakly to strongly excitatory across the wake-sleep transition, while the response to CON moves from weakly excitatory to some stimuli to non-significant or weakly suppressive during sleep. This response profile was fairly common in the population of neurons recorded across the wake-sleep boundary (see **Fig. 3.1** for similar examples).

Figure 3.4. Examples of two less common response transition types.

(A) This cell showed modest excitatory responses to both BOS and CON stimuli during wakefulness and increased response magnitude to both types of stimuli during sleep. (B) This cell showed robust excitatory responses to both BOS and CON stimuli during wakefulness with no significant changes in either type of response during sleep.

Figure 3.5. BOS-CON cells tended to show increased response magnitude to BOS and decreased response magnitude to CON across the wake-sleep transition. (A) For all cells showing excitatory response to BOS and CON stimuli during wakefulness (BOS-CON cells; n = 43) change in mean CON RS_{INDEX} from wake to sleep (x-axis) is plotted against the same change for BOS RS_{INDEX}. The majority of these cells (top left quadrant) showed increased responsiveness to both BOS and CON stimuli, while a significant majority (bottom left quadrant) showed decreased responsiveness to both kinds of

stimuli. (B) RS_{INDEX} to CON stimuli showed a significant decrease across the wake-sleep boundary in the population of BOS-CON neurons. RS_{INDEX} to BOS stimuli, in contrast, showed a significant increase across the wake-sleep boundary. (C) During sleep, in the population of BOS-CON neurons, the mean percentage of CON stimuli receiving significant excitatory responses decreased across the wake-sleep transition, while the mean percentage of CON stimuli receiving significant inhibitory responses increased across the wake-sleep transition.

Figure 3.6. Sleep auditory responses of HVC_{IN} in the first week post ts nerve transection show strong preference for the pre transection song: Example I

As was typical of cells in first week post ts nerve transection birds, response was highly tuned to the pre transection song (A). There was very little response to the first week post transaction song (B) or songs of intact conspecific (CON) birds (C). The temporal structure of song was identical in the pre and post ts nerve transection conditions, as indicated by the syntax labels (in red in A and B). In **Figures 3.6-3.13**, syntax structure of BOS songs is indicated in red. Syntax that is conserved (though spectrally altered post ts nerve transection) has letters that are the same across stimuli. Syntax elements that are new to post nerve transection song are labeled in parentheses and assigned late alphabetic letters (most commonly X). Lowercase letters denote introductory elements, which are not considered part of the motif proper and are produced in variable amounts from rendition to rendition. Letters followed by an apostrophe denote elements which are likely slightly modified versions of pre existing elements (e.g. A and A'). Each figure part (A,B, and C) in **Figures 3.6-3.13** consists, top to bottom, of a song amplitude

waveform, a spectral derivative of song (a form of time-frequency representation), a trial by trial raster of neural events, and a peri-stimulus time histogram (PSTH) of neural events normalized to spikes/s.

Figure 3.7. Sleep auditory responses of HVC_{IN} in the first week post ts nerve transection show strong preference for the pre transection song: Example II

This neuron, as the one in the previous figure from a different bird, was highly selective for the pre ts nerve transection BOS, with very little response to either the first week post transection BOS or the song of a conspecific. This bird demonstrated some degree of syntax variability both before and immediately following nerve injury.

Figure 3.8. An HVC_{IN} recorded during sleep in the second week post ts nerve transection showing strong preference for pre transection song

This bird had stable song at the time of neural recording and also at a later time point. Though this cell showed robust selectivity for pre-transection song, there was some response to at least one feature of post cut song (end of element C).

Figure 3.9. An HVC_{IN} recorded during sleep in the second week post ts nerve transection showing strong responses to both pre and post transection song

Though response to pre ts transection song was still slightly stronger than that to post ts transection song, the bias was much lower than that shown by any cells in the first week post ts nerve transection. Interestingly, this bird had begun to show song syntax plasticity by the time of neural recording, which may be a factor in the tuning bias of neurons recorded from this bird.

Figure 3.10. An HVC_{IN} recorded during sleep in the second week post ts nerve transection showing strong preference for post transection song. Several birds showed this complete reversal from the typical case in first week birds during the second week post ts nerve transection. Though this bird showed no syntax changes at the time of neural recording, he and several others went on to show syntax plasticity six week post ts nerve transection (not shown). Thus, it is possible that strong tuning preference for post ts transection song may be linked to subsequent vocal motor plasticity.

Figure 3.11. HVC_{IN} recorded in the long term post ts nerve transection all show some degree of tuning bias toward the current song: Example I. The bird in this example maintained his pre-transection syntax, though he added a variable repeat of a novel element (X) and a slightly modified version of a pre-existing element (F'). This neuron, as many in long term post ts nerve transection birds, maintained some degree of response to some features of pre-nerve transection song.

Figure 3.12. HVC_{IN} recorded in the long term post ts nerve transection all show some degree of tuning bias toward the current song: Example II. This bird showed a radical syntax rearrangement in the long term post ts nerve transection. The song became newly stereotyped conserving only a single element (A) from the original song. Cells in this bird showed very little response to features of the previous song, though I have not recorded from other birds with such radical syntax change and restabilization to evaluate whether the degree of the preference for the current song is related to the nature of the syntax changes.

Figure 3.13. HVC_{IN} recorded in the long term post ts nerve transection all show some degree of tuning bias toward the current song: Example III. This bird maintained the integrity of his original song structure (save for the common deletion of a high tonal element immediately upon nerve transection) though by the time of recordings produced a stutter of a novel element (X) a highly variable number of times. Interestingly, responses to all cells recorded in this bird were very weak or nonexistent to the novel stuttered element. This phenomenon was seen in multiple birds at both short (see **Figure 3.9**) and long timepoints relative to nerve transection.

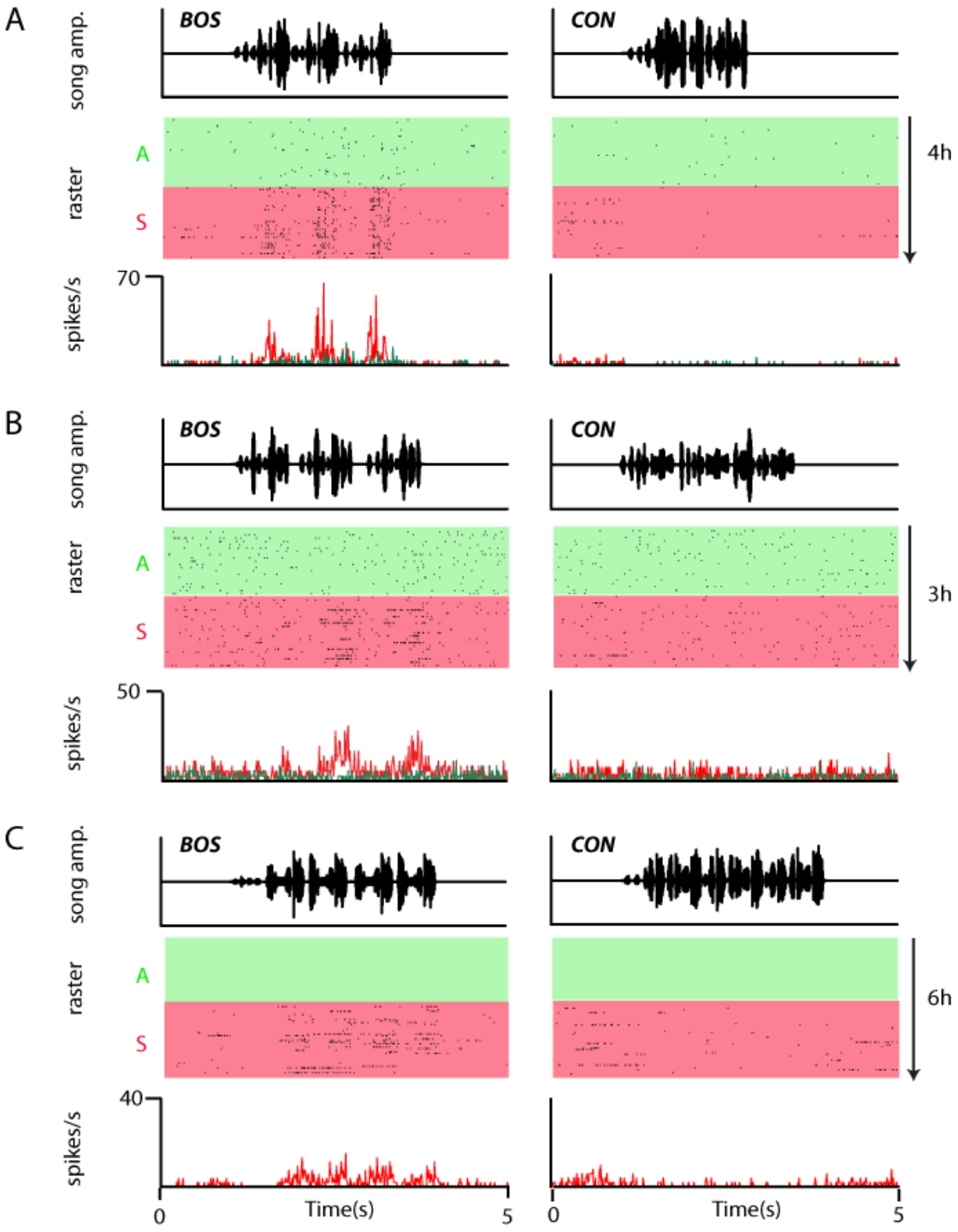
A
song amp.
BOS
CON
raster
A
S
4h
spikes/s
70
B
song amp.
BOS
CON
raster
A
S
3h
spikes/s
50
C
song amp.
BOS
CON
raster
A
S
6h
spikes/s
40
0
Time(s)
5
0
Time(s)
5

Figure 3.1

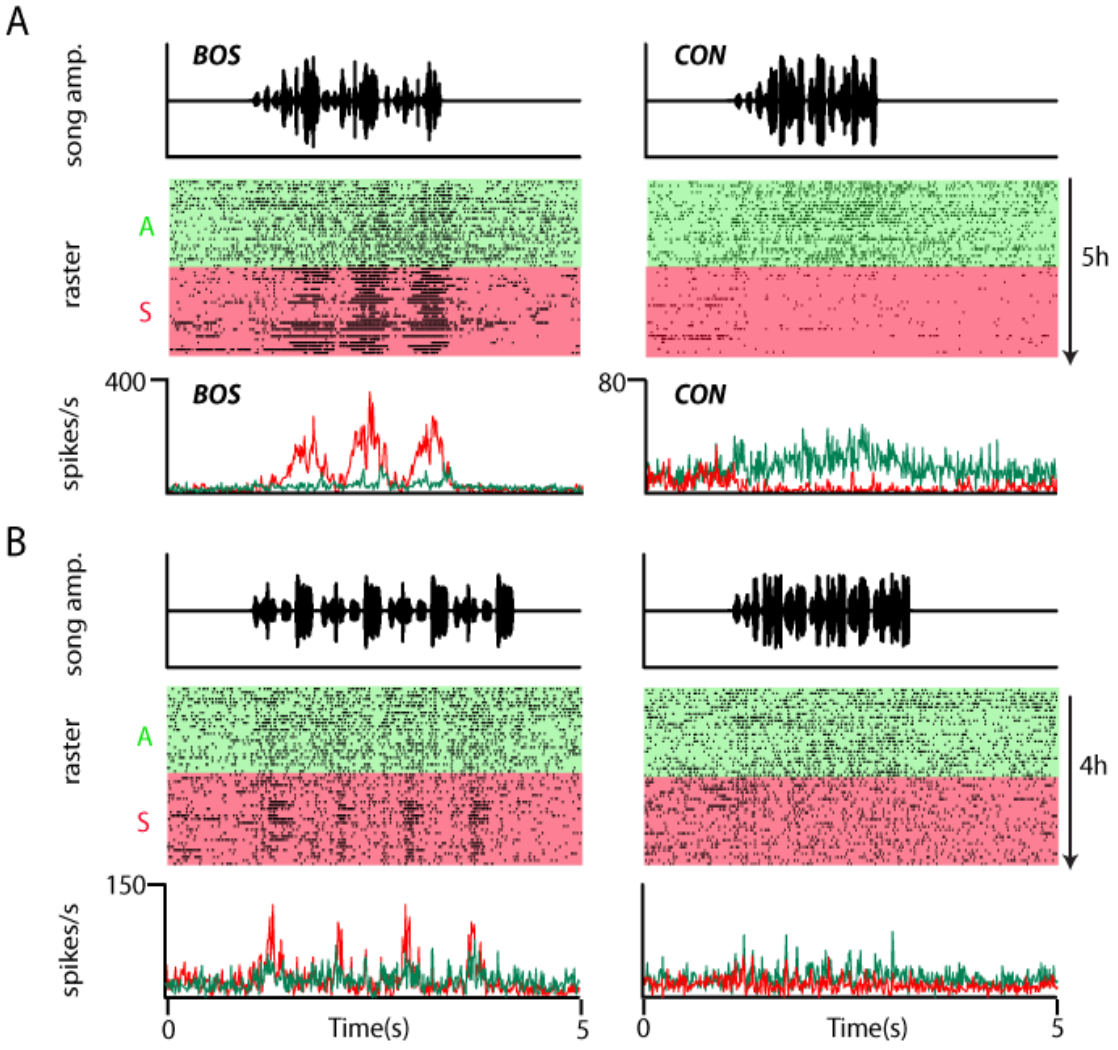
A
song amp.
BOS
CON
raster
A
S
5h
spikes/s
400
BOS
80
CON
B
song amp.
raster
A
S
4h
spikes/s
150
0
Time(s)
5
0
Time(s)
5

Figure 3.2

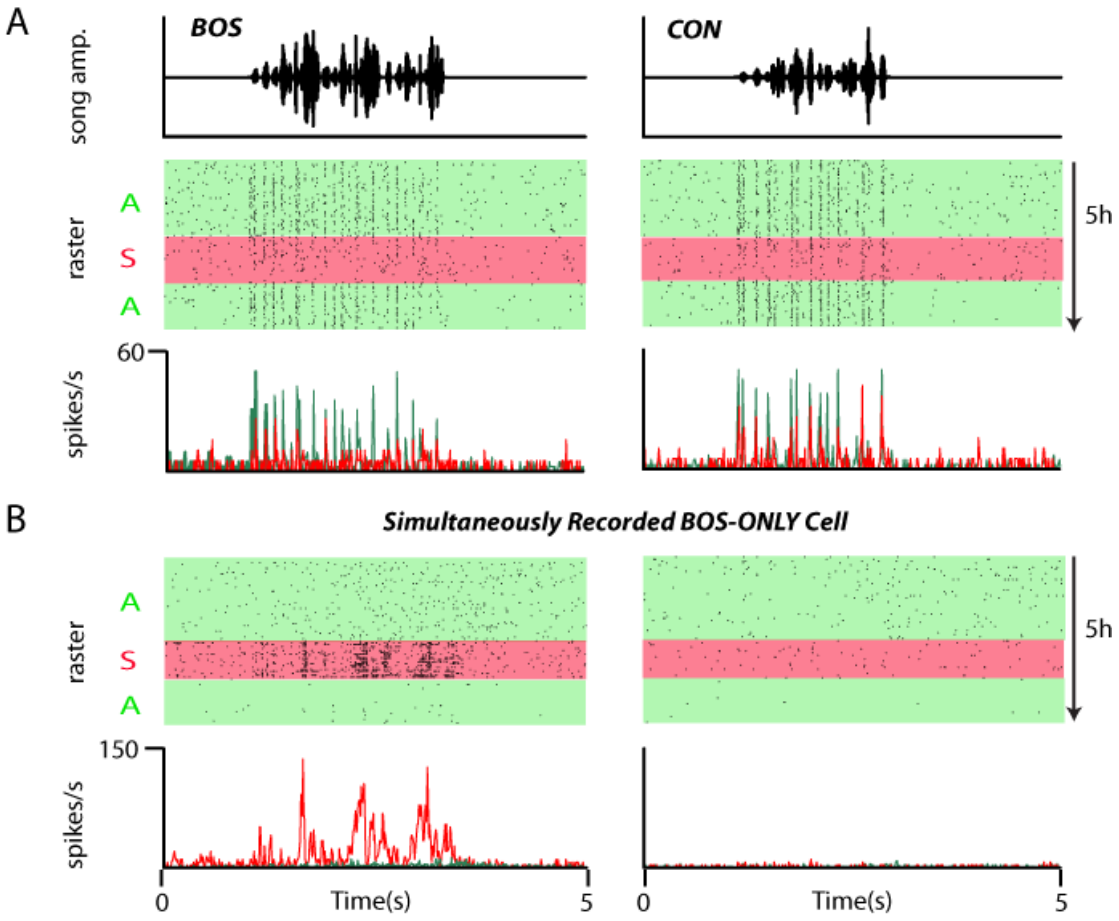
A
song amp.
BOS
CON
raster
A
S
A
5h
spikes/s
60
B
Simultaneously Recorded BOS-ONLY Cell
raster
A
S
A
5h
spikes/s
150
0
Time(s)
5
0
Time(s)
5

Figure 3.3

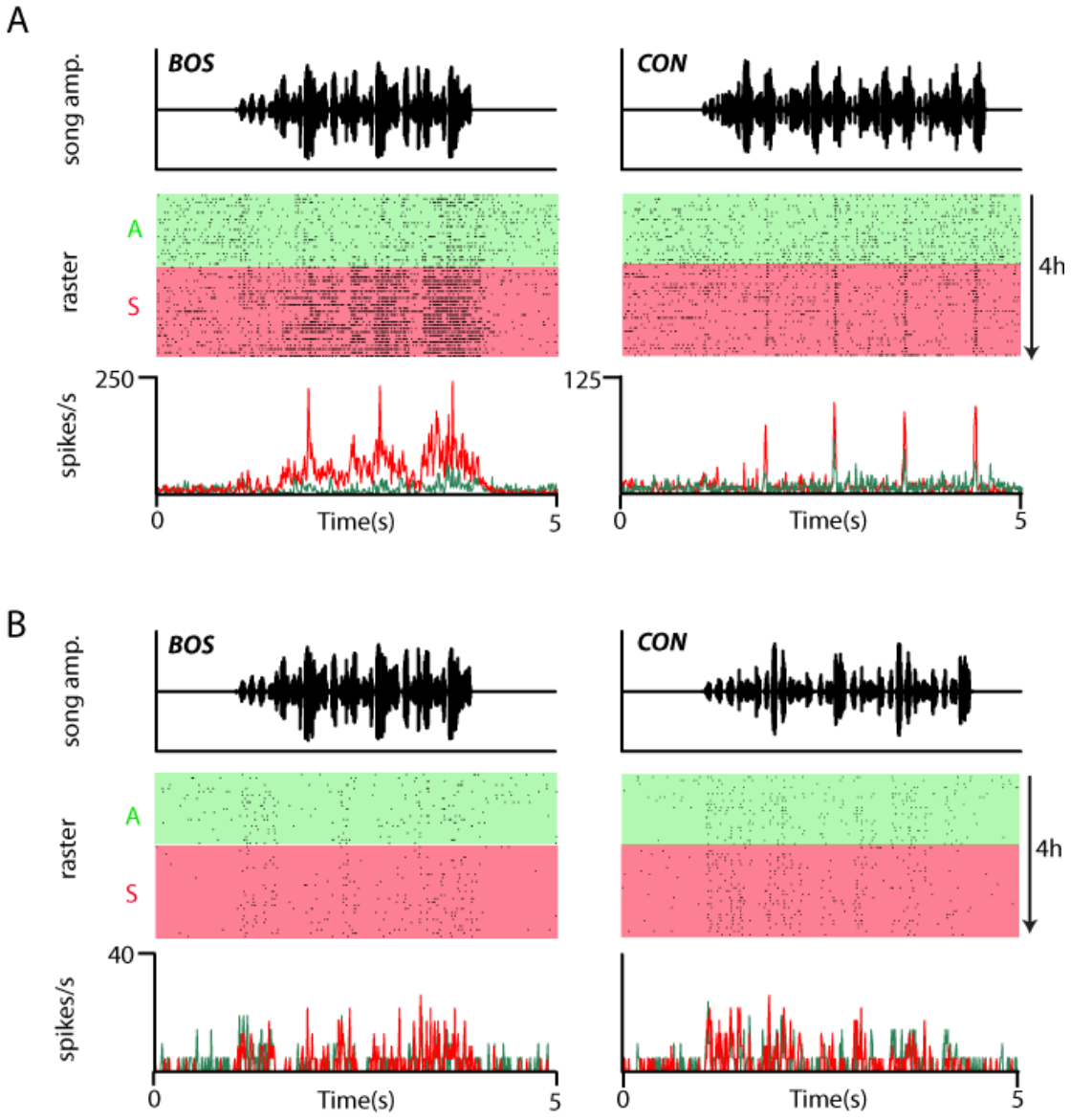
A
song amp.
BOS
CON
raster
A
S
4h
spikes/s
250
125
0
Time(s)
5
B
song amp.
BOS
CON
raster
A
S
4h
spikes/s
40
0
Time(s)
5

Figure 3.4

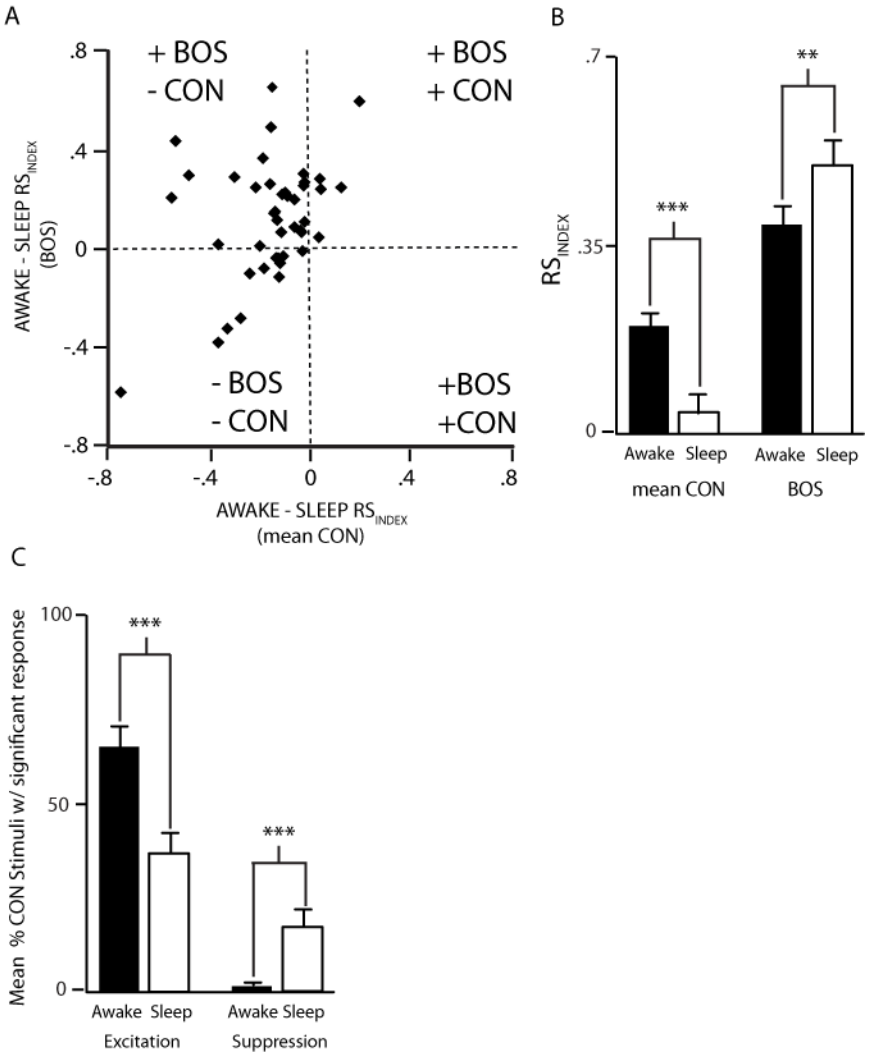
A
+ BOS
- CON
+ BOS
+ CON
- BOS
- CON
+BOS
+CON
.8
.4
0
-.4
-.8
AWAKE - SLEEP RS INDEX (BOS)
AWAKE - SLEEP RS INDEX (mean CON)
B
.7
.35
0
RS INDEX
***
**
Awake Sleep
Awake Sleep
mean CON
BOS
C
100
50
0
Mean % CON Stimuli w/ significant response
***
***
Awake Sleep
Awake Sleep
Excitation
Suppression

Figure 3.5

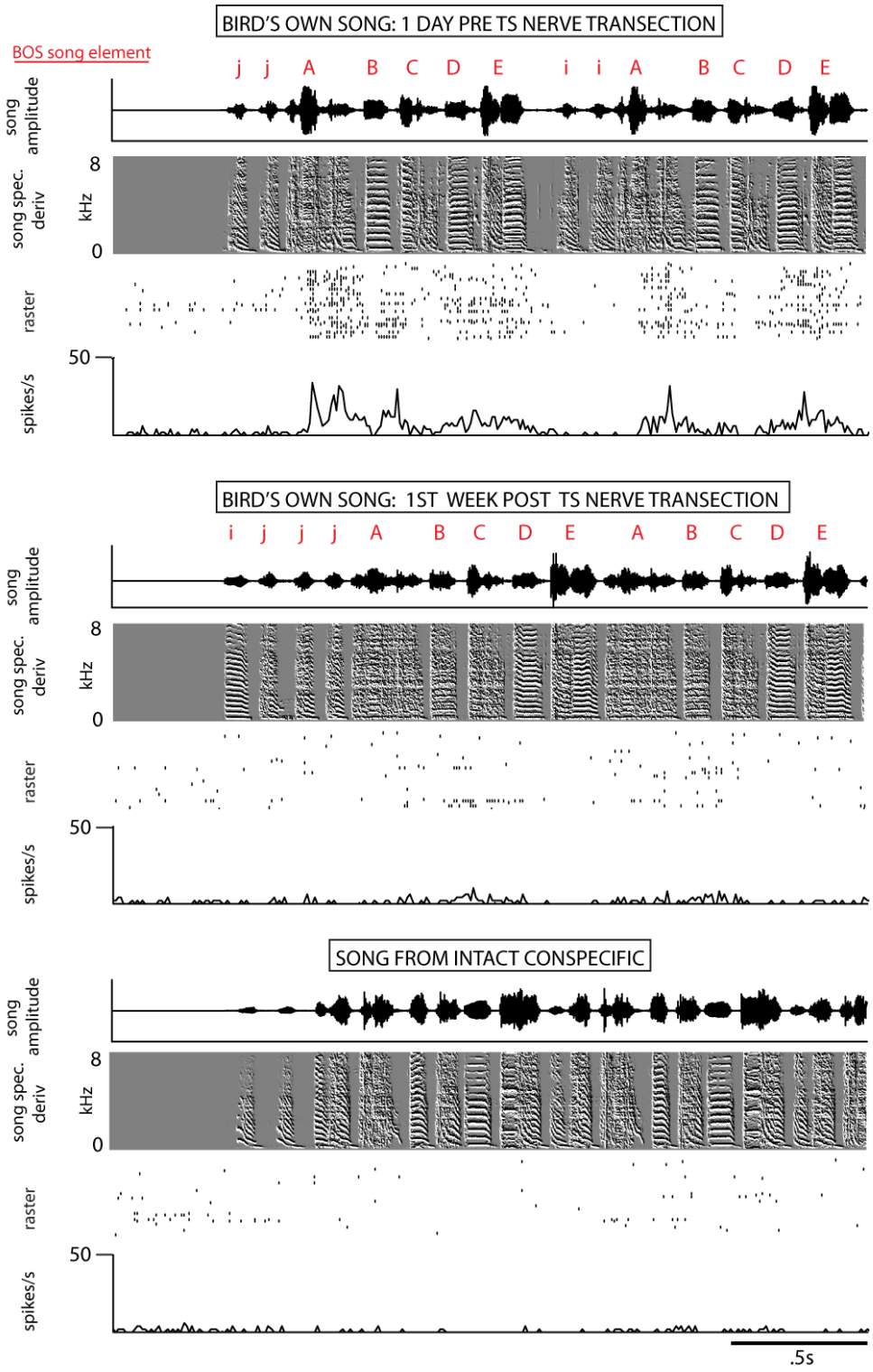
BIRD'S OWN SONG: 1 DAY PRE TS NERVE TRANSECTION
BOS song element
j j A B C D E i i A B C D E
song amplitude
song spec. deriv
8
kHz
0
raster
50
spikes/s
BIRD'S OWN SONG: 1ST WEEK POST TS NERVE TRANSECTION
i j j j A B C D E A B C D E
song amplitude
song spec. deriv
8
kHz
0
raster
50
spikes/s
SONG FROM INTACT CONSPECIFIC
song amplitude
song spec. deriv
8
kHz
0
raster
50
spikes/s
.5s

Figure 3.6

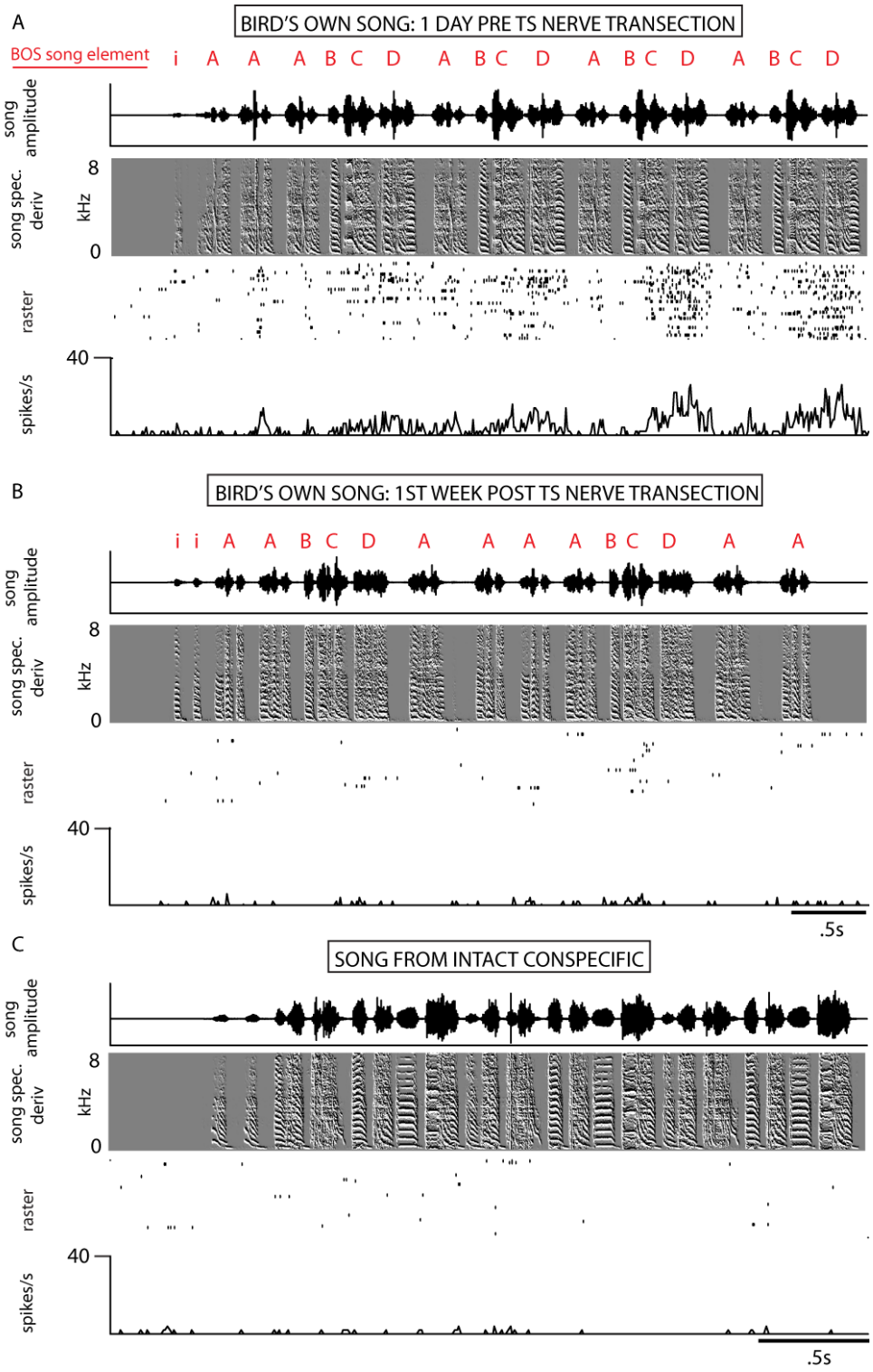
A
BIRD'S OWN SONG: 1 DAY PRE TS NERVE TRANSECTION
BOS song element
i A A A B C D A B C D A B C D A B C D
song amplitude
song spec. deriv
8
kHz
0
raster
40
spikes/s
B
BIRD'S OWN SONG: 1ST WEEK POST TS NERVE TRANSECTION
i i A A B C D A A A A B C D A A
song amplitude
song spec. deriv
8
kHz
0
raster
40
spikes/s
.5s
C
SONG FROM INTACT CONSPECIFIC
song amplitude
song spec. deriv
8
kHz
0
raster
40
spikes/s
.5s

Figure 3.7

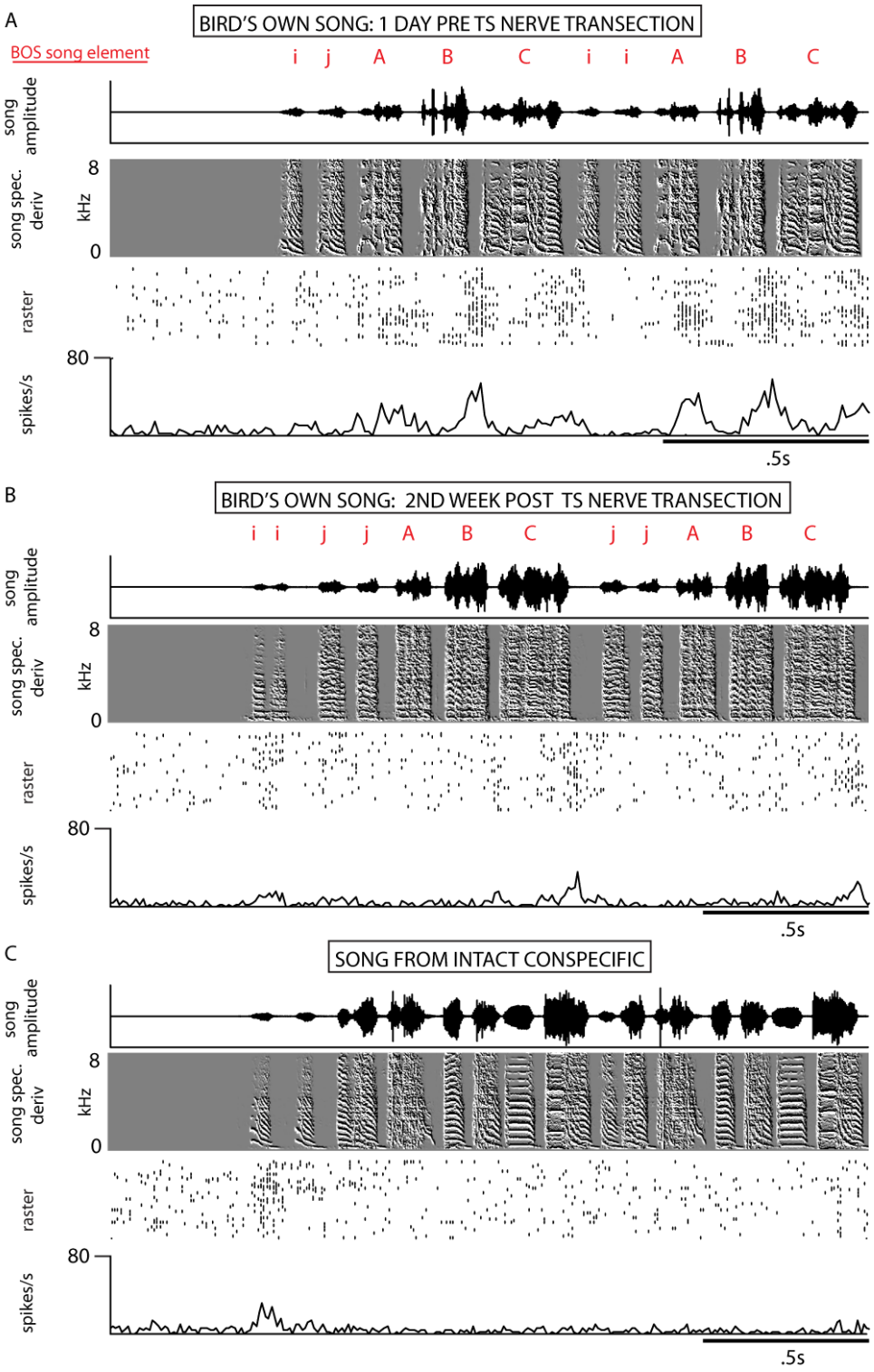
A
BIRD'S OWN SONG: 1 DAY PRE TS NERVE TRANSECTION
BOS song element
i j A B C i i A B C
song amplitude
song spec. deriv
8
kHz
0
raster
80
spikes/s
.5s
B
BIRD'S OWN SONG: 2ND WEEK POST TS NERVE TRANSECTION
i i j j A B C j j A B C
song amplitude
song spec. deriv
8
kHz
0
raster
80
spikes/s
.5s
C
SONG FROM INTACT CONSPECIFIC
song amplitude
song spec. deriv
8
kHz
0
raster
80
spikes/s
.5s

Figure 3.8

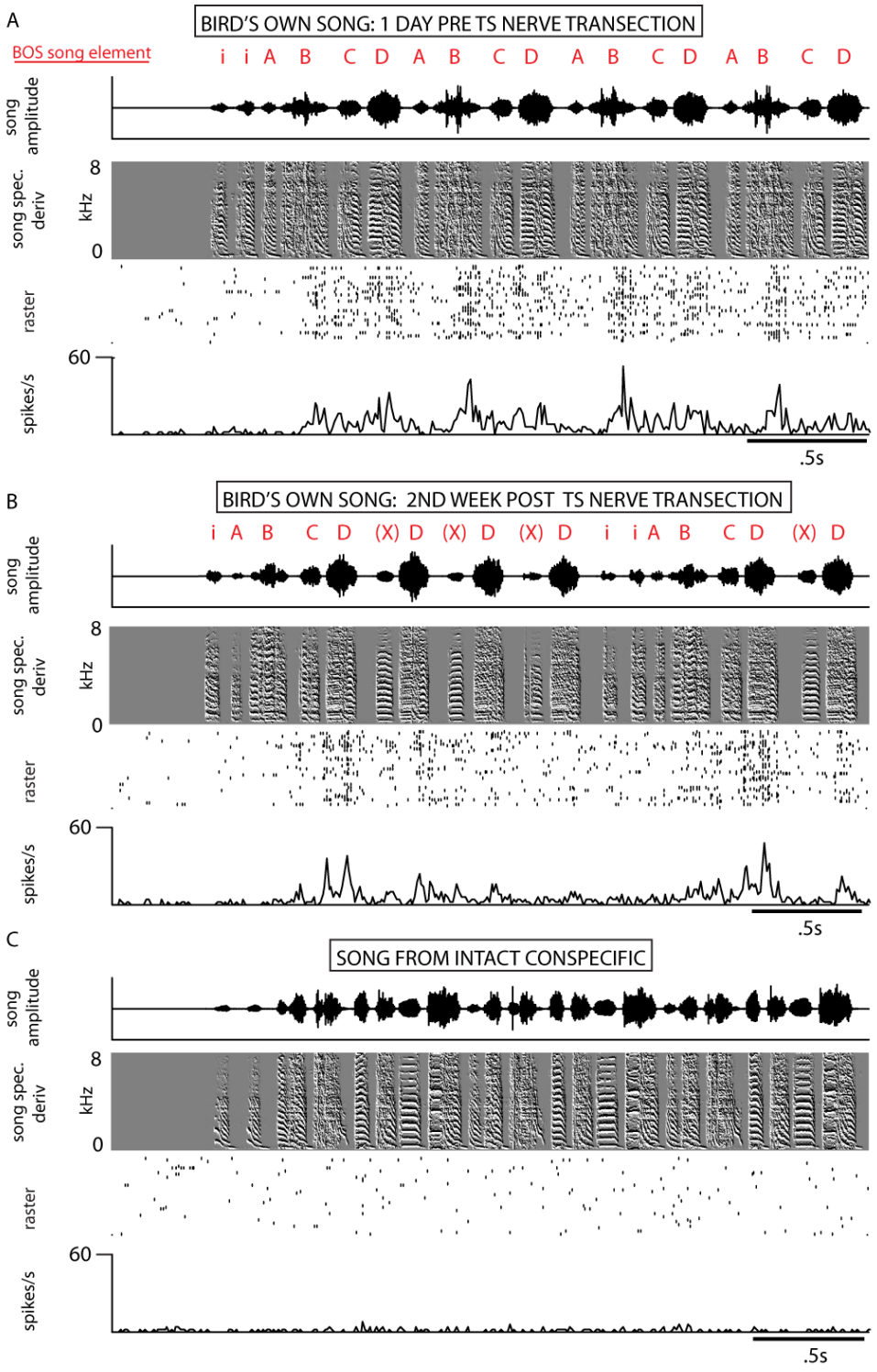
A
BIRD'S OWN SONG: 1 DAY PRE TS NERVE TRANSECTION
BOS song element
i i A B C D A B C D A B C D A B C D
song amplitude
song spec. deriv
8
kHz
0
raster
60
spikes/s
.5s
B
BIRD'S OWN SONG: 2ND WEEK POST TS NERVE TRANSECTION
i A B C D (X) D (X) D (X) D i i A B C D (X) D
song amplitude
song spec. deriv
8
kHz
0
raster
60
spikes/s
.5s
C
SONG FROM INTACT CONSPECIFIC
song amplitude
song spec. deriv
8
kHz
0
raster
60
spikes/s
.5s

Figure 3.9

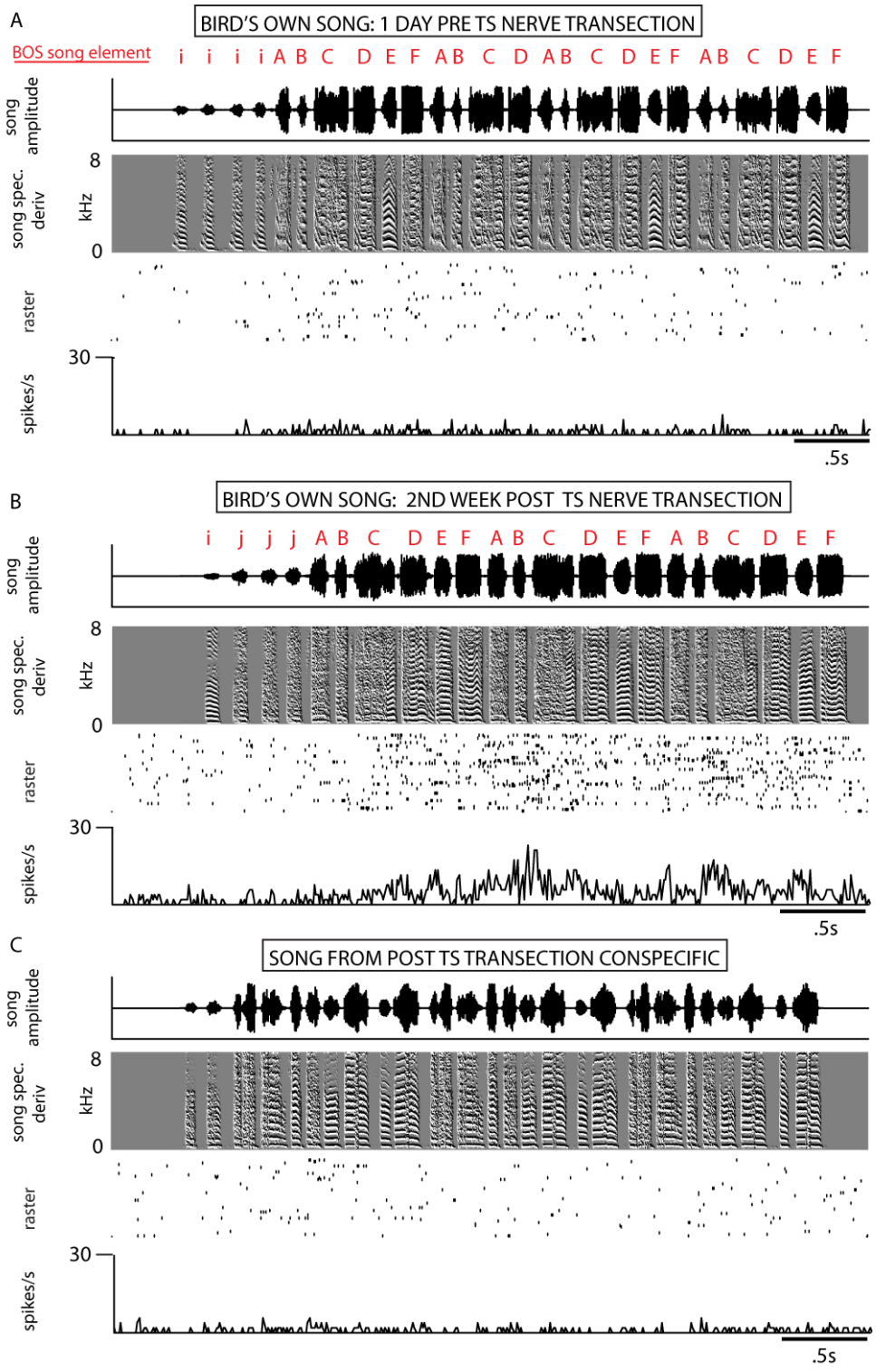
A
BIRD'S OWN SONG: 1 DAY PRE TS NERVE TRANSECTION
BOS song element
i i i i A B C D E F AB C D AB C D E F AB C D E F
song amplitude
song spec. deriv
8
kHz
0
raster
30
spikes/s
.5s
B
BIRD'S OWN SONG: 2ND WEEK POST TS NERVE TRANSECTION
i j j j A B C D E F A B C D E F A B C D E F
song amplitude
song spec. deriv
8
kHz
0
raster
30
spikes/s
.5s
C
SONG FROM POST TS TRANSECTION CONSPECIFIC
song amplitude
song spec. deriv
8
kHz
0
raster
30
spikes/s
.5s

Figure 3.10

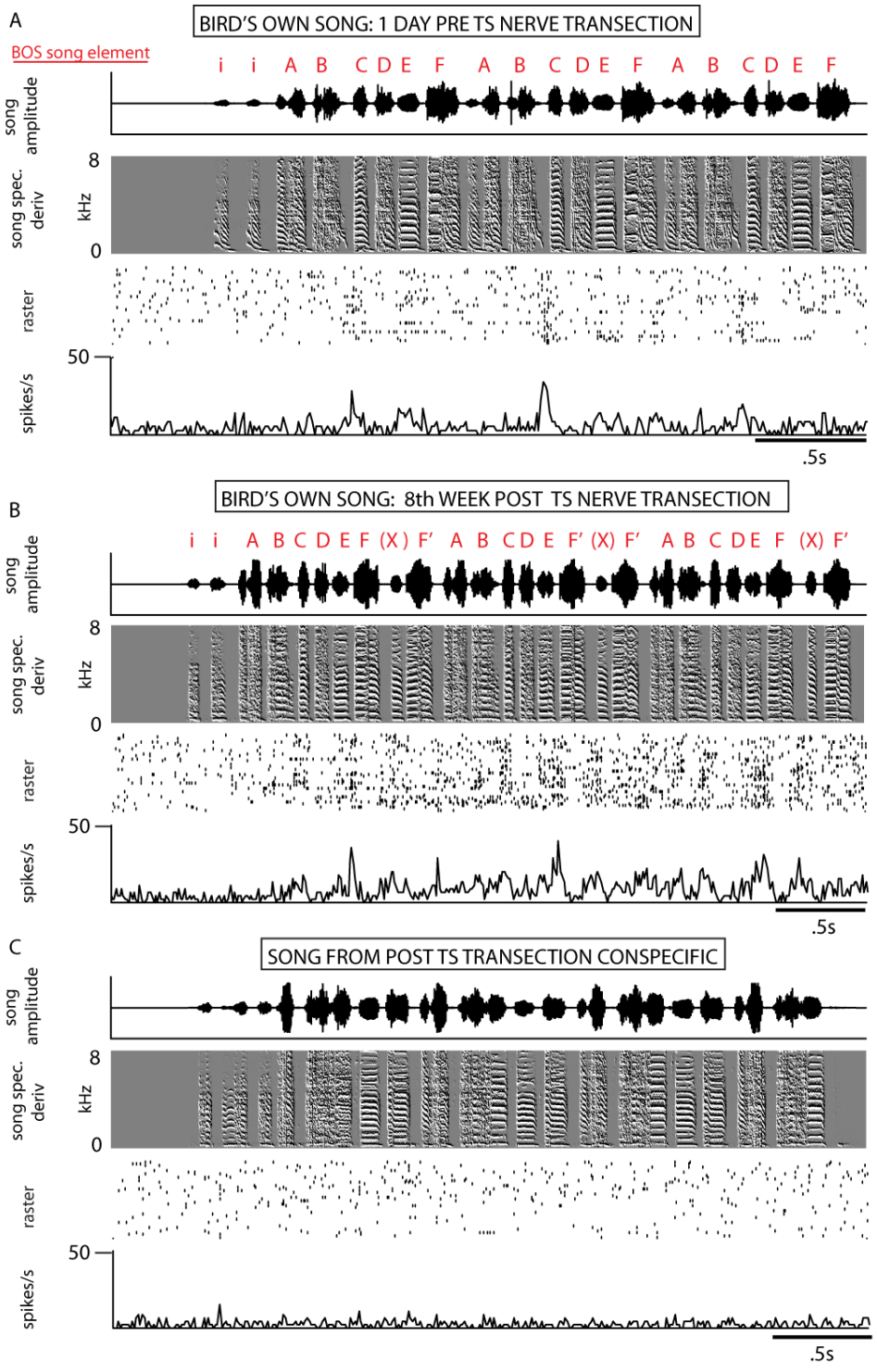
A
BIRD'S OWN SONG: 1 DAY PRE TS NERVE TRANSECTION
BOS song element
i i A B C D E F A B C D E F A B C D E F
song amplitude
song spec. deriv
8
kHz
0
raster
50
spikes/s
.5s
B
BIRD'S OWN SONG: 8th WEEK POST TS NERVE TRANSECTION
i i A B C D E F (X) F' A B C D E F' (X) F' A B C D E F (X) F'
song amplitude
song spec. deriv
8
kHz
0
raster
50
spikes/s
.5s
C
SONG FROM POST TS TRANSECTION CONSPECIFIC
song amplitude
song spec. deriv
8
kHz
0
raster
50
spikes/s
.5s

Figure 3.11

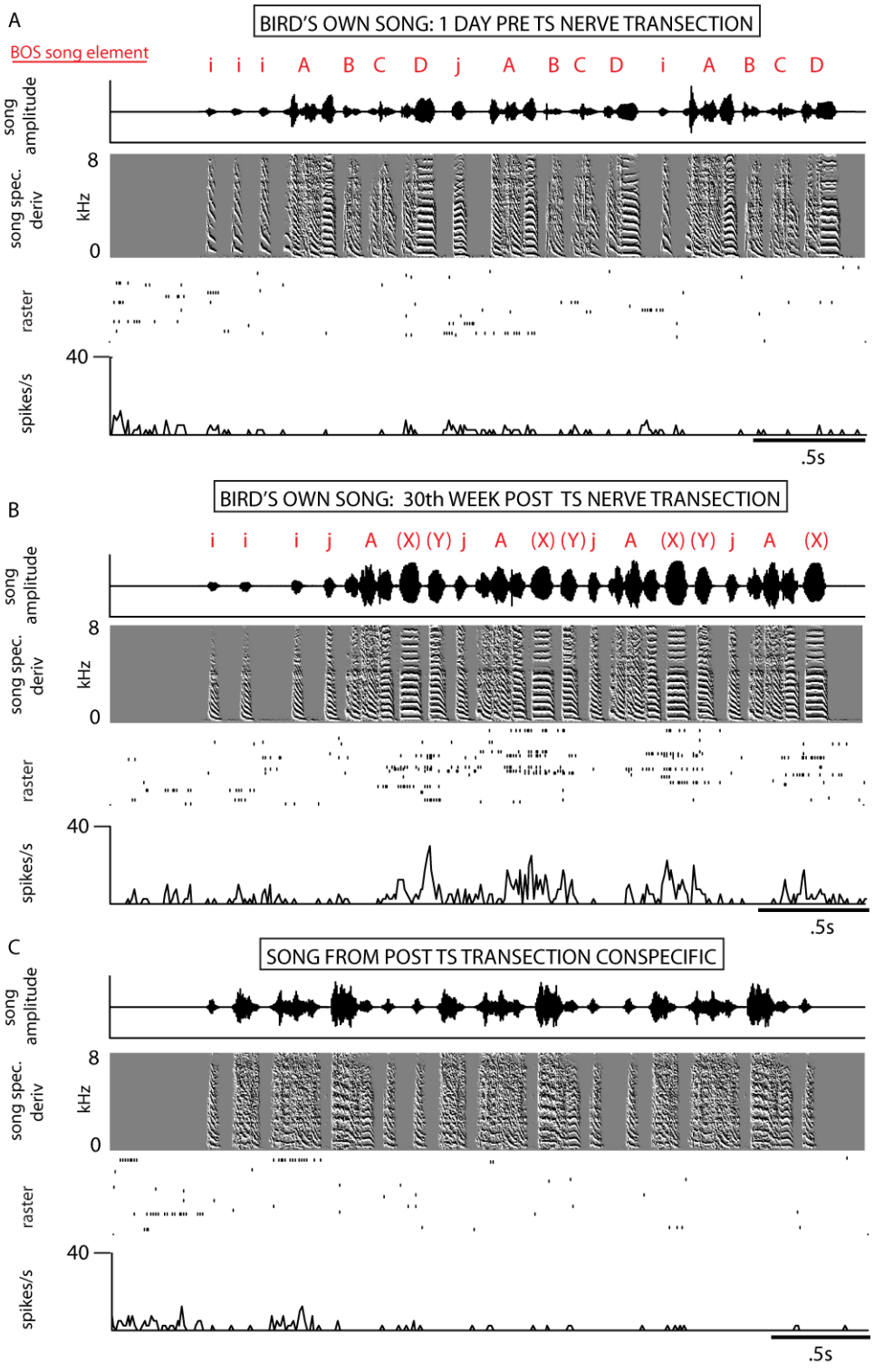
A
BIRD'S OWN SONG: 1 DAY PRE TS NERVE TRANSECTION
BOS song element
i i i A B C D j A B C D i A B C D
song amplitude
song spec. deriv
8
kHz
0
raster
40
spikes/s
.5s
B
BIRD'S OWN SONG: 30th WEEK POST TS NERVE TRANSECTION
i i i j A (X) (Y) j A (X) (Y) j A (X) (Y) j A (X)
song amplitude
song spec. deriv
8
kHz
0
raster
40
spikes/s
.5s
C
SONG FROM POST TS TRANSECTION CONSPECIFIC
song amplitude
song spec. deriv
8
kHz
0
raster
40
spikes/s
.5s

Figure 3.12

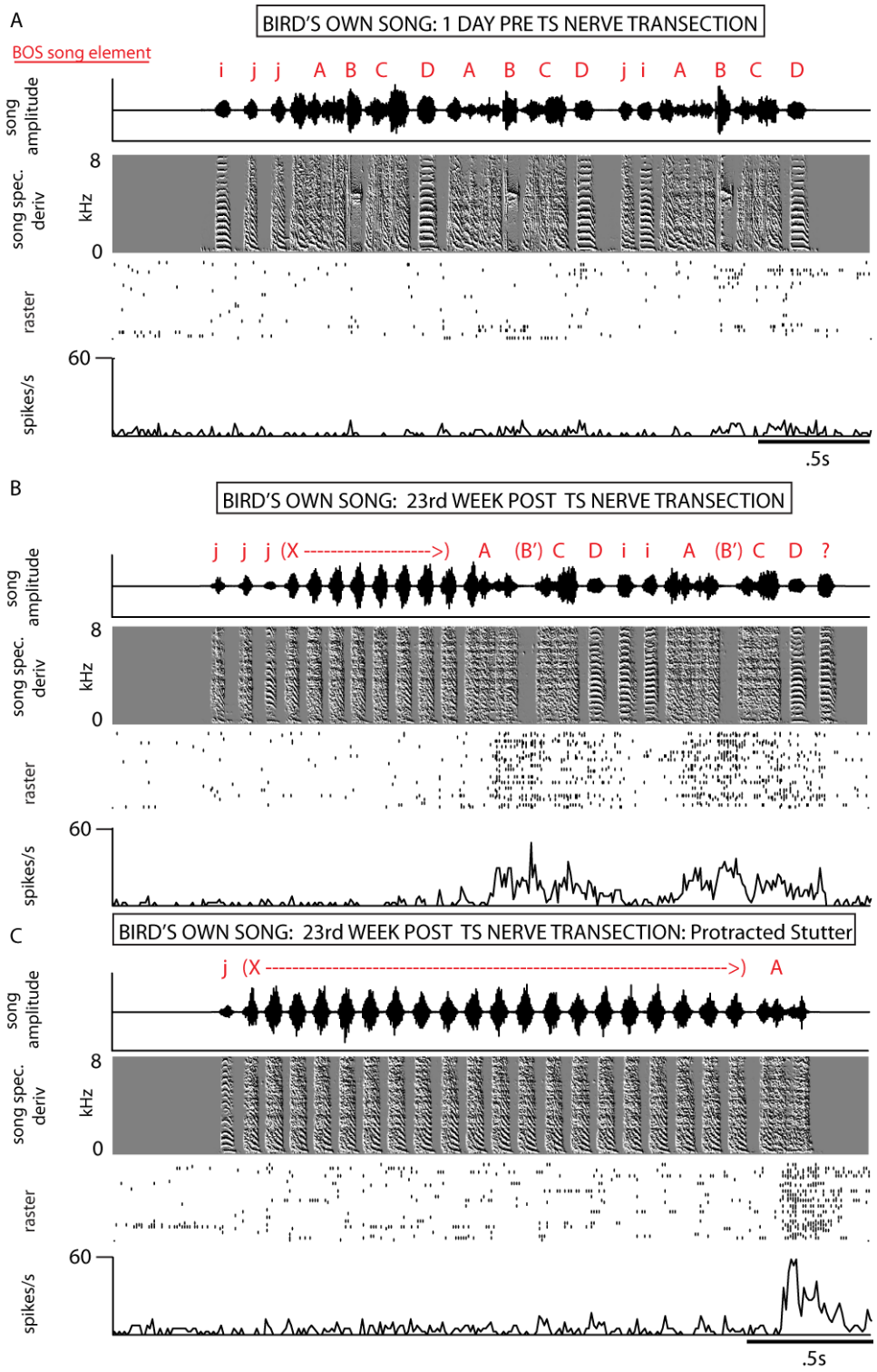
A
BIRD'S OWN SONG: 1 DAY PRE TS NERVE TRANSECTION
BOS song element
i j j A B C D A B C D j i A B C D
song amplitude
song spec. deriv
8
kHz
0
raster
60
spikes/s
.5s
B
BIRD'S OWN SONG: 23rd WEEK POST TS NERVE TRANSECTION
j j j (X ---------->) A (B') C D i i A (B') C D ?
song amplitude
song spec. deriv
8
kHz
0
raster
60
spikes/s
C
BIRD'S OWN SONG: 23rd WEEK POST TS NERVE TRANSECTION: Protracted Stutter
j (X ---------->) A
song amplitude
song spec. deriv
8
kHz
0
raster
60
spikes/s
.5s

Figure 3.13

REFERENCES

Amin N, Grace JA, Theunissen FE (2004) Neural response to bird's own song and tutor song in the zebra finch field L and caudal mesopallium. J Comp Physiol A Neuroethol Sens Neural Behav Physiol 190:469-489.

Andalman AS, Fee MS (2009) A basal ganglia-forebrain circuit in the songbird biases motor output to avoid vocal errors. Proc Natl Acad Sci U S A 106:12518-12523.

Andoni S, Li N, Pollak GD (2007) Spectrotemporal receptive fields in the inferior colliculus revealing selectivity for spectral motion in conspecific vocalizations. J Neurosci 27:4882-4893.

Appeltants D, Gentner TQ, Hulse SH, Balthazart J, Ball GF (2005) The effects of auditory distractors on song discrimination in male canaries (*Serinus canaria*). Behav Proc 69:331-341.

Aronov D, Andalman AS, Fee MS (2008) A specialized forebrain circuit for vocal babbling in the juvenile songbird. Science 320:630-634.

Ashmore RC, Wild JM, Schmidt MF (2005) Brainstem and forebrain contributions to the generation of learned motor behaviors for song. J Neurosci 25:8543-8554.

Ashmore RC, Bourjaily M, Schmidt MF (2008) Hemispheric coordination is necessary for song production in adult birds: implications for a dual role for forebrain nuclei in vocal motor control. J Neurophysiol 99:373-385.

Bauer EE, Coleman MJ, Roberts TF, Roy A, Prather JF, Mooney R (2008) A synaptic basis for auditory-vocal integration in the songbird. J Neurosci 28:1509-1522.

Brenowitz EA (1991) Altered perception of species-specific song by female birds after lesions of a forebrain nucleus. Science 251:303-305.

Buccino G, Vogt S, Ritzl A, Fink GR, Zilles K, Freund HJ, Rizzolatti G (2004) Neural circuits underlying imitation learning of hand actions: an event-related fMRI study. Neuron 42:323-334.

Cardin JA, Schmidt MF (2003) Song system auditory responses are stable and highly tuned during sedation, rapidly modulated and unselective during wakefulness, and suppressed by arousal. J Neurophysiol 90:2884-2899.

Cardin JA, Schmidt MF (2004a) Auditory responses in multiple sensorimotor song nuclei are co- modulated by behavioral state. J Neurophysiol 91:2148-2163.

Cardin JA, Schmidt MF (2004b) Noradrenergic inputs mediate state dependence of auditory responses in the avian song system. J Neurosci 24: 7745-7753.

Cardin JA, Raksin JN, Schmidt MF (2005) Sensorimotor nucleus NIf is necessary for auditory processing but not vocal motor output in the avian vocal motor system. J Neurophysiol 93:2157-2166.

Cattaneo Z, Devlin JT, Salvani F, Vecchi T, Silvanto J (2009) The causal role of category-specific neuronal representations in the left ventral premotor cortex (PMv) in semantic processing. Neuroimage [Epub ahead of print]

Chi, Z, Rauske, PL, Margoliash D (2003) Pattern filtering for detection of neural activity, with examples from HVc activity during sleep in zebra finches. Neural Comput 15: 2307-2337.

Coleman MJ, Mooney R (2004) Synaptic transformations underlying highly selective auditory representations of learned birdsong. J Neurosci 24:7251-7265.

Coleman MJ, Roy A, Wild JM, Mooney R (2007) Thalamic gating of auditory responses in telencephalic song control nuclei. J Neurosci 27:10024-10036.

Cynx J, Von Rad U (2001) Immediate and transitory effects of delayed auditory feedback on bird song production. Animal Behaviour 62:305-312.

Dave AS, Margoliash D (1998) Behavioral state modulation of auditory activity in a vocal motor system. Science 282: 2250-2254.

Dave AS, Margoliash D (2000) Song replay during sleep and computational rules for sensorimotor vocal learning. Science 290:812-816.

David SV, Mesgarani N, Fritz JB, Shamma SA (2009) Rapid synaptic depression explains nonlinear modulation of spectro-temporal tuning in primary auditory cortex by natural stimuli. J Neurosci 29:3374-3386.

deCharms RC, Blake DT, Merzenich MM (1998) Optimizing sound features for cortical neurons. Science 280:1439-1443.

Del Negro C, Gahr M, Leboucher G, Kreutzer M (1998) The selectivity of sexual responses to song displays: effects of partial chemical lesions of the HVC in female canaries. Behav Brain Res 96:151-159.

Deregnaucourt S, Mitra PP, Feher O, Pytte C, Tchernichovski O (2005) How sleep affects the developmental learning of bird song. Nature 433:710-716.

Doupe AJ, Konishi M (1991) Song- selective auditory circuits in the vocal control system of the zebra finch. Proc Natl Acad Sci U S A 88:11339-11343.

Edeline JM, Dutrieux G, Manunta y, Hennevin E (2001) Diversity of receptive field changes in auditory cortex during natural sleep. Eur J Neurosci 14:1865-1880.

Ego-Stengel V, Wilson MA (2009) Disruption of ripple-associated hippocampal activity during rest impairs spatial learning in the rat. Hippocampus [Epub ahead of print]

Elhilali M, Fritz JB, Chi TS, Shamma SA (2007) Auditory cortical receptive fields: stable entities with plastic abilities. J Neurosci 27:10372-10382.

Escabi MA, Schreiner CE (2002) Nonlinear spectrotemporal sound analysis by neurons in the auditory midbrain. J Neurosci 22:4114-4131.

Evarts, E. V. (1963). Photically evoked responses in visual cortex units during sleep and waking. J Neurophysiol *26:*229–248.

Fadiga L, Craighero, L, Olivier E (2005) Human motor cortex excitability during the perception of others' action. Curr Opin Neurobiol 15:213-218.

Fee MS, Kozhevnikov AA, Hahnloser RH (2004) Neural mechanisms of vocal sequence generation in the songbird. Ann N Y Acad Sci 1016:153-170.

Ferster D, Miller KD (2000) Neural mechanisms of orientation selectivity in the visual cortex. Annu Rev Neurosci 23:441-471.

Fogassi L, Ferrari PF, Geseierich B, Rozzi S, Chersi F, Rizzolatti G (2005) Parietal lobe:from action organization to intention understanding. Science 308:662-667.

Fortune ES, Margoliash D (1992) Temporal and harmonic combination-sensitive neurons in the zebra finch's HVc. J Neurosci 12:4309-4326.

Fortune ES, Margoliash D (1995) Parallel pathways and convergence onto HVc and adjacent neostriatum of adult zebra finches (Taeniopygia guttata). J Comp Neurol 360:413-441.

Gais S, Molle M, Helms K, Born J (2002) Learning-dependent increases in sleep spindle density. J Neurosci 22:6830-6834.

Gallese V, Fadiga L, Fogassi L, Rizzolatti G (1996) Action recognition in the premotor cortex. Brain 119:593-609.

Gentner TQ, Hulse SH, Bentley GE, Ball GF (2000) Individual vocal recognition and the effect of partial lesions to HVc on discrimination, learning, and categorization of conspecific song in adult songbirds. J Neurobiol 42:117-133.

Gentner TQ, Margoliash D (2003) Neuronal populations and single cells representing learned auditory objects. Nature 424:669-674.

George I, Cousillas H, Richard JP, Hausberger M (2005a) State-dependent hemispheric specialization in the songbird brain. J Comp Neurol 488:48-60.

George I, Cousillas H, Richard JP, and Hausberger M (2005b) New insights in to the auditory processing of communicative signals in the HVC of awake songbirds. Neuroscience 136:1-14.

George I, Cousillas H, Richard JP, and Hausberger M (2008) A potential neural substrate for processing functional classes of complex auditory signals

Gill P, Zhang J, Woolley SM, Fremouw T, Theuniussen FE (2006) Sound representation methods for spectro-temporal receptive field estimation. J Comput Neurosci 21:5-20.

Gill P, Woolley SM, Fremouw T, Theunissen FE (2008) What's that sound? Auditory area CLM encodes stimulus surprise, not intensity or intensity changes. J Neurophysiol 99:2809-2920.

Glenn LL, Steriade M (1982) Discharge rate and excitability of cortically projecting intralaminar thalamic neurons during waking and sleep states. J Neurosci 2:1387-1404.

Grace JA, Amin N, Singh NC, Theunissen FE (2003) Selectivity for conspecific song in the zebra finch auditory forebrain. J Neurophysiol 89:472-487.

Graña GD, Billimoria CP, Sen K (2009) Analyzing variability in neural responses to complex natural sounds in the awake songbird. J Neurophysiol 101: 3147-3157.

Green DM, Swets JA (1966) Signal Detection Theory and Psychophysics. New York: Wiley.

Gùcer G (1979) The effect of sleep upon the transmission of afferent activity in the somatic afferent system. Exp Brain Res 34:287-298.

Halle F, Gahr M, Pieneman AW, Kreutzer M (2002) Recovery of song preferences after excitotoxic HVC lesion in female canaries. J Neurobiol 52:1-13.

Hahnloser RH, Kozhevnikov AA, Fee MS (2002) An ultra-sparse code underlies the generation of neural sequences in a songbird. Nature 419:65-70.

Hahnloser RH, Wang CZ, Nager A, Naie K (2008) Spikes and bursts in two types of thalamic projection neurons differentially shape sleep patterns and auditory responses in a songbird. J Neurosci 28:5040-5052.

Hashimoto Y, Sakai KL (2003) Brain activations during conscious self-monitoring of speech production with delayed auditory feedback: an fMRI study. Hum Brain Mapp 20:22-28.

Hessler NA, Doupe AJ (1999) Singing-related neural activity in a dorsal forebrain-basal ganglia circuit of adult zebra finches. J Neurosci 19:10461-10481.

Hickok G (2009) Eight problems for the mirror neuron theory of action understanding in monkeys and humans. J Cogn Neurosci 21:1229-1243.

Houde JF, Jordan MI (1998) Sensorimotor adaptation in speech production. Science 279:1213-1216.

Houweling AR, Brecht M (2008) Behavioural report of single neuron stimulation in somatasensory cortex. Nature 451:65-68.

Howell P, Archer A (1984) Susceptibility to the effects of delayed auditory feedback. Percept Psychophys 36:296-302.

Howell P, Powell DJ (1987) Delayed auditory feedback with delayed sounds varying in duration.Percept Psychophys 42:166-172.

Hsu A, Woolley SM, Fremouw TE, Theunissen FE (2004a) Modulation power and phase spectrum of natural sounds enhance neural encoding performed by single auditory neurons. J Neurosci 24:9201-9211.

Hsu A, Borst A, Theunissen FE (2004b) Quantifying variability in neural responses and its application for the validation of model predictions. Network 15:91-109.

Iacoboni M, Molnar-Szakacs I, Gallese V, Buccino G, Mazziotta JC, Rizzolatti G (2005) Grasping the intentions of others with one's own mirror neuron system. PLos Biol 3:529-535.

Issa EB, Wang X (2008) Sensory responses during sleep in primate primary and secondary auditory cortex. J Neurosci 28:14467-14480.

Janata P, Margoliash D (1999) Gradual emergence of song selectivity in sensorimotor structures of the male zebra finch song system. J Neurosci 19:5108-5118.

Katz LC, Gurney ME (1981) Auditory responses in the zebra finch's motor system for song. Brain Res 221:192-197.

Keller GB, Hahnloser RH (2009) Neural processing of auditory feedback during vocal practice in a songbird. Nature 457:187-190.

Kozhevnikov AA, Fee MS (2007) Singing-related activity of identified HVC neurons in the zebra finch. J Neurophysiol 97:4271-4283.

Kudrimoti HS, Barnes CA, McNaughton BL (1999) Reactivation of hippocampal cell assemblies: effects of behavioral state, experience, and EEG dynamics. J Neurosci 19:4090-4101.

Lane H, Webster JW (1991) Speech deterioration in postlingually deafened adults. J Acoust Soc Am 89:859-866.

Lashley KS (1951) The problem of serial order in behavior. In: Cerebral Mechanisms in Behavior, edited by Jeffris LA. New York: Wiley pp. 112-136.

Lehongre K, Del Negro C (2009) Repertoire sharing and auditory responses in the HVC of the canary. Neuroreport 20:202-206.

Leitner S, Catchpole C (2004) Syllable repertoire and the size of the song control system in captive canaries (*Serinus canaria*). J Neurobiol 60:21-27.

Leonardo A, Konishi M (1999) Decrystallization of adult birdsong by perturbation of auditory feedback. Nature 399:466-470.

Leonardo A (2004) Experimental test of the birdsong error-correction model. Proc Natl Acad Sci U S A 101:16935-16940.

Lewicki MS, Arthur BJ (1996) Hierarchical organization of auditory temporal context sensitivity. J Neurosci 16:6987-6998.

Lingnau A, Gesierich B, Caramazza A (2009) Asymmetric fMRI adaptation reveals no evidence for mirror neurons in humans. Proc Natl Acad Sci U S A 106:9925-9930.

Livingstone MS, Hubel DH (1981) Effects of sleep and arousal on the processing of visual information in the cat. Nature 291:554-561.

Lombardino AJ, Nottebohm F (2000) Age at deafening affects the stability of learned song in adult male zebra finches. J Neurosci 20:5054-5064.

Low PS, Shank SS, Sejnowski TJ, Margoliash D (2008) Mammalian-line features of sleep structure in zebra finches. Proc Natl Acad Sci 105:9081-9086.

Luo M, Perkel DJ (1999) A GABAergic, strongly inhibitory projection to a thalamic nucleus in the zebra finch song system. J Neurosci 19:6700-6711.

Luo M, Ding L, Perkel DJ (2001) An Avian basal ganglia pathway essential for vocal learning forms a closed topographic loop. J Neurosci 21:6836-6845.

Margoliash D (1983) Acoustic parameters underlying the responses of song-specific neurons in the white-crowned sparrow. J Neurosci 3:1039-1057.

Margoliash D, Konishi M (1985) Auditory representation of autogenous song in the song system of white-crowned sparrows. Proc Natl Acad Sci U S A 82:5997-6000.

Margoliash D (1986) Preference for autogenous song by auditory neurons in a song system nucleus of the white-crowned sparrow. J Neurosci 6:1643-1661.

Marshall L, Born J (2007) The contribution of sleep to hippocampus-dependent memory consolidation. Trends Cogn Sci 11:442-450.

McCasland JS (1987) Neuronal control of bird song production. J Neurosci 7:23-39.

McCormick DA (1989) Cholinergic and noradrenergic modulation of thalamocortical processing. Trends Neurosci 12:215-221.

McCormick DA, Bal T (1997) Sleep and arousal: thalamocortical mechanisms. J Neurophysiol 77: 3145-3156.

Merchant H, Naselaris T, Georgopoulos AP (2008) Dynamic sculpting of directional tuning in the primate motor cortex during three-dimensional reaching. J Neurosci 28:9164-9172.

Miller LM, Escabi MA, Read HL, Schreiner CE (2002) Spectrotemporal receptive fields in the lemniscal auditory thalamus and cortex. J Neurophysiol 87:516-527.

Mooney R (2000) Different subthreshold mechanisms underlie selectivity in identified HVc neurons of the zebra finch. J Neurosci 20:5420-5436.

Mooney R, Prather JF (2005) The HVC microcircuit: the synaptic basis for interactions between song motor and vocal plasticity pathways. J Neurosci 25:1952-1964.

Murayama M, Pérez- Garci E, Nevian T, Block T, Senn W, Larkum ME (2009) Dendritic encoding of sensory stimuli controlled by deep cortical interneurons. Nature 457:1137-1141.

Nadasdy Z, Hirase H, Czurko A, Csicsvari J, Buzsaki G (1999) Replay and time compression of recurring spike sequences in the hippocampus. J Neurosci 19:9497-9507.

Nagel KI, Doupe AJ (2008) Organizing principles of spectro-temporal encoding in the avian primary auditory area Field L. Neuron 58:938-955.

Nakamura KZ, Okanoya K (2004) Neural correlates of song complexity in Bengalese finch high vocal center. Neuroreport 15:1359-1363.

Nealen PM, Schmidt MF (2006) Distributed and selective auditory representation of song repertoires in the avian song system. J Neurophysiol 96:3433-3447.

Nick TA, Konishi M (2001) Dynamic control of auditory activity during sleep: correlation between song response and EEG. Proc Natl Acad Sci U S A 98:14012-14016.

Nixdorf BE, Davis SS, DeVoogd TJ (1989) Morphology of Golgi impregnated neurons in hyperstriatum ventrale, pars caudalis in adult male and female canaries. J Comp Neurol 284:337–349.

Nordeen KW, Nordeen EJ (1993) Long-term maintenance of song in adult zebra finches is not affected by lesions of a forebrain region involved in song learning. Behav Neural Biol 59:79-82.

Nottebohm F, Stokes TM, Leonard CM (1976) Central control of song in the canary, Serinus canaries. J Comp Neurol 165:457-486.

Okanoya K, Dooling RJ (1987) Hearing in passerine and psittacine birds: a comparative study of absolute and masked auditory thresholds. J Comp Psychol 101:7-15.

Okanoya K, Yamaguchi A (1997) Adult Bengalese finches (Lonchura striata var. domestica) require real-time auditory feedback to produce normal song syntax. J Neurobiol 33:343-356.

Okanoya K (2004) The Bengalese finch: a window on the behavioral neurobiology of birdsong syntax. Ann N Y Acad Sci 1016:724-735.

Pena JL, Perez-Perera L, Bouvier M, Velluti RA (1999) Sleep and wakefulness modulation of the neuronal firing in the auditory cortex of the guinea pig. Brain Res 816:463-470.

Populin LC (2005) Anesthetics change the excitation/inhibition balance that governs sensory processing in the cat superior colliculus. J Neurosci 25:5903-5914.

Prather JF, Peters S, Nowicki S, Mooney R (2008) Precise auditory-vocal mirroring in neurons for learned vocal communication. Nature 451:305-310.

Prather JF, Nowicki S, Anderson RC, Peters S, Mooney R (2009) Neural correlates of categorical perception in learned vocal communication. Nat Neurosci 12:221-228.

Rauske PL, Shea SD, Margoliash D (2003) State and neuronal class-dependent reconfiguration in the avian song system. J Neurophysiol 89:1688-16701.

Rizzolatti G, Fogassi L, Gallese V (2001) Neurophysiological mechanisms underlying the understanding and imitation of action. Nat Rev Neurosci 2:661-670.

Rizzolatti G, Craighero L (2004) The mirror-neuron system. Annu Rev Neurosci 27:169-192.

Roy A, Mooney R (2009) Song decrystallization in adult zebra finches does not require the song nucleus NIf. J Neurophysiol 102:979-991.

Sakata JT, Brainard MS (2006) Real-time contributions of auditory feedback to avian vocal motor control. J Neurosci 26:9619-9628.

Sakata JT, Brainard MS (2008) Online contributions of auditory feedback to neural activity in the avian song control circuitry. J Neurosci 28:11378-11390.

Scharff C, Nottebohm F (1991) A comparative study of the behavioral deficits following lesions of various parts of the zebra finch song system: implications for vocal learning. J Neurosci 11:2896-2913.

Scharff C, Nottebohm F, Cynx J (1998) Conspecific and heterospecific song discrimination in male zebra finches with lesions in the anterior forebrain pathway. J Neurobiol 36:81-90.

Scharff C, Kirn JR, Grossman M, Macklis JD, Nottebohm F (2000) Targeted neuronal death affects neuronal replacement and vocal behavior in adult songbirds. Neuron 25:481-492.

Schmidt MF, Konishi M (1998) Gating of auditory responses in the vocal control system of awake songbirds. Nat Neurosci 1:513-518.

Schmidt MF (2003) Pattern of interhemispheric synchronization in HVc during singing correlates with key transitions in the song pattern. J Neurophysiol 90:3931-3949.

Sen K, Theunissen FE, Doupe AJ (2001) Feature analysis of natural sounds in the songbird auditory forebrain. J Neurophysiol 86:1445-1458.

Shaevitz SS, Theunissen FE (2007) Functional connectivity between auditory areas Field L and CLM and song system nucleus HVC in anesthetized zebra finches. J Neurophysiol 98:2747-2764.

Shank SS, Margoliash D (2009) Sleep and sensorimotor integration during early vocal learning in a songbird. Nature 458:73-77.

Shea SD, Margoliash D (2003) Basal forebrain cholinergic modulation of auditory activity in the zebra finch song system. Neuron 40: 1213-1226.

Simpson HB, Vicario DS (1990) Brain pathways for learned and unlearned vocalizations differ in zebra finches. J Neurosci 10: 1541-1556.

Singh NC, Theunissen FE (2003) Modulation spectra of natural sounds and ethological theories of auditory processing. J Acoust Soc Am 114:3394-3411.

Sober SJ, Brainard MS (2009) Adult birdsong is actively maintained by error correction. Nat Neurosci 12:927-931.

Sohrabji F, Nordeen EJ, Nordeen KW (1990) Selective impairment of song learning following lesions of a forebrain nucleus in the juvenile zebra finch. Behav Neural Biol 53:51-63.

Solis MM, Doupe AJ (1997) Anterior forebrain neurons develop selectivity by an intermediate stage of birdsong learning. J Neurosci 17:6447-6462.

Spiro JE, Dalva MB, Mooney R (1999) Long-range inhibition within the zebra finch song nucleus RA can coordinate the firing of multiple projection neurons. J Neurophysiol 81:3007-3020.

Steriade M, McCormick DA, Sejnowski TJ (1993) Thlamocortical oscillations in the sleeping and aroused brain. Science 262:679-685.

Steriade M (2000) Corticothalamic resonance, states of vigilance and mentation. Neuroscience 101:243-276.

Striedter GF, Vu ET (1998) Bilateral feedback projections to the forebrain in the premotor network for singing in zebra finches. J Neurobiol 34:27-40.

Sutter ML, Margoliash D (1994) Global synchronous response to autogenous song in zebra finch HVc. J Neurophysiol 72:2105-2123.

Swadlow HA, Gusev AG, Bezdudnaya T (2002) Activation of a cortical column by a thalamocortical impulse. J Neurosci 22:7766-7773.

Szymczak JT, Kaiser W, Helb HW, Beszczynska (1996) A study of sleep in the European blackbird. Physiol Behav 60:1115-1120.

Terleph TA, Lu K, Vicario DS (2008) Response properties of the auditory telencephalon in songbirds change with recent experience. PLoS One 3:e2854.

Theunissen FE, Doupe AJ (1998) Temporal and spectral sensitivity of complex auditory neurons in the nucleus HVc of male zebra finches. J Neurosci 18:3786-3802.

Theunissen FE, Sen K, Doupe AJ (2000) Spectral-temporal receptive fields of nonlinear auditory neurons obtained using natural sounds. J Neurosci 20:2315-2331.

Theunissen FE, Woolley SM, Hsu A, Fremouw T (2004) Methods for the analysis of auditory processing in the brain. Ann N Y Acad Sci 1016:187-207.

Thompson JA, Wu W, Bertram R, Johnson F (2007) Auditory-dependent vocal recovery in adult male zebra finches is facilitated by lesion of a forebrain pathway that includes the basal ganglia. J Neurosci 27:12308-12320.

Thompson JA, Johnson F (2007) HVC microlesions do not destabilize the vocal patterns of adult male zebra finches with prior ablation of LMAN. Dev Neurobiol 67:205-218.

Tkach D, Reimer J, Hatsopoulos NG (2007) Congruent activity during action and action observation in motor cortex. J Neurosci 27:13241-13250.

Troyer TW, Doupe AJ (2000) An associational model of birdsong sensorimotor learning I. Efference copy and the learning of song syllables. J Neurophysiol 84:1204-1223.

Vates GE, Broome BM, Mello CV, Nottebohm F (1996) Auditory pathways of caudal telencephalon and their relation to the song system of adult male zebra finches. J Comp Neurol 366:613-642.

Vicario DS (1991) Organization of the zebra finch song control system: II. Functional organization of outputs from nucleus Robustus archistriatalis. J Comp Neurol 22:486-494.

Vicario DS, Naqvi NH, Raksin JN (2001) Behavioral discrimination of sexually dimorphic calls by male zebra finches requires an intact vocal motor pathway. J Neurobiol 47:109-120.

Voigt BC, Brecht M, Houweling AR (2008) Behavioral detectability of single-cell stimulation in the ventral posterior medial nucleus of the thalamus. J Neurosci 28:12362-12367.

Wang X, Lu T, Snider RK, Liang L (2005) Sustained firing in auditory cortex evoked by preferred stimuli. Nature 435:341-346.

Wild JM (1993) Descending projections of the songbird nucleus robustus archistriatalis. J Comp Neurol. 337:32-62.

Wild JM (1994) Visual and somatosensory inputs to the avian song system via nucleus uvaeformis (Uva) and a comparison with the projections of a similar thalamic nucleus in a nonsongbird, Columba livia. J Comp Neurol 349:512-535.

Wild JM (1997) Neural pathways for the control of birdsong production. J Neurobiol 33:653-670.

Wild JM, Williams MN, Howie GJ, Mooney R (2005) Calcium-binding proteins define interneurons in HVC of the zebra finch (Taeniopygia guttata). J Comp Neurol 483:76-90.

Williams H, Crane LA, Hale TK, Esposito MA, Nottebohm F (1992) Right-side dominance for song control in the zebra finch. J Neurobiol 23:1006-1020.

Williams H, McKibben JR (1992) Changes in stereotyped central motor patterns controlling vocalization are induced by peripheral nerve injury. Behav Neural Biol 57:67-78.

Williams H, Mehta N (1999) Changes in adult zebra finch song require a forebrain nucleus that is not necessary for song production. J Neurobiol 39:14-28.

Woolley SM, Rubel EW (1997) Bengalese finches Lonchura Striata domestica depend upon auditory feedback for the maintenance of adult song. J Neurosci 17:6380-6390.

Woolley SM, Rubel EW (1999) High-frequency auditory feedback is not required for adult song maintenance in Bengalese finches. J Neurosci 19:358-371.

Woolley SM, Casseday JH (2004) Response properties of single neurons in the zebra finch auditory midbrain: response patterns, frequency coding, intensity coding, and spike latencies. J Neurophysiol 91:136-151.

Woolley SM, Casseday JH (2005) Processing of modulated sounds in the zebra finch auditory midbrain: responses to noise, frequency sweeps, and sinusoidal amplitude modulations. J Neurophysiol 94:1143-1157.

Woolley SM, Fremouw TE, Hsu A, Theunissen FE (2005) Tuning for spectro-temporal modulations as a mechanism for auditory discrimination. Nat Neurosci 8:1371-1379.

Woolley SM, Gill PR, Theunissen FE (2006) Stimulus-dependent auditory tuning results in synchronous population coding of vocalizations in the songbird midbrain. J Neurosci 26:2499-2512.

Woolley SM, Gill PR, Fremouw T, Theunissen FE (2009) Functional groups in the avian auditory system. J Neurosci 29:2780-2793.

Zann R (1993) Structure, sequence and evolution of song elements in wild Australian zebra finches. Auk 110:702−715.